DYNAMIC PERFORMANCE OF NUMERICAL DISTANCE PROTECTION RELAYS IN HEAVILY SERIES COMPENSATED NETWORKS

by

Clarence Moketjema Leoaneka

Submitted in the fulfillment of the academic requirement for the degree of Master of Science in Engineering, in the School of Electrical, Electronic and Computer Engineering, University of KwaZulu-Natal, Durban, South Africa.

June 2009

DECLARATION

I Moketjema Clarence Leoaneka declare that:

(i) The research reported in this thesis, except where otherwise indicated, is my original work.

(ii) This thesis has not been submitted for any degree or examination at any other university.

(iii) This thesis does not contain other persons' data, pictures, graphs or other information, unless specifically acknowledged as being sourced from other persons.

(iv) This thesis does not contain other persons' writing, unless specifically acknowledged as being sourced from other researchers. Where other written sources have been quoted, then:

a) Their words have been re-written but the general information attributed to them has been referenced;

b) Where their exact words have been used, their writing has been placed inside quotation marks, and referenced.

(v) Where I have reproduced a publication of which I am an author, co-author or editor, I have indicated in detail which part of the publication was actually written by myself alone and have fully referenced such publications.

(vi) This thesis does not contain text, graphics or tables copied and pasted from the Internet, unless specifically acknowledged, and the source being detailed in the thesis and in the References sections.

Moketjema Clarence Leoaneka …….. ……..
(BScEng) Signature Date

As the candidate's Supervisor I agree to the submission of this thesis.

Supervisor: Bruce Rigby …….. ……..
(BScEng, MScEng, PhD (Natal), MIEEE) Signature Date

This thesis is dedicated to my family.

ABSTRACT

Series compensating capacitors were initially introduced in transmission networks mainly to increase the power transfer capacity of long transmission lines. These series compensating capacitors bring with them significant protection challenges for relay manufacturers, utility engineers and researchers. One approach to studying the performance of advanced protection schemes in the presence of series capacitors is the use of real-time digital simulators. Real-time digital simulation allows actual relay hardware to be tested in a hardware-in-loop arrangement with detailed dynamic models of the protected power system.

This thesis, firstly, discusses an initial review carried out into the technical challenges presented when designing distance protection schemes and setting advanced numerical distance protection relays in the presence of series compensating capacitors.

The thesis then presents the results of detailed real-time simulator testing of advance numerical distance protection relays, using both hardware relays and real-time models of the relay algorithms, to determine the performance of, and appropriate settings for these advanced numerical distance relays when used to protect transmission lines.

Finally, the thesis has made use of a real-time simulation model of Eskom's heavily series compensated Western Cape transmission network, including detailed dynamic models of the non-linear metal oxide varistor (MOV) characteristics, control logic of the series capacitor protection and bypass breakers at each relevant series compensated site. This detailed dynamic simulation model has been used to study the performance of distance protection schemes for the lines in this network using the actual numerical distance relays that are used in the field, connected in closed-loop with the real-time power system model.

The results show that the real-time simulation approach allows for greater confidence when setting advanced numerical relays, where there is concern for possible under-reaching, over-reaching and malfunction of protection schemes because of the series capacitors. The results have also shown that by using actual relays for testing, in combination with a detailed real-time model of the relaying algorithms, it is possible to determine with greater confidence, when to reduce the reach of high-speed elements within the relays, and when it is genuinely not possible to use such elements. As a result of these studies it has also been possible to identify important system properties that impact on the extent to which series capacitors result in over-reaching in distance relays and to show that detailed dynamic studies are required if such relays are to be set with confidence.

ACKNOWLEGEMENTS

I would like to express my sincere gratitude to Prof. BS Rigby for his consistent supervision, support and guidance throughout the course of this research work. I would like to acknowledge Prof. BS Rigby for his commendable efforts during the write up and correction of this thesis, and for arranging funds for this research project.

Special thanks are extended to University of KwaZulu Natal, School of Electrical, Electronic and Computer Engineering, academic and support staff who have together contributed towards research environment over the years. I remember Mrs Ben Bennett, Mrs Yougie and Bruce Harrison for their administrative support. I would also like to thank Ms Fiona Higginson and Prof. E. Boje who together offered valuable advice concerning postgraduate studies.

Without thoughtful suggestions from Anura Perera (from Eskom), my thesis would have not completely fulfilled. His technical support and assistance in protection issues is highly acknowledged.

Many thanks are extended to Mr F. D'Almaine, Regina Naidoo and Ruby at Durban University of Technology for their support during my studies.

My gratefulness also goes to my friends and colleagues from Postgraduate Research Laboratory especially Rudy and Sebajoa for their support and encouragement.

The support and assistance of the University of KwaZulu-Natal, Durban University of Technology, Eskom Tertiary Education Support Programme and ABB South Africa is thankfully acknowledged. The RTPSS Centre is kindly acknowledged for financial support for the completion of this research project.

Finally, I wish to extend my profound appreciation to my family for their love, affection, and invaluable support during my studies. This acknowledgement will not be complete without thanking Almighty God for giving me strength, ability to study and providing all my needs.

Moketjema Clarence

Leoaneka

TABLE OF CONTENTS

CHAPTER 3

NUMERICAL DISTANCE PROTECTION RELAY

CHAPTER 4

REAL-TIME CLOSED-LOOP TESTING OF DISTANCE RELAYS

CHAPTER 5

REAL-TIME SIMULATION OF A HEAVILY SERIES COMPENSATED NETWORK

CHAPTER 6

THE REL531 RELAY PERFORMANCE ANALYSIS IN A HEAVILY SERIES COMPENSATED NETWORK: BAC-DRO CASE STUDY

CHAPTER 7

THE REL531 RELAY PERFORMANCE ANALYSIS FOR UNCOMPENSATED LINE WITHIN A HEAVILY SERIES COMPENSATED NETWORK: MUL-BAC CASE STUDY

CHAPTER 8

CONCLUSION AND SUGGESTION FOR FURTHER RESEARCH

APPENDIX A

HARDWARE-IN-LOOP TESTING OF THE REL531 RELAYS USING THE RTDS

APPENDIX B

DETAILED REAL-TIME CLOSED-LOOP TESTING FOR REL531 RELAY VERIFICATION

APPENDIX C

ESKOM CAPE TRANSMISSION NETWORK

REFERENCES

LIST OF FIGURES

LIST OF TABLES

LIST OF SYMBOLS

The commonly used symbols and notations adopted in this thesis are listed below. Other symbols used in the text are explained where they first occur.

Acronyms

DSP	Digital Signal Processor
HV	High Voltage
MOV	Metal Oxide Varistor
RTDS	Real-Time Digital Simulator
GUI	Graphical User Interface
CTR	Current Transformer Ratio
VTR	Voltage Transformer Ratio
A/D	Analogue to Digital converter

Symbols

Z	series impedance
Y	shunt admittance
γ	propagation constant
l	transmission line length
ZL	transmission line impedance
Δ	transmission line angle
X_S	Source reactance at sending end
E_S	Source voltage at sending end
X_R	Source reactance at sending end
E_R	Source voltage at receiving end
X_L	transmission line reactance
ZM	standard distance protection function
HS	high-speed distance protection function
PHS	phase selection function
Z1	zone 1 protection
Z2	zone 2 protection
Z3	zone 3 protection
Z1T	zone 1 time delay
Z2T	zone 2 time delay
Z3T	zone 3 time delay

Z1F	zone 1 forward direction
Z2F	zone 2 forward direction
Z3R	zone 3 reverse direction
RX	received signal
TX	transmitted signal
CR	carrier received
CS	carrier send
ZCOM	communication function
P	power transfer
$P_{W\text{-}SC}$	power transfer with series capacitor
$P_{W/O\text{-}SC}$	power transfer without series capacitor
P_O	initial power transfer
R_{MOVSC}	MOVSC equivalent series resistance
X_{MOVSC}	MOVSC equivalent series reactance
X1PP	positive sequence reactive reach setting for ph-ph fault
R1PP	positive sequence resistive reach setting for ph-ph fault
RFPP	resistive reach setting for ph-ph fault
X1PE	positive sequence reactive reach setting for ph-e fault
R1PE	positive sequence resistive reach setting for ph-e fault
X0PE	zero sequence reactive reach setting for ph-e fault
R0PE	zero sequence resistive reach setting for ph-e fault
RFPE	resistive reach setting for ph-e fault
Z_1	transmission line positive sequence impedance
Z_0	transmission line zero sequence impedance
Zsec	secondary impedance
Zpri	primary impedance

CHAPTER 1

INTRODUCTION

1.1 General Background

Series compensating capacitors were initially introduced in transmission networks mainly to increase the power transfer capacity of long transmission lines. A transmission network interconnects major generating stations and main load centers further way from generating stations. In particular, in large countries like South Africa where generating stations are several hundreds of kilometers away from load centers, series compensation is extensively utilized. The main generating stations (coal-fired) are concentrated in the northeastern part of the country, and a small nuclear power station is located in the southwestern part of the country [1]. The transmission network spans long distances to the load centers in the rest of the country, and the lines are heavily series compensated to enhance power system performance. In South Africa, Eskom introduced series capacitor compensation in 1975 [2]. The study in this thesis focuses on the heavily series compensated Eskom transmission network in the Western Cape region of South Africa.

The successful application of protection schemes in heavily series compensated networks relies on the technological advances that have been made in protection technology. Protection relaying technology was first contemplated during the early years of the 1900s. It has gone through continuous development, from the era of electromechanical relays to static or electronic relays, which were introduced in the 1960s. The present era which began in the 1980s makes use of microprocessor and microcontroller based relays [2],[3]. In 1986 numerical distance relays were developed which utilize specialized microprocessors and associated software optimized for digital signal processing (DSP) [3],[4]. These numerical distance relays provide the basis for series capacitor compensated transmission network protection, especially transmission lines compensated above 50%, because such relays have special functions to cope with the capacitive reactance introduced by series capacitors. In the first two eras of relaying technology, the degree of compensation had to be restricted to less than 50% of the line series inductive reactance to maintain security and dependability of protection [2].

The dynamic performance of a heavily series compensated network's protection depends on the reliability of present relay technology. The transient behavior of a heavily series compensated network during short-circuit faults is complex to comprehend analytically, but the network needs fast acting protection against short-circuit faults and abnormal system conditions to maintain power system stability and reliability of supply. The degree of complexity depends on the degree of compensation and the location of the series capacitor [5]. Series compensation introduced additional challenges over well known protection challenges on HV and EHV transmission networks. These challenges must be considered carefully when setting numerical distance protection relays.

The problems introduced by series compensation include voltage inversion, current inversion, subharmonic oscillations and non-linearity of the line impedance seen by the relay [6]. These problems may cause protection systems to malfunction.

The aforementioned challenges become even more problematic if the degree of series compensation is increased to over 50% of the line reactance. In the transmission networks of South Africa, a significant programme of network strengthening has been undertaken to address serious system stability and power transfer capacity constraints, but this network strengthening is also presenting considerable protection challenges as the degree of series compensation of a number of transmission lines is increased above 50%. The design of protection schemes needs careful evaluation, analysis and testing where there is possibility of apparent capacitive reactance at the relay point due to series capacitors in excess of 50%.

1.2 Thesis background and Objectives

The importance of power system protection for stability of electrical power systems is well known. However to maintain system stability provides challenges to protection schemes with regards to series capacitor compensated transmission lines. In the protection literature, protection of series capacitor compensated transmission lines is considered as one of the most difficult and complex tasks for relay manufacturers, utility engineers and researchers [5],[7],[8],[9].

The challenges to protection schemes introduced by the installation of series capacitors on transmission lines include, but are not limited to the following: voltage reversal and/or current reversal and low frequency resonances [5],[9],[10]. In addition, the series capacitor and the system inductance generate subharmonic oscillations that can cause severe underreach and overreach of the distance element [11]. These problems are compounded by the action of the devices used to protect the series capacitors themselves, namely the metal oxide varistors, (MOVs) and bypass circuit breakers, which dynamically alter the effective degree of series compensation during short-circuit faults [12]. Anderson [5] has stated: “It is clear that determining reach settings for distance measuring devices on series compensated lines is fraught with difficulties, and there is always a probability for error in the relay operation, irrespective of the rules selected for computing the settings”. Hence, relay settings and integration of series capacitor protection and line protection to maintain power system stability is a challenging task to the electrical utility practicing engineers.

The driver behind this research is that in many cases, the advanced features provided on modern numerical relays to deal with series compensated transmission lines are known and understood theoretically to practicing protection engineers, but their detailed dynamic performance under actual fault conditions in the field is not well understood.

The protection of series capacitor compensated transmission networks needs careful evaluation. Each particular application requires careful investigation to determine the most appropriate solution in respect of protection [3],[13]. A protection study for series capacitor compensated transmission network has to be conducted and a suitability of the protection scheme has to be evaluated.

1.3 Thesis Layout

Based on the research objectives, the thesis consists of the following chapters. The first chapter presents introductory information, as well as the basis and objectives of the research.

Chapter Two presents a literature review of series capacitor compensated transmission lines with regard to protection challenges. The chapter reviews the fundamentals of protection philosophies with more emphasis placed on the permissive overreaching distance protection scheme. Then the discussion is directed to series capacitor protection and its impact on distance based relays. This chapter also discusses proposed solutions for series capacitor compensated transmission lines.

Chapter Three focuses on a particular numerical distance protection relay designed for series capacitor compensated transmission lines. More emphasis is placed on the hybrid protection scheme in the relay, which combines a high-speed protection scheme in parallel with a standard distance protection scheme. The setting philosophies for compensated and uncompensated transmission lines within the vicinity of series capacitors are also discussed.

Chapter Four introduces closed-loop testing of numerical distance relays with a real time simulation model of a simple power system. A detailed model of the relays under study has also been developed, to run in parallel with the actual numerical distance relays under test. The deliberately simple power system model is used to verify the correctness of the relay model when operating in parallel with actual relays, when both are connected to series compensated transmission lines, before considering the performance on the real-time simulation model of the detail study system.

Chapter Five presents the real time simulator model of the detail heavily series capacitor compensated transmission network under study (the Western Cape transmission network).

Chapter Six presents comprehensive results of detailed real-time simulator testing of distance relays, using both physical relays and real-time models of the relay algorithms, to determine the performance of, and appropriate settings for these relays when used to protect a particular series capacitor compensated line within a heavily series capacitor compensated network.

Chapter Seven also presents comprehensive results of detailed real-time simulator testing of distance relays, using both physical relays and real-time models of the relay algorithms, to determine the performance of, and appropriate settings for these relays when used to protect an uncompensated line adjacent to heavily series capacitor compensated lines in the network.

Chapter Eight presents the conclusions of the research work as well as recommendations for further studies.

1.4 Thesis Contributions

This section highlights the main contributions of the thesis. They maybe summarized as follows:

The research work has made use of a real-time simulation model of Eskom's heavily series compensated Western Cape transmission network, including detailed dynamic models of the non-linear metal oxide varistor (MOV) characteristics, control logic of the series capacitor protection and bypass breakers at each relevant series compensated site.

A detailed real-time simulation model of the numerical distance relays themselves has been developed to allow greater insight into the reasons for the response of the real relays which cannot always be gained from fault records.

The detailed real-time simulation model of the power system and MOV-protected series capacitors is used to study the dynamic performance of distance protection schemes for the transmission lines in the network using the actual numerical distance relays currently being employed in South Africa, connected in a closed-loop testing arrangement.

The thesis has examined the performance of protection schemes in this series compensated network, under a wide range of practical fault scenarios. Using this approach, it will be possible to evaluate many more of the features of these modern numerical relays under realistic test scenarios in the future.

1.5 Research Publications

Some of the findings of this thesis have been presented at local research conferences [14],[15],[42].

CHAPTER 2

SERIES COMPENSATED LINE PROTECTION

2.1 Introduction

The previous chapter has presented the main objective of series capacitor compensation and a brief review of relaying technology development to the present day. Modern numerical relays provide the basis for series capacitor compensated transmission line protection, especially transmission lines compensated above 50% of the line reactance.

This chapter provides a brief review of transmission line protection from a general perspective. It begins with distance protection scheme performance indices. There are a variety of line protection principles and practices used to meet electrical utilities' requirements. These basic principles and practices include: overcurrent protection, distance protection, and pilot protection schemes.

This chapter further illustrates the benefits of series capacitor compensation of transmission lines. More emphasis is placed on power transfer capacity with angular and voltage stability. The series capacitor itself compensates the inductive reactance of the transmission line. Hence, series capacitor compensated transmission lines appear electrically shorter than uncompensated lines.

To an impedance relay a short-circuit fault behind a series capacitor appears to be electrically closer to the relay than it actually is, and can even appear to be located behind the relay. The action of the series capacitor's own protection modifies the degree of series compensation and, in turn, the transmission line parameters. The apparent impedance seen by the relay is therefore also modified.

Finally, this chapter examines common solutions proposed in the literature to the distance protection challenges presented by the introduction of series capacitor compensation in a transmission network.

2.2 Fundamentals of transmission line protection

2.2.1 Basic objectives of protection

Transmission systems are becoming more complex than ever before. From a simple system comprised of single source connected to a load to the present meshed networks. Hence, protection of transmission lines is becoming more and more complex. Electrical utilities adapted different protection schemes suitable to their particular network topology and system conditions.

The main purpose of a protection scheme is to detect the presence of a fault within the vicinity of the scheme as reliably and quickly as possible, and then to initiate isolation of a predefined protected zone selectively, to minimize greater blackouts and to maintain power system stability.

The performance indices of a protection scheme comprise: sensitivity; speed; selectivity; reliability; dependability; and security. The performance of directional integrity, phase selection for single-pole tripping and fault location are paramount in series capacitor compensated transmission lines.

2.2.1.1 Protection sensitivity

Protection scheme sensitivity is the ability of the scheme to detect system quantities that exceed threshold values and initiate successful protective action [5]. The smaller the percentage of the actuating quantity above threshold values, the higher the protection scheme sensitivity.

2.2.1.2 Protection speed

Protection scheme speed is referred to as the minimum operating time to clear a fault [16], in a time that will preserve power system stability. The speed is usually stated in terms of the number of cycles of the fundamental frequency required for the scheme to operate. This property is critical for power system stability and optimal power transfer in series capacitor compensated transmission lines.

2.2.1.3 Protection selectivity

Protection scheme selectivity is the ability of the scheme to isolate correctly that part of the system (protection zone) that is faulty. Protection zones are predefined to aid protection scheme selectivity. If the scheme loses this property, power system stability would be affected and result in greater blackouts.

2.2.1.4 Protection reliability

Protection scheme reliability is the capability of the scheme to operate correctly under predefined conditions. Reliability has two aspects, dependability and security [16],[17]. Dependability is the ability of the protection scheme to trip for internal short-circuit faults and security is related to the protection scheme's ability not to trip incorrectly for external short-circuit faults [18].

2.2.2 Over-current Protection

Over-current protection responds to the magnitude of fault current. When fault current exceeds a preset pickup level, a trip signal is issued after a coordination time delay. When the magnitude of a fault current greatly exceeds that of the load current, an instantaneous trip signal is typically issued. This is known as the high set or instantaneous setting value of the over-current relay. Over-current protection can be classified based on the operating characteristic, namely definite current, definite time, normal inverse, very inverse, and extreme inverse.

Over-current protection is used on radial transmission feeders to provide time-coordinated protection. However, modern transmission networks are not radial, but rather are meshed in nature. In such meshed topologies, simple over-current protection is difficult to apply where coordination, selectivity, speed, reliability, and stability are important.

In addition, over-current protection cannot discriminate load currents from fault currents, and it is therefore applicable only where the fault current exceeds the full load current [7]. In meshed-topology networks, infeed currents and coordination are problematic too when using over-current protection. Finally any changes in transmission line configuration, network topology, and network upgrading require over-current protection settings to be completely redesigned.

More sophisticated over-current protection schemes have been developed to mitigate the above mentioned problems and to accommodate series capacitor compensation of transmission lines. However, these schemes are unit protection schemes, and as such they do not provide backup protection on the adjacent lines, nor do they have backup protection for their own protected zone.

2.2.3 Step distance protection

Distance protection is so called because it is based on an electrical measure of distance along a transmission line to a fault. The distance along the transmission line is directly proportional to the series electrical impedance of the transmission line. Impedance is defined as the ratio of voltage to current. Therefore, distance protection measures distance to a fault by means of a measured voltage to measured current ratio computation.

Distance protection provides an excellent way of obtaining discrimination, selectivity, and speed of operation by allowing trip operation up to a certain range of distance. Unlike an over-current protection scheme, which does not have built-in backup protection, in a distance protection scheme backup is provided by arranging three sets of distance protection zones operating in tandem. Non-pilot application of distance relaying is called step distance protection [19]. The first zone is conventionally set to cover 80%, the second zone is set to cover 120%, and the third zone is set to cover 180% of the transmission line length.

The first zone uses high-speed tripping without intentional time delay, followed by the second and third zones with coordinated time delays. The first and second zones provide 20% margin of safety to avoid incorrect protection operation due to uncertainties in the line parameters, and the measurements obtained from the current and voltage transformers [7],[20]. These two zones provide primary protection, while the third zone provides backup protection. The distance protection zone settings and time coordination typically used in a distance protection scheme are illustrated in Figure 2.1, where AB is the protected line

and BC is an adjacent line. Lines AB and BC are assumed here to have equal length. Tripping time is represented in number of cycles of the fundamental system frequency.

The zones of protection are defined by a variety of tripping characteristics. The two commonly used characteristics are the Mho and Quadrilateral tripping characteristics. Figure 2.2 shows these two characteristics on an R-X impedance plane, showing the three zones of protection covered by the relay in each case. The quadrilateral characteristic provides higher resistive coverage.

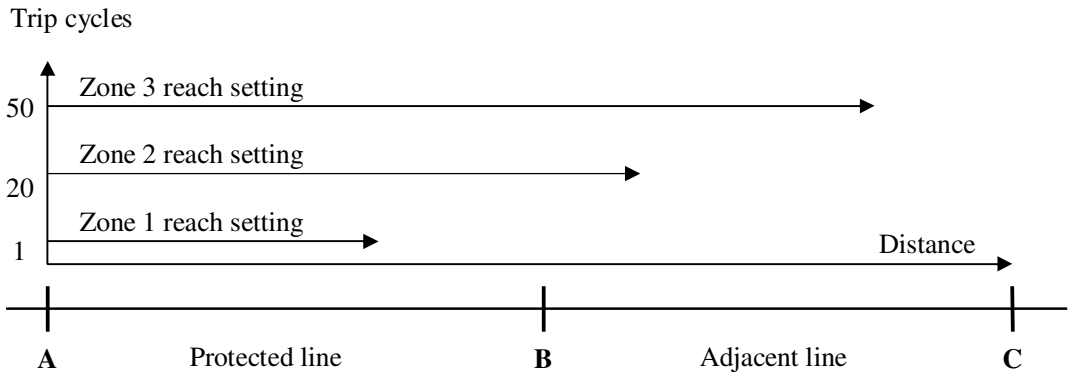

Figure 2.1: Typical coordinated distance protection settings.

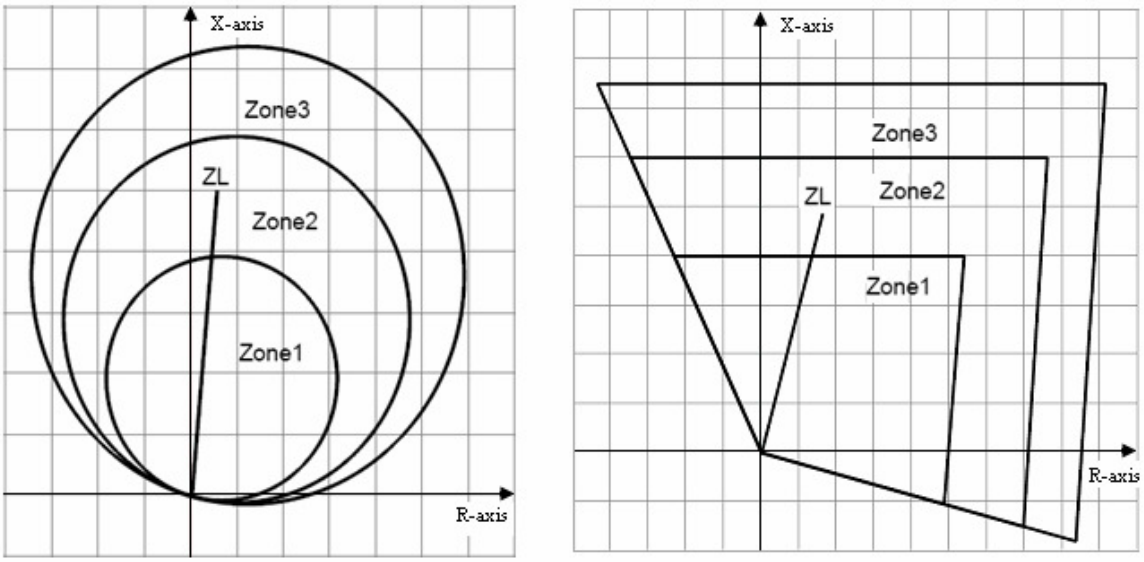

Figure 2.2: Mho and Quadrilateral tripping characteristics.

The time coordination and distance protection settings are easy to apply, and are less affected by changes in the system conditions than over-current protection schemes. Stand-alone distance protection provides satisfactory protection for many applications. However, it is not satisfactory on transmission lines where high-speed tripping of both line ends is critical to maintain power system stability. Pilot protection

schemes have been developed to meet the requirement of high-speed tripping of both ends of a faulty unit. However, distance protection performance is significantly affected by series capacitor compensation of transmission lines, since distance relays are designed to protect inductive transmission lines.

2.2.4 Pilot protection scheme

A protection scheme that utilizes pilots (communication channels) between two ends of the protected unit is referred to as pilot protection in the literature. The protection systems at both ends of the protected unit determine whether the protected zone is healthy or unhealthy. Then a decision is made to isolate unhealthy zones and keep healthy zones. This approach enhances fault clearing time and power system stability. Pilot protection is suitable for high-speed tripping, fault clearing selectivity, and power system reliability, particularly where system stability and protection security and dependability are important.

There are varieties of pilot protection classification in the literature. Pilot protection schemes are broadly classified into two categories: unit protection schemes and non-unit protection schemes [5],[26]. However, pilot protection schemes can also be classified by their principle of fault detection and/or the information contained in their communication channels. The classifications are shown diagrammatically in greater detail in Figure 2.3. These classifications will be adopted here as a convenient grouping of protection schemes, but non-unit protection schemes are classified and described in greater detail in this study by the manner in which the transferred signaling is used, and how such signaling is handled at the receiving end.

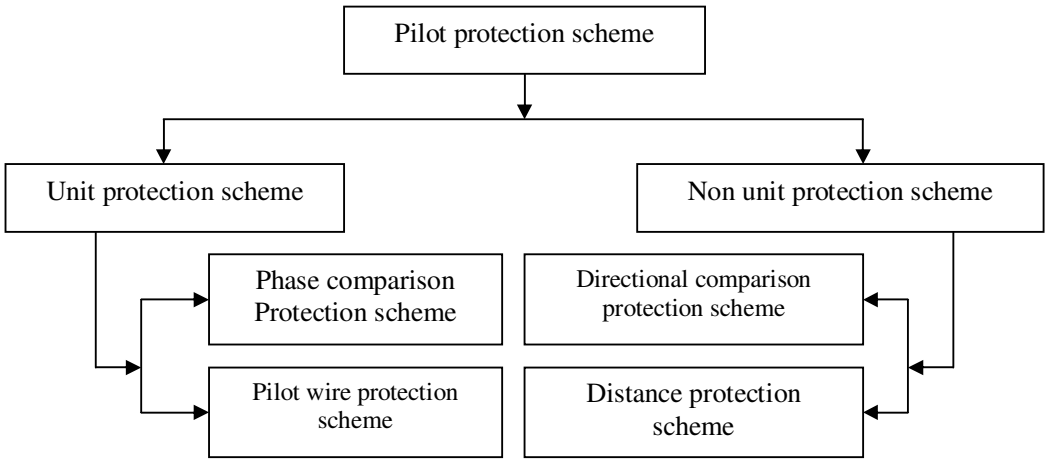

Figure 2.3: Classification of pilot protection schemes [5],[26].

2.2.4.1 Non-unit protection schemes

Non-unit protection schemes are all distance based protection schemes. The setting principle is the same as stepped distance protection, but with the inclusion of a communication system. These schemes take measurements of voltage and current at both ends of the protected zone, and process the measurements at each end to determine whether a fault is within a distance reach setting. This information is exchanged between the two protection systems at each end of the zone. The transferred information would be in the

form of transfer trip signaling, blocking trip signaling, and / or a combination of the two, and unblocking trip signaling. The particular type of signaling used defines the various protection schemes in common use namely, transfer trip schemes, blocking trip schemes, and unblocking trip schemes.

2.2.4.2 Blocking trip scheme

This scheme is fundamentally based on fault detection in the forward and reverse directions. Hence, it is also referred to as a directional comparison scheme based on the fault detection principle. When a fault is in the reverse direction, a blocking signal is sent to the remote end to prevent tripping. For internal faults, a blocking signal is not sent so that tripping is allowed. However, both ends have to wait for a period of time called the coordination time. This time delay is used to ensure that an external fault was not detected before initiating a trip. An under-reaching scheme is incorporated into the scheme logic to provide instantaneous tripping and an over-reaching scheme to provide backup protection. However, when the pilot (communication channel) fails, fast tripping occurs for external faults. This scheme is less secure in instances of pilot channel failure.

2.2.4.3 Unblocking trip scheme

An unblocking trip scheme is normally-blocked for tripping, and an unblocking signal is sent to the remote end for internal faults only. In the event of pilot failure, tripping is permitted (i.e. the communication channel is not required for tripping to occur). However, the pilot channel is monitored by a continuous guard signal, called the blocking signal. The guard-signal (blocking signal) increases the scheme security. This signal needs to be removed for internal faults. This scheme provides improved security over a blocking scheme, but additional circuits are necessary for the additional functionality. The fast clearing of internal faults depends on pilot channel communication delay.

2.2.4.4 Transfer trip scheme

Under the general heading of transfer trip schemes, there are specific sub-categories namely direct tripping schemes and permissive tripping schemes. These schemes could be set to operate in under reach mode (the under-reaching element, zone 1, sends the trip signal) or over reach mode (the over-reaching element, zone 2, sends the trip signal). These schemes are also known as directional comparison schemes.

Direct tripping schemes send a trip command to the remote end via the pilot channel. The remote end issues a trip signal locally without acknowledgement of receipt of the command. This approach can cause false trips due to pilot channel excitation by storms, mutual induction, or other means [5].

In a permissive under reaching scheme, an under reaching zone 1 normally sends a permissive trip signal to the remote end. The main purpose of the zone 1 setting is to provide instantaneous tripping upon detection of a fault within its reach. The drawback of this scheme is the restriction of zone 1 from covering the entire protected line.

The main advantage of permissive trip schemes over direct trip schemes is that spurious trips are not allowed. The permissive over reaching scheme is discussed in detail in the next section. The operation is similar to an under reaching scheme except that the over-reaching element (zone 2) is used to send the permissive trip signal.

2.2.4.5 Permissive over-reaching scheme

A permissive over-reaching distance protection scheme is a non-unit pilot protection scheme with directional features. Such schemes are a widely used form of protection for HV and EHV transmission lines that are easy to understand and apply, as they use basic distance protection principles. Figure 2.4 illustrates the application of the scheme to protect a transmission line between substations A and B.

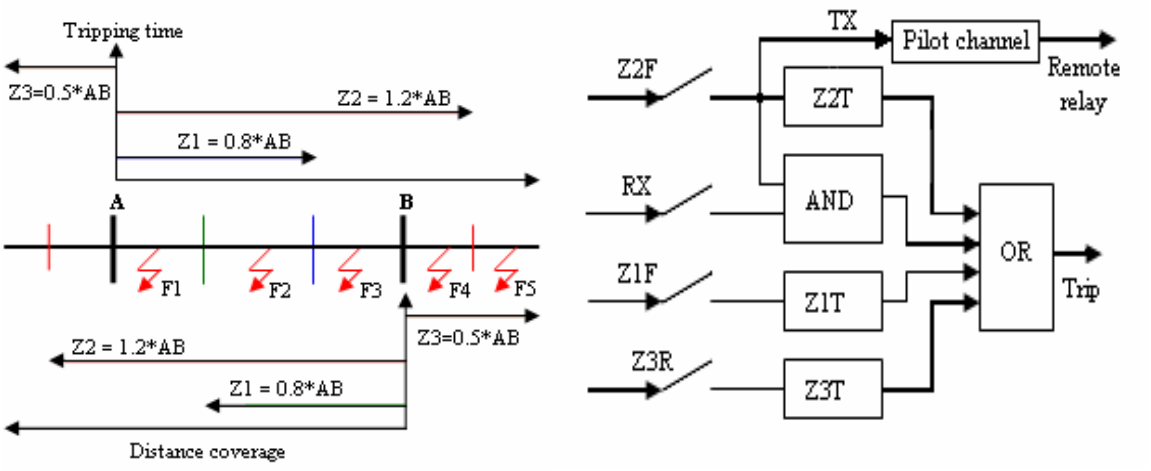

(a) (b)

Figure 2.4: (a) Permissive over-reaching distance protection scheme settings, (b) Trip logic.

Figure 2.4 (a) shows the protected transmission line AB and sections of adjacent lines on either side of AB. The line AB itself is protected by distance protection relays at A and B aided by permissive signals that are exchanged between the relays over a dedicated communication channel, as depicted in Figure 2.4 (b). The distance relays at both ends of the protected line are set to detect all internal faults, as well as external faults within close proximity of the protected line. At each substation A and B, the zone 1 and zone 2 elements of the relay are set to “look” into the protected line towards the relay at other end (i.e. in the forward direction), while the zone3 element is set to “look” outside the protected line (i.e. in the reverse direction).

The zone 2 elements are set to over-reach the protected line with sufficient margin of safety to detect all internal faults and to provide backup bus-bar protection. This approach ensures that the protected line is fully covered. These elements are normally set to cover 120% of the protected line with a settable time delay. The time delay is typically 400 ms for zone 2.

The zone 3 elements looking behind the relays are set to over-reach the zone 2 reach of relays at the remote end. These reverse looking zone 3 elements are needed for use in a number of enhanced logic options in distance protection schemes, namely: current reversal logic, weak in-feed logic, and echo keying logic [20]. These elements cover 50% of the adjacent line. The zone3 timer is typically set to 1 second.

The permissive over-reaching distance protection scheme utilizes a pilot communication channel to accelerate tripping on the protected line. When zone 2 elements detect a fault, they send permissive trip signals, TX to the relay at the remote end. The permissive trip signal TX from the sending relay is wired via the pilot communications channel to the permissive receive input RX of the remote-end relay. If a relay at either end sees a fault in its zone 2, and it receives a permissive trip signal from the remote end, the zone 2 timer is bypassed and the relay trips at high-speed. Practically, a permissive trip will occur in the zone 1 time plus the short time (≈ 10 ms) taken for the communication between the relays. With this arrangement, provided there is no communication failure, the protection scheme should be able to issue a high-speed trip signal for faults at any position along the protected line AB. Should the pilot communication link fail, high-speed clearance will not occur for faults that are not located in the zone 1 reach of the relay: without receipt of a permissive signal from the remote end, tripping will only occur in the zone 2 time of 400ms for faults outside of zone 1.

To illustrate further how the complete scheme operates, consider fault locations at each of the positions F1 to F5 shown in Figure 2.4 (a). For the fault at F1, the zone 1 element of the relay at substation A would issue an instantaneous trip, and the zone 2 element at A would send a permissive trip signal, TX to the remote-end relay at substation B. The relay at substation B would issue a trip only on receipt of the permissive trip signal, since the fault is in relay B's zone 2, but the breakers at both ends of the protected line open almost simultaneously. The fault at F3 would be cleared in a similar manner to the fault at F1, but with B sending the permissive signal. For the fault at F2, which lies within the intersection of both relays' zone 1 elements, trip signals are issued by both relays instantaneously, without intentional time delay, by the respective zone 1 elements.

Faults external to the line are expected to be cleared with high-speed by the primary protection of the adjacent lines. However, backup protection is provided by the over-reaching zone 2 elements of the remote-end relays and the zone3 elements at the local-end relays. For example, the relay at substation A would issue a trip signal after 400 ms if the fault at F4 is not cleared by primary and secondary protection of the line beyond substation B. The zone3 element at substation B would operate if the zone 2 element at the remote-end were to under-reach the fault at F4, and it would also operate for faults at F5 if and only if the fault persists for the zone3 time delay setting, of 1 s.

2.2.4.6 Unit protection schemes

In general, unit protection schemes are current based schemes. The zone of protection is considered as a unit. The magnitude and / or phase angle of the currents at both ends of the protected zone are compared to determine whether the unit is healthy or unhealthy. Unit protection is classified into two schemes: phase comparison schemes and pilot wire protection schemes (also known as current differential schemes).

2.2.4.7 Phase comparison scheme

A phase comparison scheme compares the phase angle between the currents at the two ends of a protected zone. If the two currents are in phase, the protected zone is healthy. If these two currents are out of phase by 180^{o}, the protected zone is unhealthy, and isolation of the faulted unit is initiated.

Phase comparison schemes provide protection only for internal faults in the protected zone. They do not provide backup protection on the adjacent zone(s), nor do they have backup protection for their own protected zone. In addition, since these systems operate only on line currents, they are not subject to tripping problems as a result of power swings or out-of-step conditions [22]. Likewise, series capacitors have no effect on the operation of current-only schemes [23]. Therefore, phase comparison schemes are an attractive alternative for series capacitor compensated transmission line protection.

2.2.4.8 Pilot wire protection scheme

These schemes employ a pilot wire and measure the currents at both ends of the protected zone for comparison in order to determine whether the protected zone is healthy or not. Unlike phase comparison schemes which use only the phase angle of the currents, pilot wire protection schemes use both phase angle and amplitude of the currents. These schemes are completely dependent on the pilot wire to operate, and as with phase comparison schemes, there is no backup protection. This scheme is also applicable in series capacitor compensated transmission line protection.

2.3 Series capacitor compensated transmission lines

2.3.1 Power transfer

Series compensated transmission lines utilize series capacitors to reduce the net series inductive reactance of the line in order to enhance the power transfer capability of the line. The power transfer along a transmission line is often explained in terms of the simple two-source power system shown in Figure 2.5 (a) without series capacitor (W/O SC) and Figure 2.5 (b) with series capacitor (W SC). The active power, P transferred by the uncompensated and compensated transmission lines are computed using equations (2.1) and (2.2) respectively, where $X_T = X_S + X_L + X_R$ is the total uncompensated reactance between the sending end voltage, E_S and receiving end voltage, E_R, δ is the transmission angle between the sending and receiving end voltages, and X_C is the series capacitor's compensation reactance.

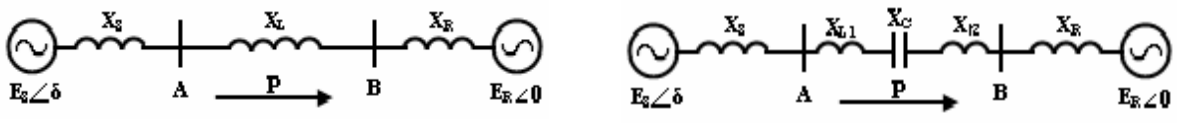

$$P = \frac{|E_S| * |E_R|}{X_T} * Sin(\delta) \qquad (2.1)$$

(a)

$$P = \frac{|E_S| * |E_R|}{X_T - X_C} * Sin(\delta) \qquad (2.2)$$

(b)

Figure 2.5: A two-source power system (a) without series capacitor, (b) with series capacitor.

The merits of series capacitor compensation can be illustrated by computing power transfer where transmission angle, δ is a variable and calculating load bus voltage, V_B where the load is a variable. This gives a graphical visualization in Figure 2.6. The maximum power transfer in the compensated line $P_{W\text{-}SC}$ is significantly higher than $P_{W/O\text{-}SC}$ in the uncompensated line.

To illustrate further the benefits of series capacitor compensation, consider a given power transfer, P_O shown in Figure 2.6. The power transfer, P_O in the compensated line is further away from steady state maximum power transfer capacity, which indicates increased angular and voltage stability margins for the same power transfer level. The uses of series capacitors also allows increased power transfer for the same transmission angle, δ_O and enhances the voltage profile of the line. Since, series capacitors compensate the inductive reactance of the line, reactive transmission line losses are significantly reduced.

In addition, series compensating capacitors allow power transfer at the same voltage level over longer transmission lines than uncompensated lines. This better utilizes the existing transmission network, which is cost effective and quicker rather than building new or additional parallel lines [26].

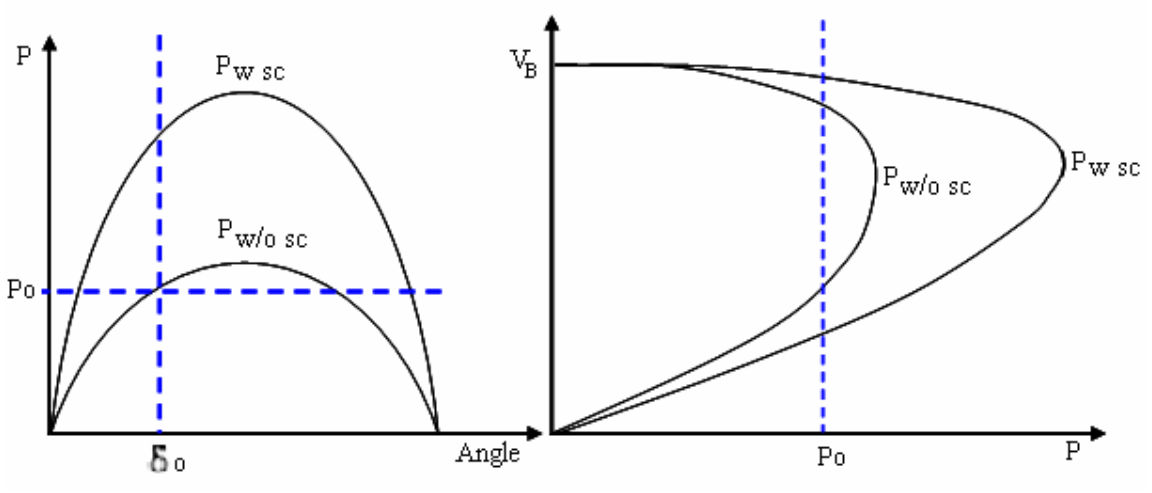

Figure 2.6: Power-angle curves and PV curves [24],[25].

Modern HV and EHV transmission lines are series compensated to improve power system performance; enhance power transfer capacity; enhance power flow control and voltage control; decrease transmission losses; environmental impact reduction; decreased capital investment [10]. Series compensation of transmission lines is widely used for very long transmission lines. However, the literature reveals that heavily-loaded, short transmission lines are also typically series compensated to gain the aforementioned benefits [26]. However, these benefits also bring with them significant transmission line protection challenges, particularly in heavily series compensated networks.

2.3.2 Series capacitor protection

The introduction of series capacitors presents a number of technical challenges when setting distance protection relays, because of the combined effects of the series capacitor's compensating reactance and the series capacitor's own protective equipment, on the measured impedance to a short-circuit fault. During a short-circuit fault, the fault current through the capacitor produces overvoltages across the terminals of the series capacitor. Therefore, protection is provided to limit voltage across the series capacitor.

In the mid 1970s a metal oxide varistor (MOV) was announced as a means of series capacitor protection, which superseded spark gaps previously used to protect series capacitors [12],[27]. The MOV is a non-linear resistive device, which starts to conduct at specific instantaneous voltage and ceases to conduct when the voltage falls below the same voltage at each half cycle of the power frequency. The result is that there is a non-linearly time-varying degree of series compensation during a fault, due to the non-linear impedance characteristics of the parallel MOV-series capacitor combination.

This non-linear voltage-current characteristic of the MOV allows it to provide overvoltage protection across the capacitor when connected in parallel with it. The MOV holds the voltage across the capacitor within the permissible range of the capacitor by allowing a self-regulating amount of current through itself automatically. This non-linear relationship between the voltage and current is shown in Figure 2.7 (a). The MOV protective voltage is the instantaneous voltage across the series capacitor at a specified current when the MOV starts conducting. The protective voltage is typically chosen above normal operating conditions, power system swing, and overloads as illustrated in Figure 2.7 (a) [12],[28],[29].

Figure 2.7 (b) shows the equipment used to protect the series capacitor bank against overvoltages. The MOV itself is protected against excessive absorption of energy by a bypass switch. As the MOV conducts current, energy accumulates within the MOV itself. The MOV has a maximum amount of energy that it can absorb before it breaks down. Hence, the MOV is bypassed at a preset energy level to avoid break down. The bypass breaker operates when the energy absorbed by the MOV is greater than the preset value. This bypasses both the MOV and series capacitors and re-inserts them when the energy falls below

the preset value. The impedance seen by the relay transits rapidly from compensated impedance to uncompensated impedance during severe short-circuit faults.

Goldsworthy [12] has introduced an equivalent series capacitive reactance and resistance of a MOV-protected series capacitor as a function of normalized line current based on the capacitor's protective level current. The equivalent model is depicted in Figure 2.7 (c).

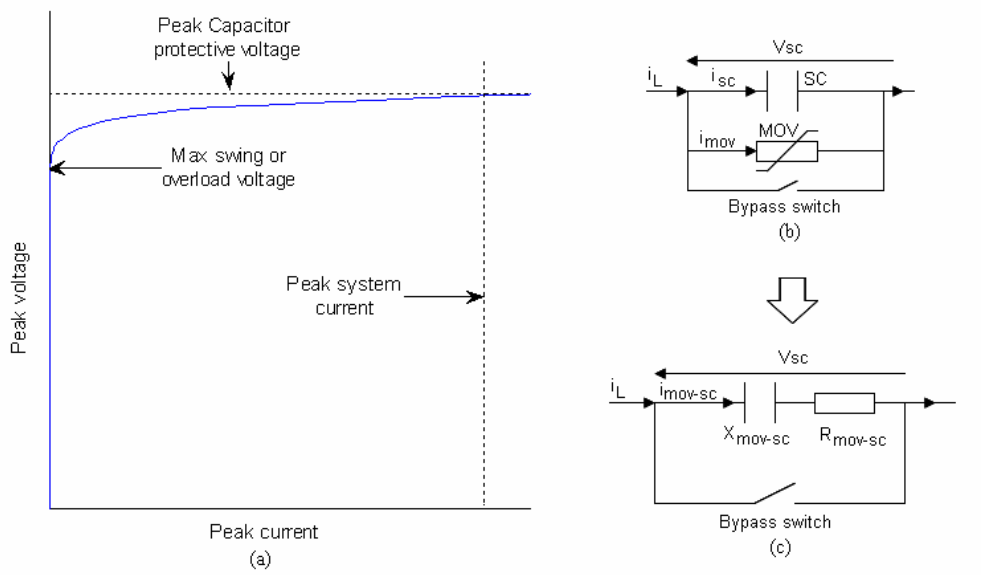

Figure 2.7: (a) MOV V-I characteristic; (b) MOV protected series capacitor; (c) Equivalent model.

The MOV-protected series capacitor equivalent model parameters under short-circuit currents can be determined by equations (2.3) and (2.4).

$$R_{MOVSC}=X_{SC}(0.0745 + 0.49e^{-0.243I\,pu} - 35.0e^{-5.0I\,pu} - 0.6e^{-1.4I\,pu}) \quad (2.3)$$

$$X_{MOVSC}=X_{SC}(0.1010 - 0.005749I_{pu} + 2.088e^{-0.8566I\,pu}) \quad (2.4)$$

Where I_{pu} is fault current expressed in per unit of capacitor protective level current.

The MOV-protected series capacitor's normalized equivalent model characteristic, based on the series capacitor's reactance, is illustrated in Figure 2.8 (a). The Goldsworthy model viewed in the complex impedance plane is depicted in Figure 2.8 (b). This shows the normalized impedance characteristic of the MOV-SC combination in the same R-X plane used to define the reach of the protective zones of the distance relays.

Figure 2.8 shows that the MOV-SC's impedance is composed of non-linear resistive and capacitive reactance components that are functions of normalized fault current through the MOV-SC. The impedance decreases with increasing fault current above one per-unit in a non-linear relationship.

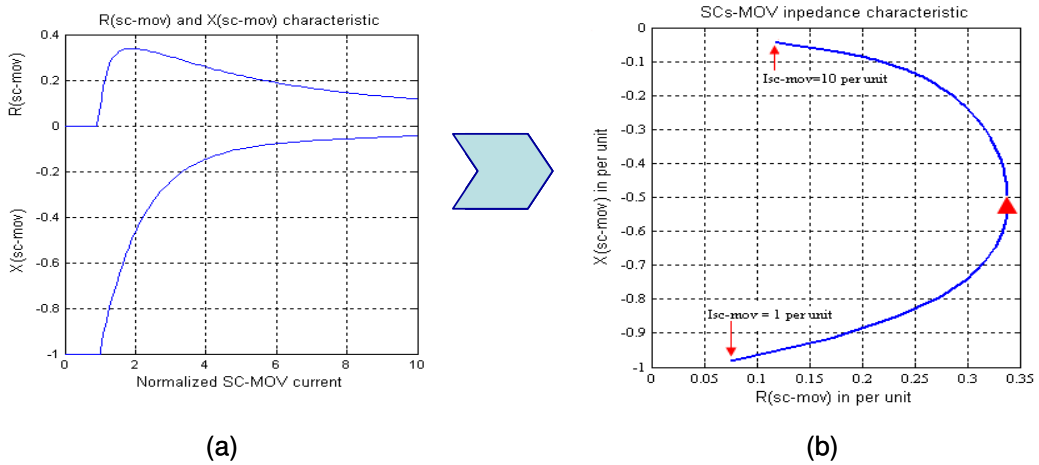

Figure 2.8: Normalized MOV-SC equivalent (a) resistance and reactance (b) impedance [14].

The benefits of MOV protection schemes include: instantaneous and automatic re-insertion and restoration of power transfer that can considerably increase power system transient stability; optimized capacitor design; increased reliability; predictability of performance; reduced maintenance [27],[28].

These benefits are associated with increased transmission line protection challenges. The complex, non-linear time-varying impedance behavior of series capacitors and their protection devices during a fault presents challenging problems to protection engineers in so far as to how to set the relays.

2.3.3 Protection challenges of series compensated network

A series compensating capacitor reduces the net fault impedance for all faults behind it; consequently such a fault appears closer to the relay depending on the amount of series compensation, fault current and the fault location. A comprehensive depiction of the effect of fault resistance and the MOV-series capacitor impedance characteristic on a distance relay is illustrated in Figure 2.9 on the R-X plane.

The fault resistance, R_F shifts the impedance seen by the relay to the right and lowers the fault impedance angle to δ'. The MOV and series capacitor combination also reduces the impedance seen by the relay and lowers the fault impedance angle further to δ''. This shifting of the fault impedance seen by the relay could affect the relay's performance.

The first challenge is the dynamic changes that occur in the total impedance presented by the series capacitor and its protection devices. The unknown state of the series capacitor, whether it is in service,

by-passed, or partly in service and partly by-passed, complicates the reach settings of zone 1 elements. If the capacitor is in service, over-reaching occurs and if the capacitor is by-passed, under-reaching occurs depending on the assumption made when setting zone elements. The fault position follows the curve CDE during MOV conduction.

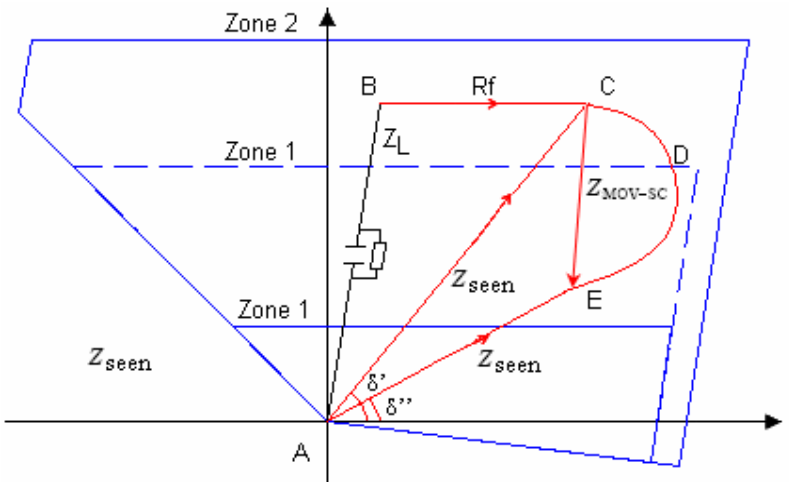

Figure 2.9: The effect of R_F and MOV and series capacitor on the impedance seen by the relay.

The second challenge is the effect of series capacitor location and degree of compensation. The series capacitor can practically be located at the middle of the line, or at the line terminals. It is apparent that for a high degree of compensation and a fault close to the series capacitor, the net reactance seen by a relay could be capacitive. Since the relays are designed for inductive reactance, the relay would see such a fault in the reverse direction.

The third and obvious challenge is that the impedance seen by the relay is smaller than would be the case in an uncompensated line, and is no longer a true measure of distance to a fault, so that the relay over-reaches the fault. These problems are compounded by the action of the devices used to protect the series capacitors themselves which dynamically alter the effective degree of series compensation during a fault [12]. Hence, restriction of the reactive and resistive reach of zone 1 is necessary (as illustrated by the dotted versus solid zone 1 polygons shown in Figure 2.9).

2.3.4 Voltage and current inversion

To demonstrate more challenges, consider a heavily compensated line with the series capacitors in the middle of the line, as in Figure 2.10 (a), for faults at various locations between substation B and the series capacitors. For the relay at substation A, this variable-location fault is always behind the capacitors. However for faults at the far end of the line (near B), the relay at substation A sees the impedance to the fault as inductive, and the system impedance to the fault (i.e. the impedance between E_S and F) are also inductive. The fault current at substation A then lags the system voltage E_S and the measured voltage at

substation A by 90° as shown in Figure 2.10: (b). Since the relays are designed for inductive systems, the potential problem is over-reaching due to compensated reactance.

If the fault is now moved from substation B towards the capacitors, a situation can occur where the total system impedance to the fault is inductive, but the impedance from substation A to the fault is net capacitive, so that the voltage measured at the relay point is capacitive (i.e. the fault current leads the measured voltage at relay A by 90°). This phenomenon is referred to as voltage inversion [28], and the relay at A would see the fault in the reverse direction; the voltage inversion is illustrated in Figure 2.10 (c).

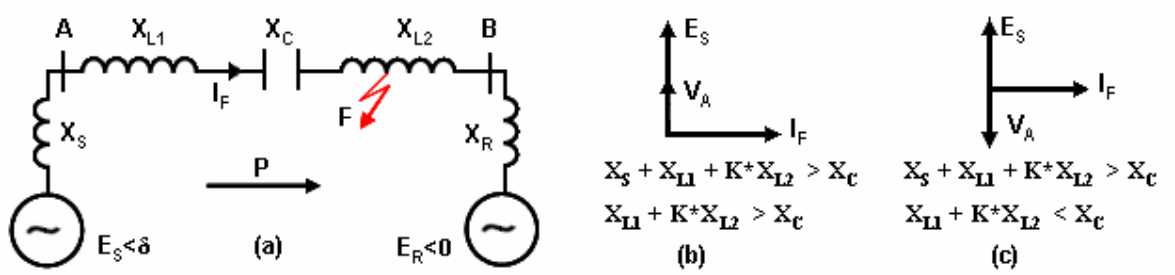

Figure 2.10: (a) Series capacitor in the middle; (b) Normal conditions; (c) Voltage inversion conditions.

A second phenomenon that can present a challenge is current inversion [28] which occurs when the overall system impedance to a fault is capacitive. Then the fault current would be capacitive, i.e. the fault current leads the system emf and the measured voltage at the relay by 90°. Again the fault current leads the measured voltage at the relay by 90°. Current inversion is likely to occur for series capacitors installed at the line terminals as shown in Figure 2.11 (a). The relay again would see a fault in the reverse direction. The current inversion phenomenon is illustrated in Figure 2.11: (c).

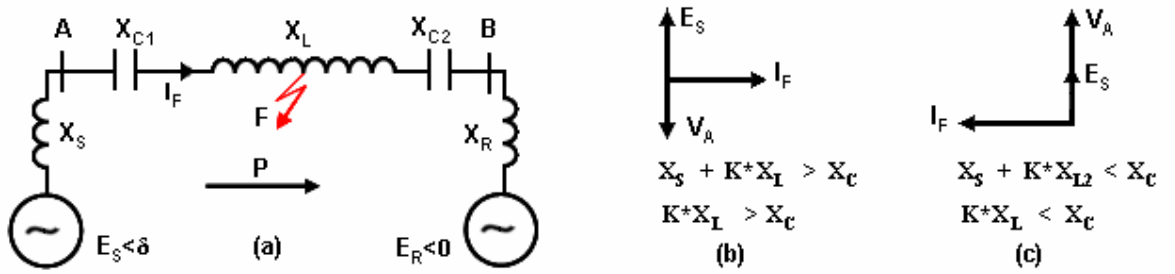

Figure 2.11: (a) Series capacitors at both ends; (b) Voltage inversion; (c) Current inversion conditions.

The fundamental challenge to the successful operation of distance relays in series compensated networks is that the electrical impedance measured by the relay is no longer always a true reflection of the physical distance from the relay to the fault [5]. This phenomenon is illustrated in Figure 2.12.

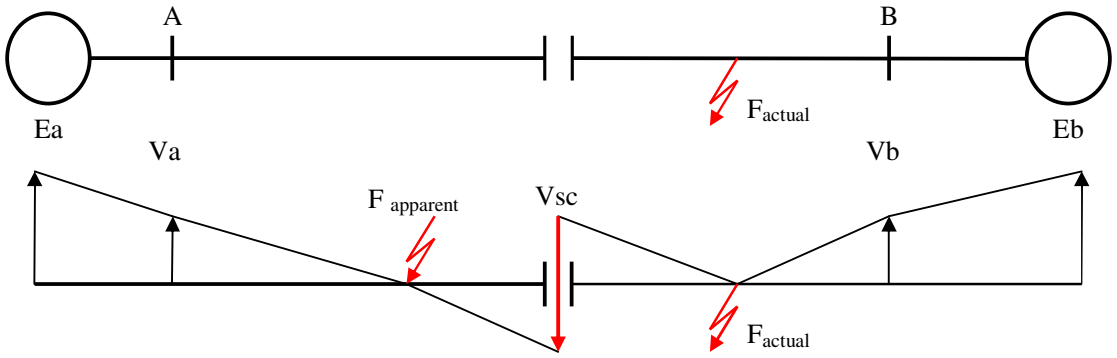

Figure 2.12: Voltage profile of series compensated line under short-circuit fault.

A fault behind the series capacitor appears in front of the relay at substation A due to voltage inversion at the series capacitor substation. If the relays were installed closer to series capacitor substation, they would experience voltage inversion and would underreach or overreach depending on the system configuration during a fault. To a relay seeing a fault through a series capacitor, the fault position appears electrically closer.

2.3.5 Common solutions to protection challenges in series compensated lines

The challenge to protection engineers is to provide secure, dependable, high-speed and selective protection schemes for series compensated transmission lines under low and high fault currents, resistive faults, and weak infeed conditions that are easy to adapt to different network topologies.

The challenges imposed by series capacitor compensation to transmission line protection are dealt with in a number of ways. Practically, the phenomenon of current inversion is unlikely to occur, since the MOV should not allow overvoltages across the series capacitor. The MOV would conduct and reduce the amount of series compensation as explained before. Hence the MOV maintains the overall system impedance to the fault inductive, and prevents the current inversion. The problem of voltage inversion has also been addressed by voltage memory and cross polarization for proper directional measurement [9].

The simplest, but far from satisfactory solution to the problem of lack of proportionality between the actual distance to the fault and the measured impedance is to set the first zone at about 30% of the line length [30] (ie to significantly reduce the reach of the zone 1 elements). In addition, series compensation generates subharmonics that can cause distance elements to overreach [11].

For the case of capacitors located at the line terminal substations, the relaying voltage is typically measured on the line-side of the capacitor instead of on the bus-side. This avoids loss of directional integrity and the overreaching problem for forward faults. This approach would be expected to be

appropriate, but according to Marttila [32], with the voltage measured on the line side of the capacitor there is no discrimination between forward and reverse faults.

Another approach is to estimate voltage drop or capacitor impedance using artificial neural networks to compensate for faults behind the capacitor. This requires an additional algorithm to determine whether a fault is in front of, or behind the capacitor. Such methods require either special hardware, or utilize novel approaches that are not sufficiently tested nor widely accepted by relay vendors and utilities [30].

A travelling wave protection algorithm has also been proposed [9]. This method is not affected by the presence of series capacitors [5],[33]. The drawback, however, is that it is not based on a continuous measuring algorithm, and thereby requires combined operation with an impedance measuring device [34].

2.4 Conclusion

This chapter has reviewed the fundamentals of transmission line protection, in particular performance indices of protection schemes, overcurrent protection, distance protection, and pilot protection schemes. Permissive overreaching distance protection schemes have been treated in some detail because this type of scheme is incorporated in the dynamic performance study of numerical distance protection relays under investigation.

The chapter further highlighted the benefits of series capacitor compensation of transmission lines and the accompanying protection challenges. More emphasis is placed on power transfer capacity with angular and voltage stability. The common solutions to these problems introduced by series capacitor compensation, and their drawbacks were also reviewed.

In conclusion, it is difficult to foresee the impact of dynamic behavior of the series capacitor compensated transmission network when setting distance protection schemes. This motivates the need to carry out detailed study, analysis, evaluation and testing of such protection schemes on a case by case basis, especially in the case of distance protection schemes in heavily series capacitor compensated transmission networks.

The next chapter describes the particular numerical distance protection relay designed for use in series compensated line that has been used in this study.

CHAPTER 3

NUMERICAL DISTANCE PROTECTION RELAY

3.1 Introduction

The previous chapters discussed the fundamentals of transmission line protection, series capacitor compensation, capacitor protection, transmission line protection challenges and how these challenges have been solved.

HV and EHV transmission lines are predominantly inductive in nature, with a small series resistive component. The measured fault currents at the relay locations are also inductive. That is, the measured fault current lags the measured fault voltage by the transmission line angle. Hence, standard distance protection relays were designed for inductive networks.

The introduction of series capacitors in transmission networks upsets the relationship between measured fault current and measured fault voltage. The distance relays designed to protect inductive transmission lines experience capacitive reactance under certain fault conditions, and hence fail to operate properly. This apparent capacitive reactance during a fault on part of the network complicates protection of compensated transmission lines and adjacent transmission lines in the neighborhood of series capacitors. The effect of series capacitors is also to generate transients during a fault which have adverse effects on protection performance.

This chapter describes a particular numerical distance protection relay designed for use in series capacitor compensated transmission lines. More emphasis is placed on application of a fast hybrid protection scheme within the relay, which combines a high-speed protection scheme in parallel with a modified standard distance protection scheme. The setting philosophies for compensated and uncompensated transmission lines within the vicinity of series capacitors are also discussed in detail.

The particular relay described in this chapter was chosen for study in this thesis, because it is the device used in all new protection schemes at transmission voltage levels by the national electricity utility in South Africa at the time of this thesis research project.

3.2 Hybrid protection philosophy of the REL531 relay

The REL531 relay is a high-speed numerical distance protection relay designed with series compensating capacitors in transmission lines in mind. This relay provides the basic protection requirements for series compensated transmission lines and adjacent transmission lines, which could be exposed to capacitive reactance during a fault. It has a high-speed protection function and a special directional function to cope with the capacitive reactance introduced by series compensating capacitors.

The numerical relay is a complex multifunction device consisting of standard and advanced protection functions, control functions, logical gates, recording and monitoring functional modules. The internal protection scheme in the REL531 relay is configured using a graphical programming language, the CAP531 configuration tool. The configuration is made according to the specific protection scheme's application requirements. All functional modules in the relay are represented by graphical function blocks in the CAP531 configuration tool. Each function has several setting parameters which have to be chosen carefully to make the protection relay behave as intended. Setting the parameters of the configured protection scheme is done via the CAP540 software and human machine interface of the relay.

The fast hybrid distance protection scheme philosophy implemented in the REL531 relay has been developed by ABB, Sweden [34]. This philosophy is used in heavily loaded transmission lines where fast fault clearance is critical in order to maintain power system stability. High-speed protection allows high power transfer in heavily series compensated transmission networks without compromising power system stability. A catastrophe in a heavily loaded transmission network is system-wide instability caused by short-circuit faults that are not cleared with sufficient speed. According to the designer of the relay, this hybrid scheme is reliable and provides high-speed protection to enhance power system stability and prevents cascading blackouts [35].

The fast hybrid distance protection scheme configuration consists of a standard distance protection function (ZM) and a high-speed distance protection function (HS) operating in parallel as represented diagrammatically in Figure 3.1. The scheme is aided with a communication scheme (ZCOM) and single-phase and three-phase trip logic. The phase selection logic (PHS) operates as a complement to the standard distance protection function for secure faulted phase identification; it is an independent phase selection function used for faulted phase selection purposes and secures tripping of the correct faulted phase on single-pole tripping applications. The high-speed function has its own built in high-speed phase selection logic.

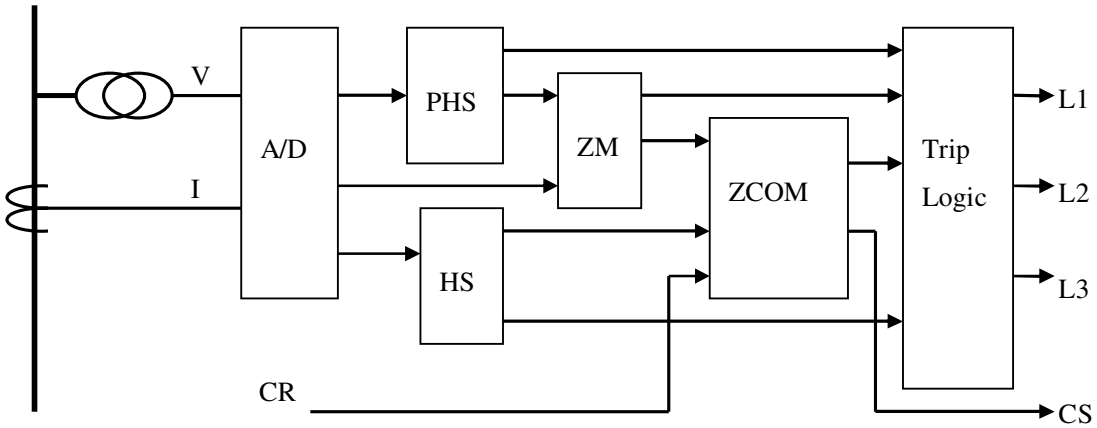

Figure 3.1: Fast hybrid distance protection scheme.

The standard distance protection function has an embedded special directional function to cope with voltage reversal on series compensated networks. The directional function needs to identify all forward and reverse faults that can cause voltage reversal at the local bus. In order to maintain directional integrity, a polarizing voltage is based on healthy phases and memory positive sequence voltage. The standard distance protection function has five zones of protection. The directional function and each of the five zones are set independently for phase-to-phase faults and phase-to-ground faults.

The principle behind the standard distance protection function is based on measured apparent impedance at the transmission line terminals. The apparent impedance is computed from fundamental power frequency components of measured instantaneous voltage and current signals. The apparent impedance is given by:

$$Z_{apparent} = \frac{V_{measured}}{I_{measured}} \tag{3.1}$$

A one cycle Fourier transform is typically used to extract the fundamental power frequency components from the voltage and current for impedance calculation in a distance relay. The speed of operation of this impedance calculation cannot be improved without affecting protection accuracy. Hence, combining the high-speed function with a standard protection function is considered necessary in the REL531 relay.

The high-speed distance protection is a full distance protection scheme with two zones of protection: a high-speed underreaching trip zone and a fast overreaching carrier send zone for permissive overreaching schemes. The high-speed permissive overreaching scheme is complementary to the standard distance protection permissive overreaching scheme, as the high-speed function picks up faults more rapidly and sends permissive signals earlier than the standard distance protection. The high-speed impedance measurement is performed during a time window of less than a cycle of the power frequency, whereas conventional measurement is carried out over one cycle of the fundamental power frequency. The high-speed function has been designed specifically with the requirements of protection of series compensated networks in mind, since the high-speed distance protection function is less influenced by series capacitors than the standard distance protection function due to the time window over which the measurement is performed [20].

The high-speed function operates on the basis of the superposition principle and makes decisions on the fault direction and fault position before voltage reversal develops [34]. Following a short-circuit fault, the apparent impedance measured at the relay deviates from the pre-fault impedance. This deviation or incremental impedance is superimposed on the steady state pre-fault impedance. The incremental impedance ΔZ can be determined as follows.

$$\Delta Z = \frac{\Delta V}{\Delta I} = \frac{V_{prefault} - V_{postfault}}{I_{prefault} - I_{postfault}} \tag{3.2}$$

A short-circuit fault causes a traveling wave to propagate at the speed of light (c = $300*10^8$ m/s) in a lossless transmission line towards the terminals of the protected line. The associated superimposed current and voltage waveforms also propagate at the speed of light from a fault position towards the relay measuring point [45]. These high-speed traveling waves form the basis of high-speed protection functions.

The high-speed protection function utilizes superimposed voltages and currents during a short interval of time after fault inception, which is faster than full-cycle Fourier transform methods. This principle is not a new concept; it has been used in high-speed protection of transmission lines [36]. However, it is not a continuously-measuring function, so, it is packed together with the continuous impedance measurement function (standard distance protection function in the REL531 relay) [4].

The main objective of combining the high-speed distance protection function and the modified standard distance protection function is to improve speed and reliability of series compensated transmission line protection. The outputs of the two protection functions are combined effectively to achieve accurate single-pole tripping, high-speed fault detection and signaling. Since the two protection functions make use of different operating principles and run in parallel, they back each other up in case the other one fails.

3.3 Quadrilateral polygon impedance setting philosophy

While series compensating capacitors enhance power system performance, when setting individual protection functions in the relay's hybrid protection scheme, the settings philosophy must take careful recognition of the presence of the series capacitors. Before understanding how the hybrid protection functions are set in series compensated networks, it is important to consider first how the protection settings are carried out in uncompensated transmission networks. This understanding will then be extended to the protection of compensated transmission lines and uncompensated transmission lines adjacent to compensated lines.

The standard distance protection scheme consists of five independent impedance measuring zones of protection, while the high-speed protection scheme has two zones of protection. Each zone of protection comprises three impedance measuring loops for phase-to-phase faults (L1-L2, L2-L3, and L3-L1) and phase-to-ground faults (L1-G, L2-G, and L3-G). The phase-to-phase impedance measuring loops also operate for multiphase faults, whilst the phase-to-ground impedance measuring loops operate only for single line-to-ground faults. The phase selection function provides faulted phase information in order to select the particular fault loop to be used to calculate impedance to a fault.

The setting parameters of each zone define the shape and size of the operating area of protection. The operating area of each zone is a quadrilateral polygon impedance characteristic as shown in Figure 3.2 and Figure 3.3.

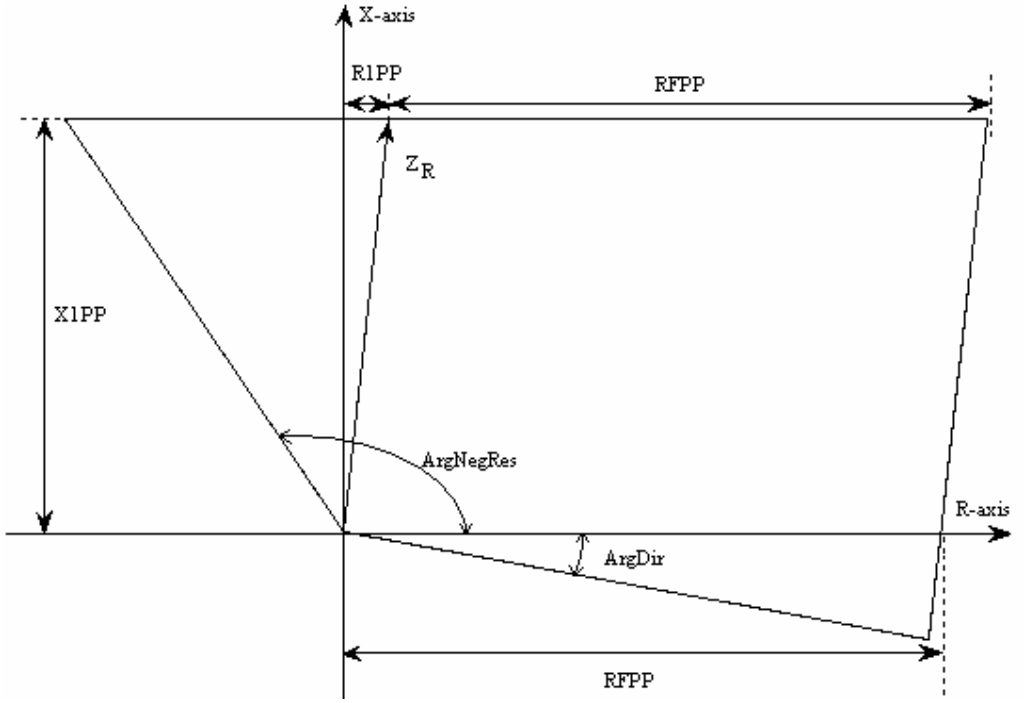

Figure 3.2: The operating characteristic of the phase-to-phase measuring loop.

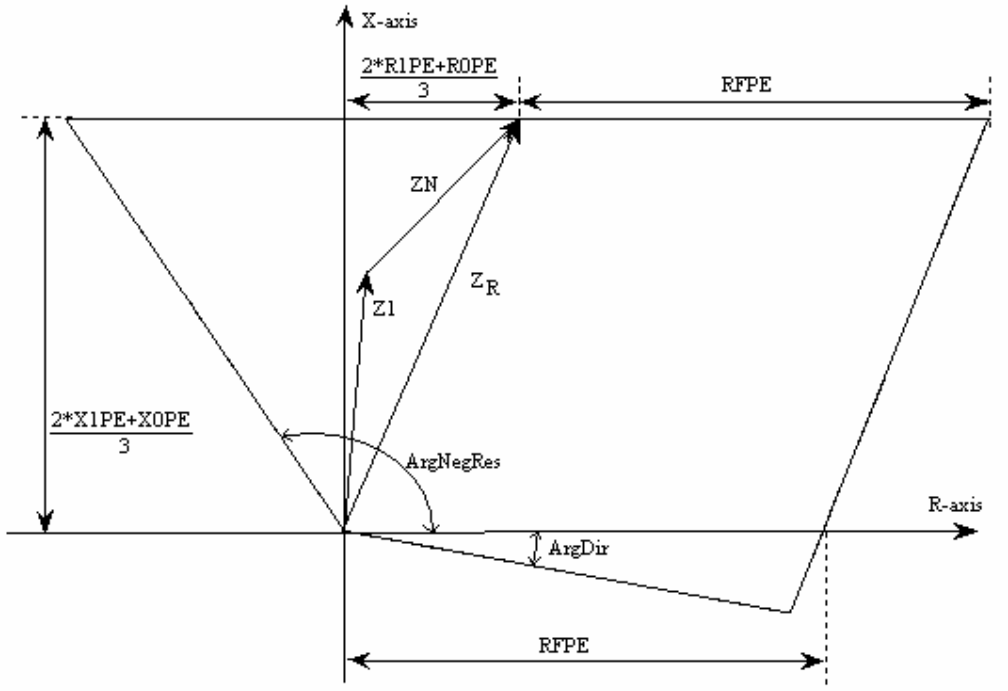

Figure 3.3: The operating characteristic of the phase-to-ground measuring loop.

These characteristics involve the combination of three measuring functions, namely the reactive boundary (top line), resistive boundary (right line), and directional boundary (left and bottom lines). The reactive boundary is parallel to the R-axis and the resistive boundary is parallel to the line impedance (Z_R). The second quadrant directional line is at an angle of 25^0 with the X-axis and the corresponding fourth quadrant directional line is at an angle of 15^0 with the R-axis. The operating zone is the area enclosed by these protection boundaries.

In order to apply the quadrilateral impedance characteristic within the REL531 relay for a particular zone of protection, the user must set the zone's operating time delay, the line reactance reach (X1PP), line resistance reach (R1PP), fault resistance coverage (RFPP), and the directional angles (ArgDir =15^0, and ArgNegRes = 115^0) for phase-to-phase protection zones. The setting visualization of the quadrilateral polygon impedance characteristic for phase-to-phase faults is illustrated in Figure 3.2.

In the case of single line to ground faults, the operating region of the quadrilateral polygon impedance characteristic is extended in the reactive and resistive directions to compensate for earth return impedance, ZN. This enables zero sequence compensation for single line to ground faults.

The user-settable parameters for ground faults include the operating time delay, line reactance reach (X1PE), line zero sequence reactance reach (X0PE), line resistive reach (R1PE), line zero sequence resistance reach (R0PE), fault resistance coverage (RFPE), and directional angles (ArgDir and ArgNegRes). The settings visualization of the quadrilateral polygon impedance characteristic for single line-to-ground faults is illustrated in Figure 3.3. The earth return impedance is calculated automatically by the relay using the following equations:

$$ZN = \frac{1}{3}(Z0 - Z1) \tag{3.3}$$

where

$$Z0 = R0PE + jX0PE \tag{3.4}$$

$$Z1 = R1PE + jX1PE \tag{3.5}$$

Most modern numerical distance relays provide this type of quadrilateral polygon impedance setting characteristic, because it is highly flexible in terms of fault impedance coverage for phase-to-phase faults and phase-to-ground faults. It is important to understand the relay's operating characteristics as well as its behaviour under realistic power system fault conditions in order to determine if the relay will operate as expected.

3.4 Protection settings for an uncompensated transmission network

Consider two power system networks interconnected by an uncompensated transmission line as shown in Figure 3.4. The two networks are represented by Thevenin equivalent circuits behind each end of the transmission line, i.e. busbar A and busbar B. The normal pre-fault load current flowing depends on the source voltages and equivalent impedance at each end of the protected transmission line, A-B. The transmission line is protected at each end with REL531 relays equipped with the fast hybrid protection scheme.

Generally, the electrical utility setting philosophy is developed in line with manufacturer's setting recommendations and IEEE standard C37.113-1999 [19]. The manufacturer's setting guide covers most aspects that need to be considered in distance protection settings, but is not specific to the performance requirements of the particular power system network under consideration. Hence each zone has to be set according to the specific scheme requirements, system conditions and transmission network topology of the particular application. In addition, adjustment is often necessary to optimize relay settings after detailed dynamic fault studies have been carried out.

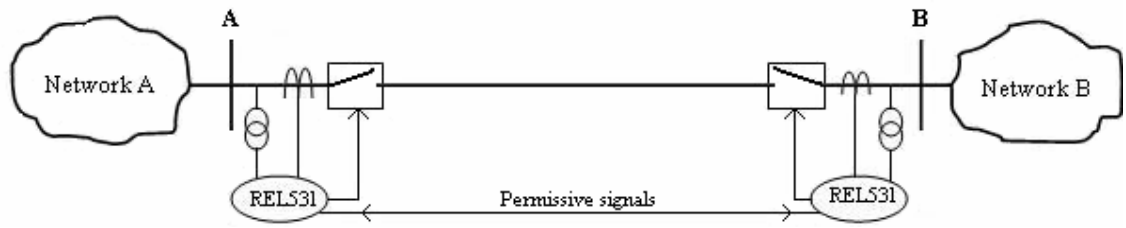

Figure 3.4: Uncompensated transmission network.

The relay reach settings must also be matched to the primary parameters of the network, as the relay is connected to the secondary side of the current and potential transformers (CTs and PTs). To convert primary impedances to secondary impedances for the adjustment of a distance relay, the following relation is used:

$$Z_{\text{sec}} = Z_{pri} * \frac{CTR}{VTR} \tag{3.6}$$

where CTR and VTR are the current and potential transformers turns ratios.

The setting of the complete fast hybrid distance protection scheme involves a comprehensive set of parameters, and hence only the zones of protection actually configured in this study are discussed. The fast hybrid distance protection scheme has independent settings for each of the standard distance protection functions and for each of the high-speed distance protection functions for phase-to-phase faults and phase-to-ground faults. The standard distance protection function is a complete protection scheme

with three measuring zones, having quadrilateral polygon impedance characteristics. Each zone of the distance protection has settings that are independent of those of other zones in terms of direction, operating time delay, and impedance coverage for phase-to-phase faults and phase-to-ground faults. For this application, the directional functions of zones 1 and 2 monitor forward faults while the directional function of zone 3 monitors reverse faults.

For an uncompensated transmission network such as Figure 3.4, the recommended impedance setting of zone 1 is 80% of the protected transmission line's positive sequence impedance. The zone 1 provides instantaneous tripping without intentional time delay. The 20% margin of security is provided to avoid overreaching due to parameter uncertainties of the transmission line, voltage and current transformer errors, and load transfer. The remaining 20% of the line is covered by zone 2 protection with a permissive overreaching scheme.

The recommended minimum impedance setting for zone 2 is 120% of the protected transmission line's positive sequence impedance. The main purpose of zone 2 protection is to cover the entire protected transmission line with sufficient margin of safety (of 20%) to avoid underreaching the protected transmission line. The zone 2 time delay setting ensures coordination with zone 1 protection on the protected line and the protection zones of adjacent transmission lines. The zone 2 protection on both ends of the protected transmission line provides accelerated tripping for internal faults through the permissive overreaching scheme.

It is recommended that the reverse looking zone3 protection is set to overreach the zone 2 protection of the remote end. The zone3 protection is needed for use in a number of enhanced logic options in the hybrid protection scheme such as communication logic, weak infeed logic and current reversal logic. It also provides backup busbar protection. The coordination of zone3 protection with the primary protection of the transmission lines must be taken into consideration.

The phase selection function is a complementary function to the standard distance protection function for secure faulted phase identification, since the standard distance protection algorithm is not sufficient to accurately identify faulted phases under certain system conditions. Secure faulted phase identification is necessary, because of the need for single-pole tripping to enhance power system stability in case of single phase-to-ground fault. During single phase-to-ground faults, the idea is to isolate the faulted phase. The proper setting of this function is critical for proper operation of the standard distance protection scheme. The setting parameters of the phase selection function are independent from each other for phase-to-phase faults and phase-to-ground faults. The phase-to-phase loops operate also for three-phase faults. It is recommended to cover the protected transmission line only with sufficient margin, so that the phase selection function always covers zone 2 protection with a safety margin of 10% to 15%.

The high-speed protection function is generally used in parallel with the standard distance protection functions when high-speed tripping is required to maintain power system stability during short-circuit faults. The function has two independent high-speed protection zones, an underreaching zone 1 and an overreaching zone 2, and high-speed phase selection logic. The high-speed distance protection function's settings must meet security and dependability requirements as for standard distance protection function settings. The maximum impedance setting of the high-speed zone 1 is 75% of the secondary positive impedance of the protected line while the high-speed zone 2 is generally set greater than 150% of the secondary positive impedance of the protected line.

The suggested setting equations for uncompensated lines are tabulated in Tables 3.1 and 3.2. The hybrid protection scheme settings values are determined using the results of these calculations.

Table 3.1: Standard distance protection zone settings [20].

Parameter	Zone 1 Forward Dir	Zone 2 Forward Dir	Zone 3 Reverse Dir	Phase selection
X1PP	$\leq 0.8 * X1$	$\geq 1.2 * X1$	$\leq 0.5 * X1$	$\geq 1.1 * X1PP_{Z2}$
R1PP	$= \frac{X1PP}{X1} * R1$	$= \frac{X1PP}{X1} * R1$	$= \frac{X1PP}{X1} * R1$	N/A
RFPP	$\leq 3 * X1PP$ $\leq 1.6 * Z_{Load\min}$	$\leq 3 * X1PP$ $\leq 1.6 * Z_{Load\min}$	$\leq 3 * X1PP$ $\leq 1.6 * Z_{Load\min}$	$\geq 1.1 * RFPP_{Z2}$ $\leq 1.35 * R_{L\min}$
X1PE	$\leq 0.8 * X1$	$\geq 1.2 * X1$	$\leq 0.5 * X1$	$\geq 1.1 * X1PE_{Z2}$
R1PE	$= \frac{X1PE}{X1} * R1$	$= \frac{X1PE}{X1} * R1$	$= \frac{X1PE}{X1} * R1$	N/A
X0PE	$= \frac{X1PE}{X1} * XO$	$= \frac{X1PE}{X1} * XO$	$= \frac{X1PE}{X1} * XO$	$\geq 1.1 * XOPE_{Z2}$
R0PE	$= \frac{X1PE}{X1} * RO$	$= \frac{X1PE}{X1} * RO$	$= \frac{X1PE}{X1} * RO$	N/A
RFPE	$\leq 0.83 * (2 * X1PE + X0PE)$ $\leq 0.8 * Z_{Load\min}$	$\leq 0.83 * (2 * X1PE + X0PE)$ $\leq 0.8 * Z_{Load\min}$	$\leq 0.83 * (2 * X1PE + X0PE)$ $\leq 0.8 * Z_{Load\min}$	$\geq \left(\frac{2 * R1PE_{Z2} + R0PE_{Z2}}{3} \right)$ $+ RFPE_{Z2}$

The Tables 3.1 and 3.2 highlight the relationship between reactive reach settings and the rest of the relay's setting parameters. The settings for line resistance (R1PP and R1PE), and line zero sequence resistance (R0PE) cover the same percentage of transmission line section as are covered by the reactive reach settings (X1PP and X1PE). The line zero sequence reactance reach (X0PE) covers the same line section as is covered by X1PE. The resistive coverage (RFPP and RFPE) must (together with the R1PP setting) include line resistance, expected fault resistance, and earth return compensation resistance for phase-to-ground faults. However, all resistive coverage settings for phase-to-ground faults and phase-to-phase faults are restricted by transmission line impedance loading. The earth return compensation

resistance for phase-to-ground faults includes the expected tower footing resistance; however, in cases where impedance measurement cannot detect ground faults due to excessively-high tower footing resistances, an optional earth fault overcurrent element can be used to overcome the problem [20].

Table 3.2: High-speed function protection zone settings [20].

Parameter	Zone 1	Zone 2
X1PP	$\leq 0.75 * X1$	$= \left(\frac{11.25}{X1_{pri}} + 1.5\right) * X1$
RFPP	$= RFPP_{Z1} + 0.75 * R1 * 2$	$= RFPP_{Z2} + \left(\frac{11.25}{X1_{pri}} + 1.5\right) * R1 * 2$
X1PE	$\leq 0.75 * X1$	$= \left(\frac{11.25}{X1_{pri}} + 1.5\right) * X0$
X0PE	$= \frac{X1PE}{X1} * X0$	$= \frac{X1PE}{X1} * X0$
RFPE	$= RFPE_{Z1} + 0.75 * \frac{2 * R1 + R0}{3}$	$= RFPE_{Z2} + \left(\frac{11.25}{X1_{pri}} + 1.5\right) * \frac{2 * R1 + R0}{3}$

The resistive coverage is set to avoid the minimum load impedance by a 20% margin of safety. The recommended settings are calculated using eqns. 3.7 and 3.8 as follows.

$$RFPE < 0.8 * Z_{loadmin} \tag{3.7}$$

$$RFPP < 1.6 * Z_{loadmin} \tag{3.8}$$

The minimum load impedance, $Z_{loadmin}$ in equations 3.7 and 3.8 is determined by:

$$Z_{load\,\min} = \frac{U_{\min}}{\sqrt{3} * I_{\max}} * \frac{CTR}{VTR} \tag{3.9}$$

where U_{min} is the minimum phase-to-phase voltage and I_{max} is the maximum load current. The primary current rating of the current transformer can be used as the maximum expected load current, I_{max} [3].

The resistive coverage is thus not determined by the total fault resistance, but by the reactance of the transmission line and minimum load impedance. In addition, resistive coverage is adjusted to prevailing system conditions to avoid underreaching short-circuit faults on the protected zone or overreaching short-circuit faults beyond the protected line.

The operating characteristic of the hybrid protection functions are presented in Figures 3.5 and 3.6. These operating characteristics for phase-to-ground faults and phase-to-phase faults are developed using the

setting guides in Tables 3.1 and 3.2 respectively. The phase selection function must cover all types of faults on the protected zone. Figure 3.5 shows the phase selection operating characteristics (PHS_FWD and PHS_RVD) covering all distance protection zones within the hybrid protection scheme. The phase selection function has different operating characteristics for phase-to-phase faults (PHS_FWD and PHS_RVD) and three-phase faults (PHS_3PH_FWD and PHS_3PH_RVD) and these are both presented together with the zones of protection in Figure 3.6. It is important to understand thoroughly the settings parameters and the operating characteristics in order to determine if the hybrid protection scheme would function as expected.

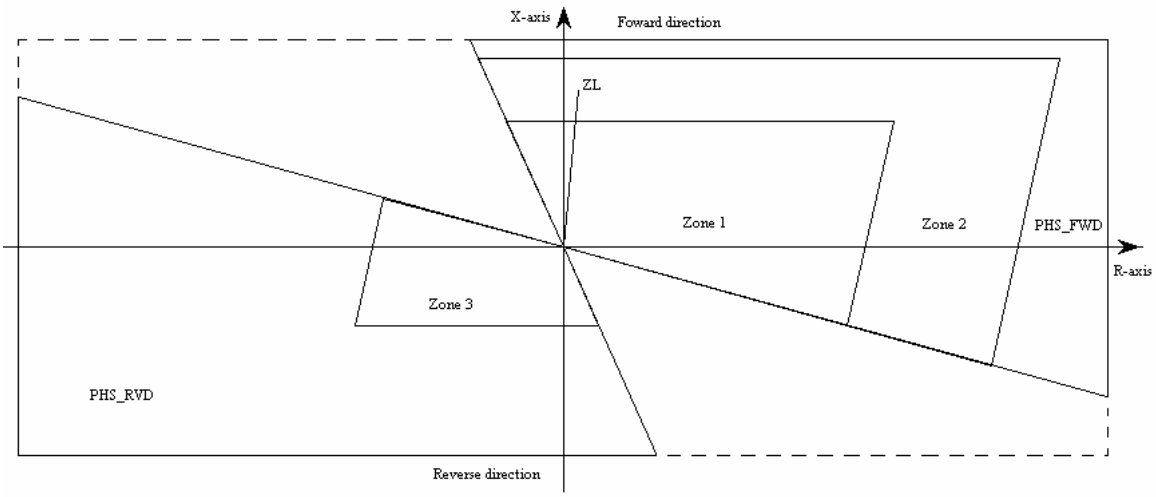

Figure 3.5: Settings visualization operating characteristic for phase-to-ground faults.

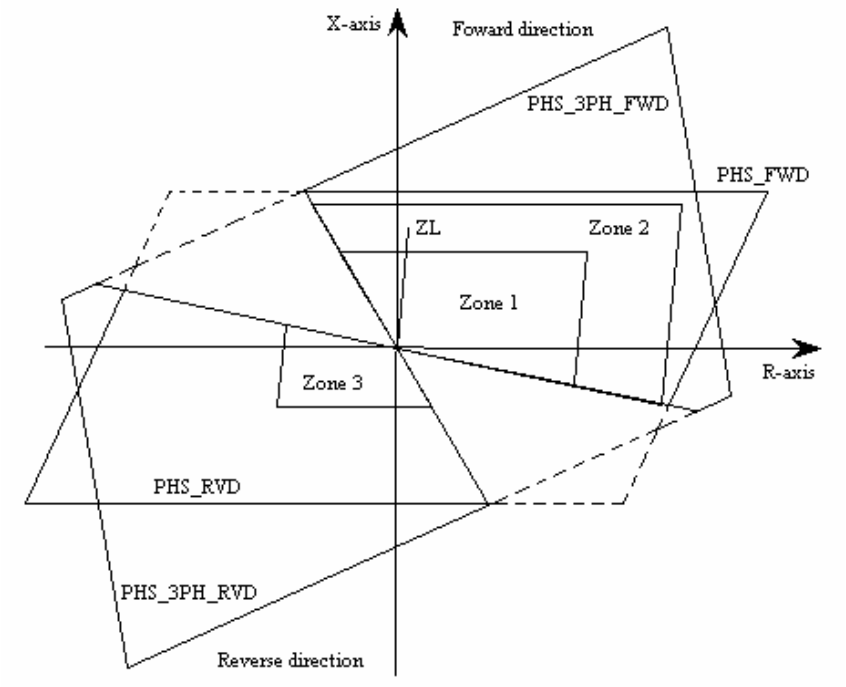

Figure 3.6: Settings visualization operating characteristic for phase-to-phase and three-phase faults.

3.5 Protection settings for series compensated transmission networks

The protection settings for a series capacitor compensated transmission line must meet the same basic protection requirements as those for an uncompensated transmission line. Series capacitor compensation affects the distance protection scheme on the compensated line itself and on adjacent lines. The effect of series capacitors on a transmission line protection scheme depends on the location of the capacitors, the degree of compensation and the capacitor protection scheme. Consider a simple power system network feeding a mid-line series capacitor compensated transmission line in Figure 3.7. The transmission line is protected by REL531 relays with the fast hybrid protection scheme. Thus, the effect of series capacitor compensation must be included in determining proper settings for the fast hybrid protection scheme. In practice, greater setting margins are employed to ensure a reliable application.

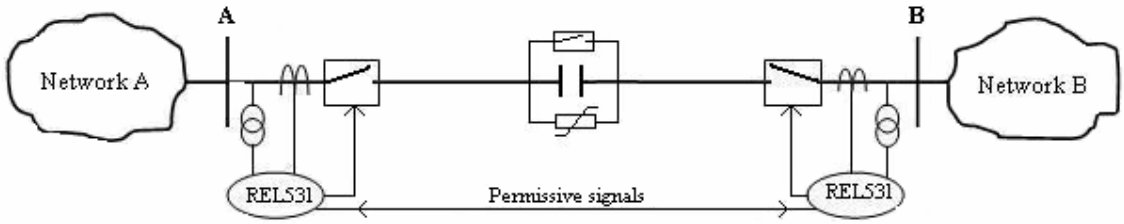

Figure 3.7: Compensated transmission network.

The standard instantaneous zone 1 distance protection elements applied on series capacitor compensated transmission networks are critical to the overall reliability of the hybrid protection scheme. The scheme must be both secure (not operate outside the designated zone 1 protection) yet dependable (operate as intended on the desired 80% zone 1 protection coverage), but these performance requirements are somewhat conflicting. Hence, security outweighs dependability on series compensated transmission network applications. Normally, the zone 1 setting is based on the compensated impedance of the transmission line, but the resulting coverage is too small, and hence it is considered unsatisfactory.

To illustrate the protection setting challenges on a series capacitor compensated network, consider the power system shown in Figure 3.7 with 60% compensation (i.e. the reactance of the series compensating capacitor is 60% of the transmission line's reactance). If the zone 1 protection is set to cover 80% of uncompensated impedance of the line, and when the series capacitor is in service (not bypassed), zone 1 covers 140% of the uncompensated impedance. The zone 1 protection will thus see and respond instantaneously to short-circuit faults beyond the protected line, which compromises the security of the hybrid protection scheme. Hence, zone 1 needs to be set with restricted coverage.

In practice, zone 1 is set to cover 80% of the compensated impedance of the line. For a 60% compensated transmission line, the actual zone 1 coverage is thus 32% when the series capacitor is out of service (bypassed). Further zone 1 reduction is required to avoid overreaching due to subharmonic oscillations

caused by series capacitors during short-circuit faults. The application manual of the REL531 relay provides a graph to determine the zone 1 percentage reach setting as shown in Figure 3.8; the curve in this graph is based on real time simulations and field experience [24].

The y-axis in Figure 3.8 represents the percentage reach setting, P for the underreaching zone 1 with respect to subharmonic oscillations. The degree of compensation, C on the x-axis of Figure 3.8 is not the percentage transmission line compensation; rather, it represents the ratio of the series capacitor's reactance to the total reactance from the source behind the relay to the fault at the end of the zone 1 reach. The analysis has indicated that zone 1 protection coverage is severely restricted due to the negative reactance of the series capacitor and further reduction is due to subharmonic oscillations.

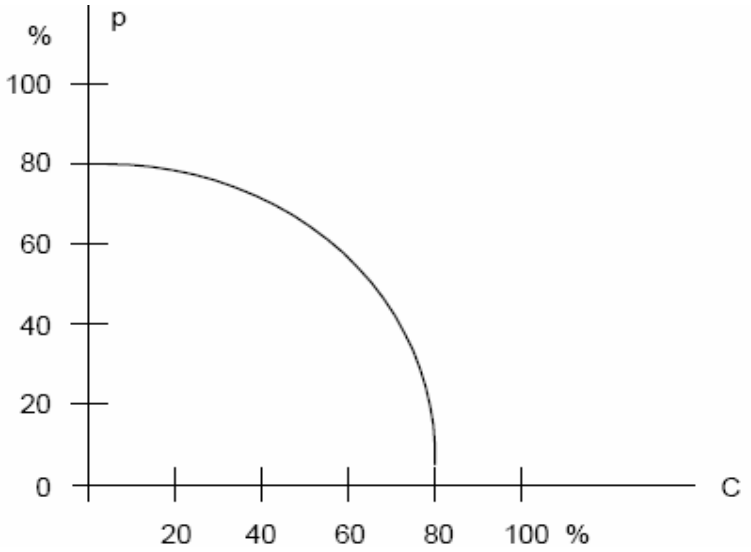

Figure 3.8: Reduced zone 1 reach due to subharmonic oscillations at different degrees of compensation [20]

In a heavily series capacitor compensated network, where zone 1 is restricted in reach, high-speed tripping will be achieved by means of the permissive overreaching scheme. It is important to ensure that the overreaching zone 2 protection (at both ends of the protected line) can detect all internal short-circuit faults and initiate a permissive trip signal with the series capacitor in service and out of service. Hence, zone 2 is set to cover 120% of the uncompensated impedance of the protected line. The actual coverage is then 180% (for 60% transmission line compensation) if the series capacitor is in service, since the capacitor's own protection is designed such that the series capacitors remain in service for external short-circuit faults. This significant overreaching for external faults can cause coordination problems with stepped distance protection on the adjacent transmission lines. For example, when a long series compensated line is adjacent to a much shorter line, even faults beyond the immediately-adjacent line could be seen by the overreaching zone 2 elements (in other words, the protection in one series-compensated line could overreach into lines beyond those directly connected to it). This excessive overreaching can be mitigated by increasing the stepped distance zone 2 time delay to secure selectivity.

The zone 2 protection must cover the protected line under all power system conditions. During heavy short-circuit currents, the bypass breaker operates and takes the series capacitor out of the fault loop. Hence, the overreaching zone 2 protection should be set excluding the series capacitive reactance.

The reverse looking zone3 protection must have sufficient reach to detect all types of short-circuit faults beyond the protected line that will also be detected by the remote overreaching zone 2 protection. The proper operation of communication logic, weak infeed logic and current reversal logic on a series capacitor compensated network is dependent on the proper coordination between zone3 protection and zone 2 protection at the remote end. In practice, the reverse looking zone3 is set to cover the remote zone 2 protection reach with a margin of safety.

The high-speed protection function meets the requirements for protection of a series capacitor compensated transmission line and of an uncompensated transmission line affected by series capacitors in adjacent lines. However, the high-speed function is less affected by series capacitors than a standard distance protection scheme. The underreaching zone 1 reactive reach setting for phase-to-phase faults and phase-to-ground faults is recommended to cover a maximum of 50% of the protected line.

The summaries of how to calculate individual setting parameters for the hybrid scheme are shown in Tables 3.3 and 3.4. Similar operating characteristics to those shown in section 3.4 are obtained when using the settings calculations from these tables.

Table 3.3: Standard distance protection zone settings for a compensated line [20].

Parameter	Zone One Forward Dir	Zone Two Forward Dir	Zone Three Reverse Dir	Phase selection
X1PP	$\leq 0.8*(X1-XC)$	$\geq 1.2*X1$	$\leq 1.2*X1PP_{Z2}-0.5*(X1-XC)$	$\geq 1.1*X1PP_{Z2}$
R1PP	$=\frac{X1PP}{X1}*R1$	$=\frac{X1PP}{X1}*R1$	$=\frac{X1PP}{X1}*R1$	N/A
RFPP	$\leq 3*X1PP$ $\leq 1.6*Z_{Load\min}$	$\leq 3*X1PP$ $\leq 1.6*Z_{Load\min}$	$\leq 3*X1PP$ $\leq 1.6*Z_{Load\min}$	$\geq 1.1*RFPP_{Z2}$ $\leq 1.35*R_{L\min}$
X1PE	$\leq 0.8*(X1-XC)$	$\geq 1.2*X1$	$\leq 1.2*X1PE_{Z2}-0.5*(X1-XC)$	$\geq 1.1*X1PE_{Z2}$
R1PE	$=\frac{X1PE}{X1}*R1$	$=\frac{X1PE}{X1}*R1$	$=\frac{X1PE}{X1}*R1$	N/A
X0PE	$=\frac{X1PE}{X1}*XO$	$=\frac{X1PE}{X1}*XO$	$=\frac{X1PE}{X1}*XO$	$\geq 1.1*XOPE_{Z2}$
R0PE	$=\frac{X1PE}{X1}*RO$	$=\frac{X1PE}{X1}*RO$	$=\frac{X1PE}{X1}*RO$	N/A
RFPE	$\leq 0.83*(2*X1PE+X0PE)$ $\leq 0.8*Z_{Load\min}$	$\leq 0.83*(2*X1PE+X0PE)$ $\leq 0.8*Z_{Load\min}$	$\leq 0.83*(2*X1PE+X0PE)$ $\leq 0.8*Z_{Load\min}$	$\geq\left(\frac{2*R1PE_{Z2}+R0PE_{Z2}}{3}\right)$ $+RFPE_{Z2}$

The fault loop resistance includes transmission line resistance, earth return resistance for phase-to-ground faults, fault resistance and resistance across the MOV protected series capacitor. According to Goldsworthy [12] the maximum apparent resistance of series capacitor and MOV combination is about 34% of the series capacitor reactance; this resistance appears twice in a phase-to-phase fault because two series capacitors are in the fault loop.

Table 3.4: High-speed function protection zone settings for a compensated line [20].

Parameter	Zone One	Zone Two
X1PP	$\leq 0.5 * X1$	$= \left(\frac{11.25}{X1_{pri}} + 1.5 \right) * X1$
RFPP	$= RFPP_{Z1} + 0.5 * R1 * 2$	$= RFPP_{Z2} + \left(\frac{11.25}{X1_{pri}} + 1.5 \right) * R1 * 2$
X1PE	$\leq 0.5 * X1$	$= \left(\frac{11.25}{X1_{pri}} + 1.5 \right) * X0$
X0PE	$= \frac{X1PE}{X1} * X0$	$= \frac{X1PE}{X1} * X0$
RFPE	$= RFPE_{Z1} + 0.5 * \frac{2 * R1 + R0}{3}$	$= RFPE_{Z2} + \left(\frac{11.25}{X1_{pri}} + 1.5 \right) * \frac{2 * R1 + R0}{3}$

Series compensating capacitors are normally employed on parallel and adjacent transmission lines. Hence the impact of series capacitors in adjacent and parallel lines must be considered, in terms of subharmonic oscillations and resulting negative reactance, on the protected line during short-circuit faults. The series capacitors in the adjacent lines are not considered if and only if there is assurance that there is sufficient infeed current for external faults so that the bypass breaker will operate on the internal series capacitors.

3.6 Conclusion

This chapter has presented the characteristics of a high-speed distance protection relay, the REL531 designed with series capacitor compensated transmission line protection in mind. Emphasis has been placed on the application of the fast hybrid protection scheme in the relay. The different operating characteristics for phase-to-phase faults and phase-to-ground faults have been explained in detail. This chapter also included a detailed description of setting philosophies for uncompensated and series capacitor compensated transmission lines.

The settings of a distance protection scheme in a heavily series compensated network remain a challenge. It is very difficult to calculate optimum distance protection settings by following relay setting manuals and standard practices in a large complicated network. Network-specific dynamic simulations, with the series capacitor protection modelled in detail, are practically necessary for fine tuning distance protection settings. Practical simulation of a simple power system, and closed loop testing of distance relays are introduced in the next chapter.

CHAPTER 4

REAL-TIME CLOSED-LOOP TESTING OF DISTANCE RELAYS

4.1 Introduction

Protection challenges in the application of distance protection schemes on series capacitor compensated transmission lines have been described theoretically in the previous chapters.

In this chapter, a real-time simulation model of a simple series capacitor compensated transmission line has been developed, including detailed dynamic models of the non-linear characteristics and control logic of the series capacitors' metal oxide varistors (MOVs) and bypass breakers. This model is used to study the performance of a distance protection scheme using the actual numerical relays that are used in the field, connected in a closed-loop configuration with the real-time power system model.

A detailed model of the relays under study has also been developed to run in parallel with the physical relays under test, in order to gain a better insight into the reasons for the response of the real relays, which cannot always be gained from relay fault records. Initially the system is tested for an uncompensated transmission line, and thereafter the tests include series compensating capacitors in the line.

The real-time closed-loop testing approach enables relay setting optimization and provides assurance of a more reliable protection scheme. The closed-loop testing of distance relays with a real-time digital simulator (RTDS) is done in real time so as to be able to re-create their operation under actual power system conditions.

4.2 Real-Time Closed-Loop Testing Configuration

The use of the RTDS simulator is a safe and realistic testing environment, since the dynamic performance of actual relays can not easily be verified and tested on an actual power system. The RTDS simulator performs power system simulations in real time. When conducting real-time closed-loop testing of distance relays, the simulator provides continuous real time outputs of breaker status, voltages and currents of the simulated power system to the external relays being tested. The relays directly control the breakers of the simulated power system. Since the power system is being simulated, all types of short-circuit faults experienced by the actual power system can easily be studied so as to evaluate the performance of the numerical distance protection relays under test. The RTDS simulator provides an outstanding benefit and advantage over traditional testing methods such as allowing the interaction of more than one protection relay with the real-time power system model to be studied.

Figure 4.1 illustrates real-time closed-loop testing of a permissive distance protection scheme using the REL531 high-speed distance protection relays. In order to conduct such closed loop testing with the RTDS, the user has to develop a real time simulation model of the power system to be studied, including any faults to be applied, circuit breakers, potential and current transformers for voltage and current measurements. The relays are fed with voltages and currents at the levels that actual relays in the field would experience. The simulated voltages and currents at the relay measurement point are sent out of RTDS simulator via a digital-to-analogue converter output card, and then on to the relay through an analogue amplifier. The breaker status is also sent to the relay through a digital output port and subsequent digital amplification. The relays then process these inputs and feedback breaker control signals into the RTDS simulator, via a digital input port, so as to operate their respective circuit breakers to isolate the faulty zone. The real-time closed-loop testing hardware setup is depicted diagrammatically in Figure 4.2. (Figure A1 of Appendix A shows hardware-in-loop testing of the REL531 relays using the RTDS)

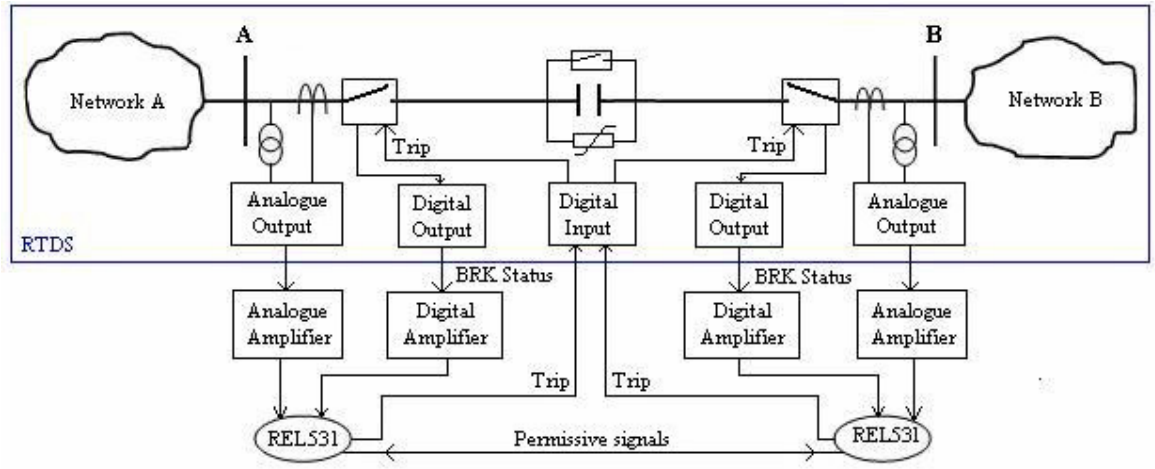

Figure 4.1: Real-time closed-loop testing of a permissive distance protection scheme using REL531 relays.

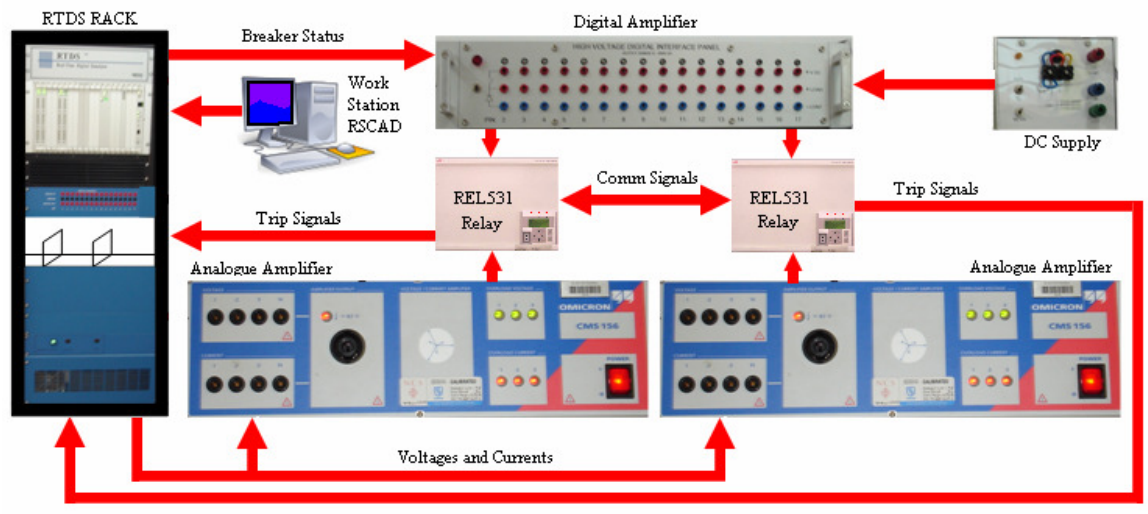

Figure 4.2: Diagrammatic representation of the real-time closed-loop testing hardware setup.

The hardware on the RTDS rack employs parallel operation of high-speed digital signal processors (DSPs), in order to carry out the solution of the power system simulation model in real time [37]. The simulator software installed on the workstation (PC) is called RSCAD and includes a graphical user interface (GUI), detailed power system components, and control library models. The technical details of the RTDS simulator can be found in the literature [37],[38],[39], and hence are not treated in detail here.

4.3 Real-time simulation model of the distance relay

A simulation model of the actual distance relay under test is helpful for settings optimization and understanding the relay's response under different operating conditions and different types of short-circuit faults. The relay model can be used to evaluate and gain further insight into the dynamic performance of the actual hardware relays during the real-time simulation and testing. The model is also capable of showing an impedance locus in the complex plane during a short-circuit fault, an insight which cannot always be gained from fault records of the actual relay under test.

The distance relay operates on the basis of measured impedance from the relay location to the fault point. The relay makes use of the voltage and the current values on the secondary side of potential and current transformers to compute impedance. The basic principle used to calculate impedance involves sampling of secondary voltages and currents, and extraction of voltage and current fundamental power frequency components. Then, phase-to-phase and phase-to-ground fault impedance calculation is accomplished. The actual relay's settings characteristics have also been included as part of the real-time model to show whether the measured impedance locus fell inside or outside the protected zones during a short-circuit fault. The impedance locus plot on an R-X plane can be used to determine optimal settings of the relays under test, especially in series compensated networks.

To evaluate the dynamic performance of distance relays under test, the relay must be modelled as accurately as possible or the real relays must be tested. However, there is not enough information available to model the specific relay in such detail. Therefore, a generic relay model has been developed to resemble the relay under test. It should also be noted that the actual REL531 relay hardware is always tested in the studies of this thesis in a detailed hardware in loop arrangement as previously explained. The real-time simulation model of the relay was developed to run in parallel with the actual relay hardware during these tests, for further insight and explanation, and not to make any predictions on the performance of the relay itself. For these reasons, a simple generic distance relay model was considered adequate. The following subsections describe the real-time simulation model developed for the REL531 distance relay, as part of this thesis using standard, pre-coded RSCAD real-time library components.

4.3.1 Sampling of voltages and currents

The voltage and current transformers step down high voltage and current levels to relay rated values of 110 V and 1 A respectively. In the REL531 relay, the secondary voltages and currents that are applied to the relay are sampled at the rate of 2 kHz, or 40 samples per cycle in a 50 Hz power system. These 40 samples are then down sampled to 20 samples per cycle with a moving average filter [4]. High-speed sampling provides high quality recording of the voltage and current waveforms during short-circuit faults.

Figure 4.3 shows the sampling stages in the real-time distance relay model. The relay model samples the secondary voltages and currents at 2 kHz, 40 samples per 50 Hz power frequency cycle. The 2 kHz sampled data is down sampled to 8 samples per cycle with a 5-sample moving average filter. Then the output data of the moving average filters is sampled and held at the rate of 8 samples per cycle, since the next stage needs data 8 times per cycle. Each of the 8 samples per cycle is the average of 5 consecutive samples calculated by the moving average filter. The purpose of the moving average filter is to match high-speed sampling with slower protection algorithms; it also suppresses random noise [40].

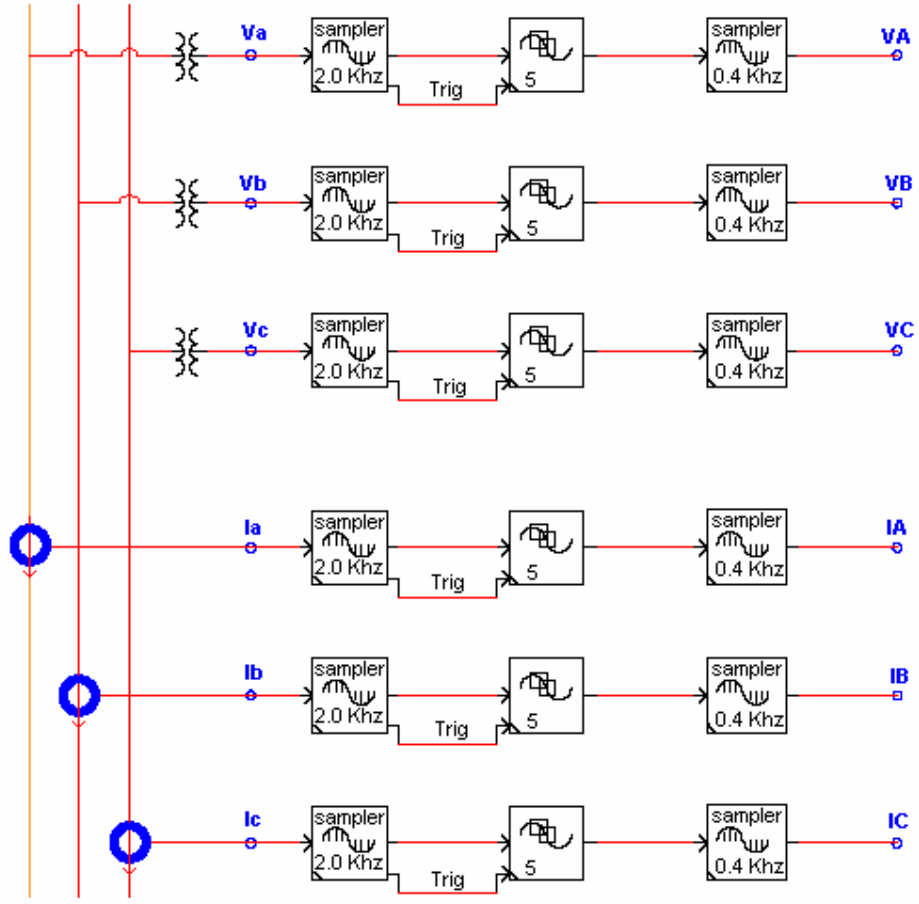

Figure 4.3: Sampling of voltages and currents in the real-time model of the relay.

4.3.2 Extraction of fundamental power frequency components

Figure 4.4 illustrates extraction of the fundamental power frequency components of the phase voltages and currents in the relay model. This stage processes data at 8 samples per cycle provided by the upstream sampling stage. A one cycle discrete Fourier transform (DFT) is used to convert instantaneous voltages and currents into fundamental power frequency phasors, as the Fourier transform principle is used in many numerical relays [41].

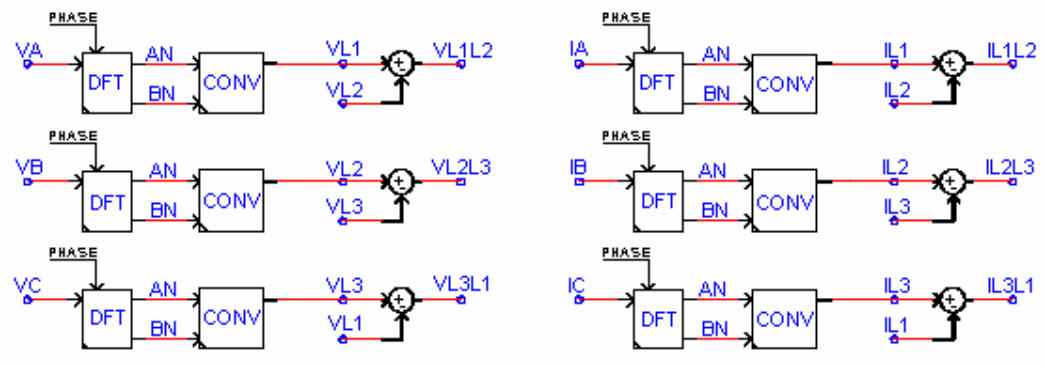

Figure 4.4: Extraction of fundamental frequency components of the voltage and current in the real-time model of the relay.

The outputs A_n and B_n of each DFT can be related to their input sampled voltage or current by the following relationship:

$$A_n^v = \frac{2}{N}\sum_{k=1}^{N} V(k)\cos(k\theta) \tag{4.1}$$

$$B_n^v = \frac{2}{N}\sum_{k=1}^{N} V(k)\sin(k\theta) \tag{4.2}$$

$$A_n^i = \frac{2}{N}\sum_{k=1}^{N} i(k)\cos(k\theta) \tag{4.3}$$

$$B_n^i = \frac{2}{N}\sum_{k=1}^{N} i(k)\sin(k\theta) \tag{4.4}$$

where N is the number of samples per cycle, and kθ is the instantaneous angle of the fundamental frequency reference phasor.

The DFT is capable of extracting the fundamental frequency components, while rejecting any multiples of the fundamental frequency. The one cycle discrete Fourier transform is based on the extraction of the

fundamental frequency phasor components that represent the fundamental frequency behaviour of the instantaneous input signal. The outputs of the DFTs are then converted to complex number format to enable complex mathematical operations on those phasors in the rest of the relay model. The outputs of this stage are complex phasor voltage and current representations of the 50 Hz fundamental frequency instantaneous input signals.

4.3.3 Phase-to-phase and phase-to-ground impedance calculation

A standard distance protection relay has six positive sequence impedance measurement fault loops, three for phase-to-phase faults and three for phase-to-ground faults. The complex phasor voltages and currents described in the previous section are used to calculate the impedances measured by the distance relay. These measured impedance loci can then be plotted on a complex R-X plane onto which one can overlay the reach characteristics (settings) of the distance relays.

The calculations used in the phase-to-phase positive sequence impedance measurement loops follow in eqns. 4.5 to 4.7.

$$Z_{L1L2} = \frac{V_{L1L2}}{I_{L1L2}} = \frac{V_{L1} - V_{L2}}{I_{L1} - I_{L2}} \tag{4.5}$$

$$Z_{L2L3} = \frac{V_{L2L3}}{I_{L2L3}} = \frac{V_{L2} - V_{L3}}{I_{L2} - I_{L3}} \tag{4.6}$$

$$Z_{L3L1} = \frac{V_{L3L1}}{I_{L3L1}} = \frac{V_{L3} - V_{L1}}{I_{L3} - I_{L1}} \tag{4.7}$$

The calculations used in the phase-to-ground positive sequence impedance measurement loops follow in eqns. 4.8 to 4.11.

$$Z_{L1G} = \frac{V_{L1}}{I_{L1} + k_n I_n} \tag{4.8}$$

$$Z_{L2G} = \frac{V_{L2}}{I_{L2} + k_n I_n} \tag{4.9}$$

$$Z_{L3G} = \frac{V_{L3}}{I_{L3} + k_n I_n} \tag{4.10}$$

$$I_n = I_{L1} + I_{L2} + I_{L3} = 3I_0 \tag{4.11}$$

$$k_n = \frac{1}{3}\frac{Z_0 - Z_1}{Z_1} \tag{4.12}$$

where I_n is current in the neutral conductor and k_n is earth return compensation factor.

The implementation of eqns. (4.5) to (4.7) and (4.8) to (4.10) in the real-time model of the distance relay is shown in Figures 4.5 and 4.6 respectively.

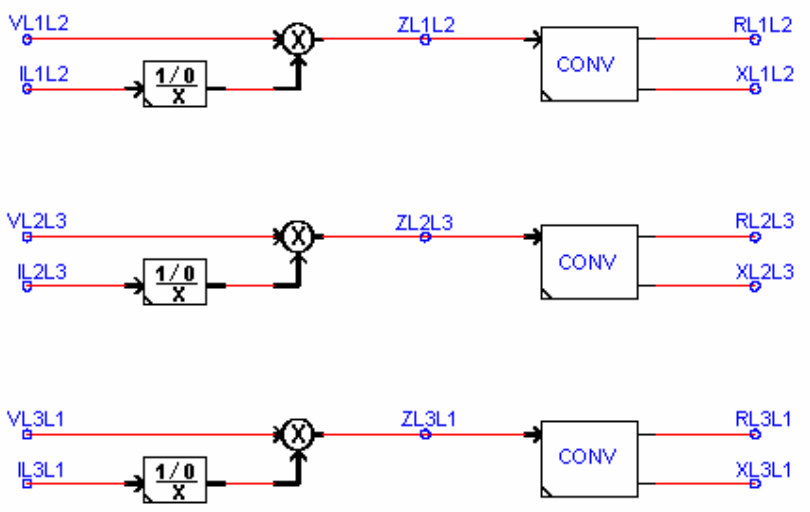

Figure 4.5: The phase-to-phase positive sequence impedance measurement loops in the real-time model of the relay.

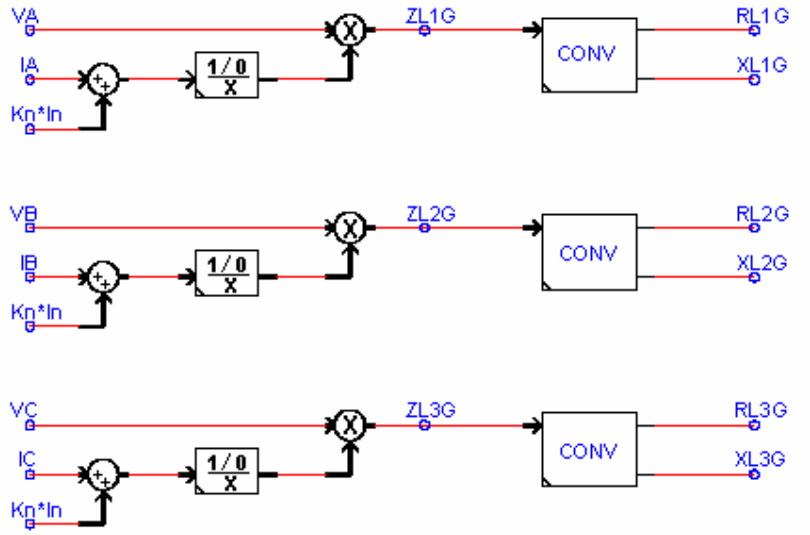

Figure 4.6: The phase-to-ground positive sequence impedance measurement loops in the real-time model of the relay.

The operating characteristic in the complex plane has also been developed as part of the real-time model and the impedance measured by the relay model plotted on the same plane. The impedance locus in the complex plane directly indicates whether a short-circuit fault is inside or outside the protected zone. Under normal operating conditions, the impedance locus remains outside the operating characteristic and the physical relay under test is not expected to operate. For internal faults, the measured impedance locus will fall within the operating characteristic and the physical relay is expected to issue a trip command. The locus of the measured impedance in the complex plane directly indicates the fault position on the faulted transmission line.

4.4 Uncompensated transmission line simulation studies

4.4.1 Power system simulated

Figure 4.7 depicts the power system model adopted for verification and validation of the real-time model and distance protection zone settings of the REL531 relay. The transmission line is represented using a distributed parameter, traveling-wave model and the generators with simple voltage sources behind the relays. The real-time power system simulation model has made use of actual power system parameters tabulated in Table 4.1. The REL531 relays are connected in closed-loop configuration with the real-time model of the power system and operate the circuit breakers at their respective ends of the real-time model.

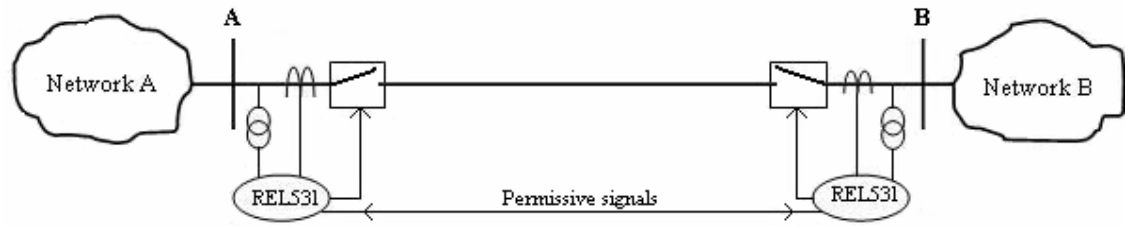

Figure 4.7: Power system model for the verification of the real-time relay model of the uncompensated line.

Table 4.1: Test system parameters (uncompensated line).

Parameter		Value	Units
Transmission line	Length	249.07	km
	Positive sequence reactance (XL)	0.2784	Ω/km
	Positive sequence resistance (RL)	0.04693	Ω/km
	Zero sequence reactance (X0)	1.10113	Ω/km
	Zero sequence resistance (R0)	0.40767	Ω/km
Source	Positive sequence impedance (Z1)	0.5 + j5	Ω
	Zero sequence impedance (Z0)	0.3 + j50	Ω
System voltage	Voltage	400	k V
Voltage transformer	Primary voltage	400	kV
	Secondary voltage	110	V
Current transformer	Primary current	2.4	kA
	Secondary current	1	A

The performance of the real-time model of the relay is first verified and validated against that of the actual REL531 relay in the simplest possible test system in which the transmission line does not have series compensating capacitors installed. Thereafter, the performance of the real-time model is verified for a series compensated line.

4.4.2 Real-time relay model validation

A set of simulation studies was carried out for various fault locations and a range of short-circuit faults were applied on the protected line to show the validity of the relay model. The relay model can be verified by comparing the measured reactance and resistance with the transmission line reactance and resistance from the relay location to the fault position. Figure 4.8 shows the voltages and currents sampled by the model to calculate resistance and reactance for a single-phase-to-ground fault at the end of the protected line. The current waveform of the faulted line is displaced by an exponentially decaying dc offset component.

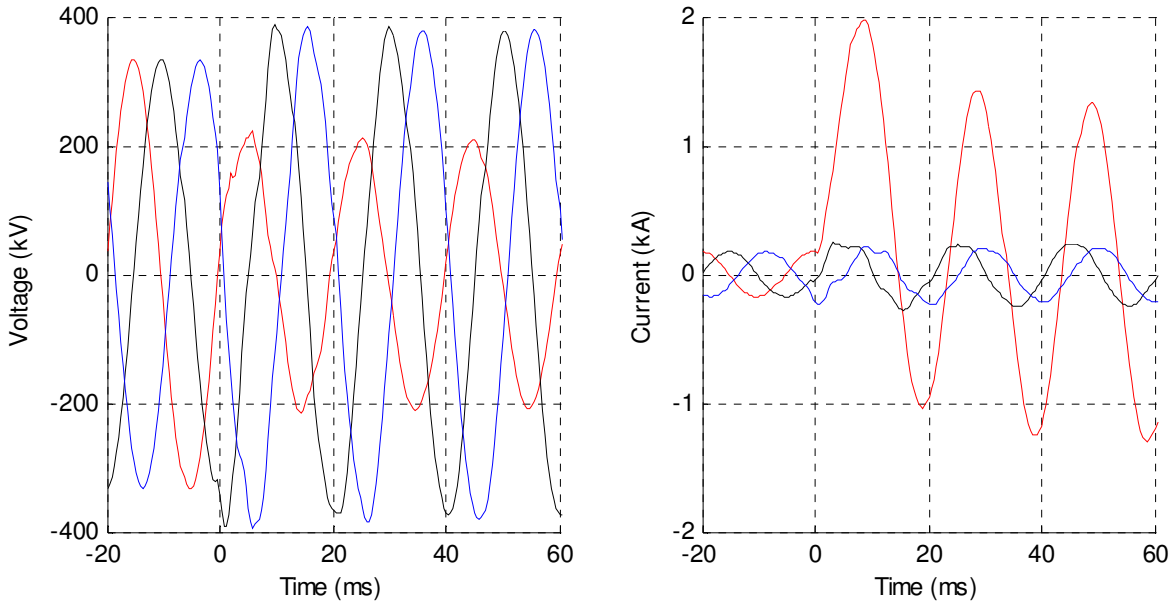

Figure 4.8: The voltages and currents at the relay model location for a single phase-to-ground fault at the end of the transmission line.

The most significant results for model validation are presented in Figures. 4.9 and 4.10 for the phase-to-ground fault loop for various fault locations (0% to 100% of the line length in steps of 10%) on the protected line. The measured impedance transits from the prefault state to the fault state. The transition period is equal to a full cycle of the DFT data window. The initial data used by the DFT at the moment of fault inception is purely prefault data. After 20 ms, the DFT data window contains the first full cycle of fault data and the impedance seen by the relay is close to the actual transmission line impedance to the point of the fault.

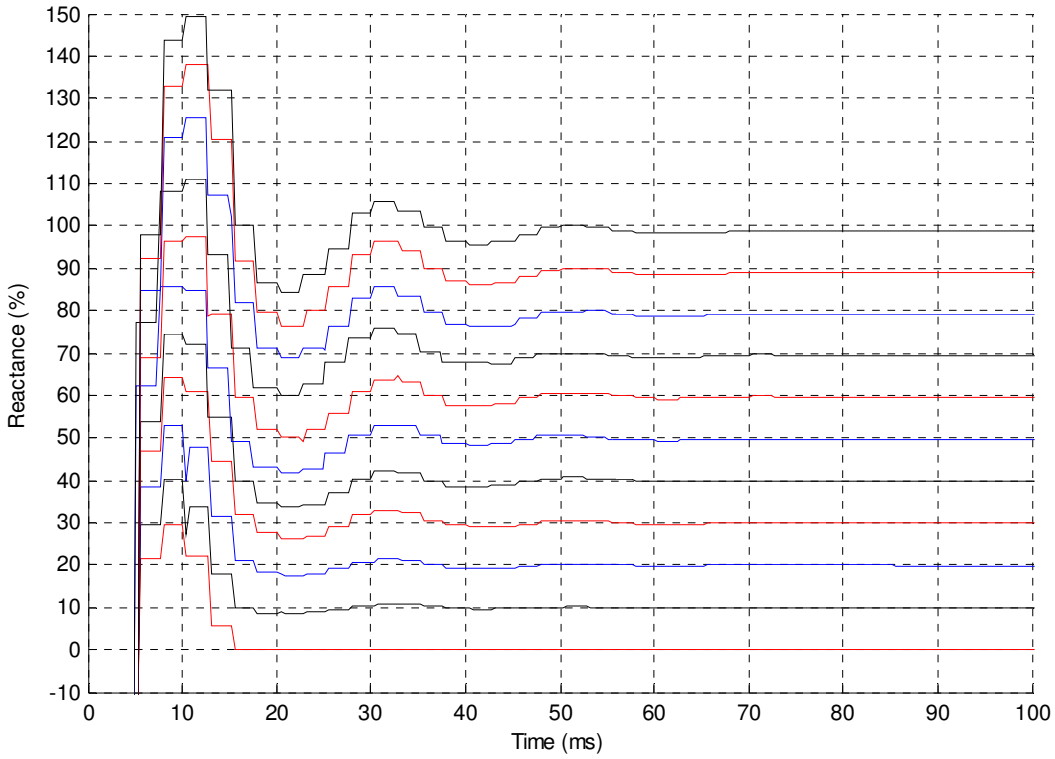

Figure 4.9: Measured reactance for phase-to-ground fault loop in the real-time model of the relay at various locations of the fault along the line length.

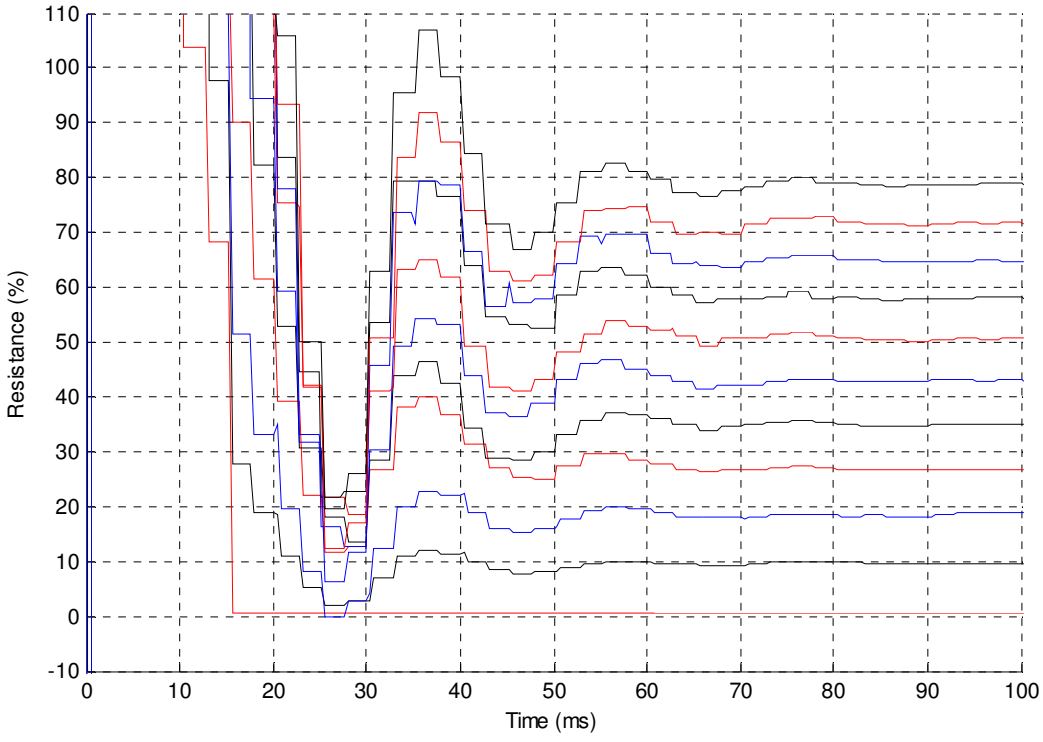

Figure 4.10: Measured resistance for phase-to-ground fault loop in the real-time model of the relay at various locations of the fault along the line length.

The calculated impedance is influenced by the high frequency component obvious in the measured input voltage and the exponentially decaying dc component in the measured input current. The effect is seen as decaying oscillations in the reactance and resistance that settle, in time, to the required levels. Another way of viewing the measured reactance and resistance response is to plot the impedance seen by the distance relays during the faults on a complex R-X plane as presented in Figure 4.11. The measured impedance is also corrupted with high frequency and exponentially decaying dc components. The effect is seen as the decaying spiral in the impedance locus around the final fault location. The impedance locus seen by the relay is clearly visualized and the fault location can also be estimated from the plot. The relay model can also be verified by comparing the impedance location on the complex R-X plane with the fault location calculation of the physical relay under test.

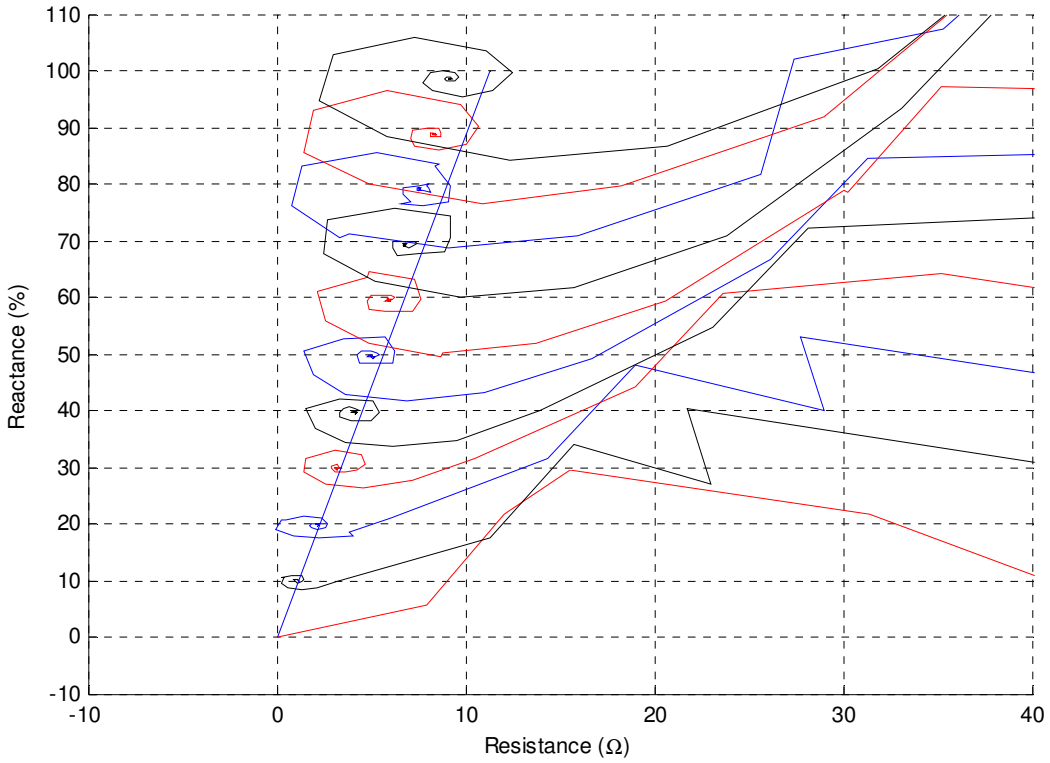

Figure 4.11: Phase-to-ground impedance measurement loop in the real-time model of the relay at various locations of the fault along the line length.

The measured impedance deviation from the transmission line (fault position) is noticeable for fault locations greater than 80 km (20%) due to the long transmission line effect. In long transmission lines, the shunt capacitance between lines, and from each line to ground, is significant as well as charging current. The series impedance is no longer linear, instead it is hyperbolic in nature and the zero sequence compensation factor has different values along the transmission line [44]. The effect of distributed parameters of a long transmission line is best explained by reference to equivalent JI model of long transmission line as shown in Figure 4.12. Considering the equivalent model, the series impedance, Z and

the shunt admittance, Y are corrected by the factors sinh (γl)/(γl) and tanh (γl/2)/(γl/2) respectively. This causes uncertainty in the setting of zero sequence compensation factor.

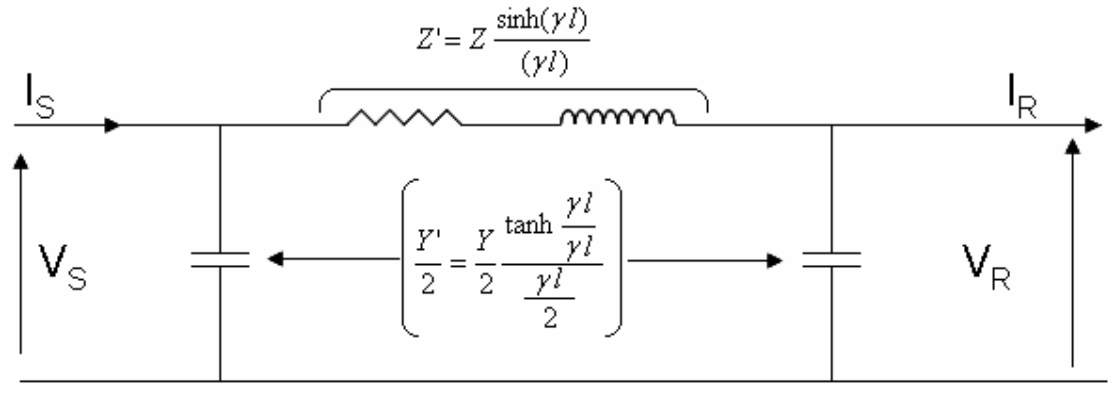

Figure 4.12: A long transmission line equivalent ЛI model [46].

Where:

Z series impedance
Y shunt admittance
γ propagation constant
l transmission line length

The analysis of long transmission lines and the results in Figure 4.11 show that the effect of distributed shunt capacitance in long transmission lines must be considered when setting distance protection relays.

The relay operating characteristic can also be shown on the same plot to check whether the fault is inside or outside the protected zone. In this study there was no attempt to remove high frequency and dc components from the measured voltage and current respectively. A low-pass filter and a Mimic high pass filter are used in distance protection relays to remove high frequency components and exponentially decaying dc component respectively. The setting visualization on the same complex plane (R-X plane) with the impedance locus would allow protection setting optimization.

4.4.3 The REL531 distance relay settings

The settings for the REL531 relay can be determined based on the transmission line parameters using the CAP540 software as shown in Figure 4.13. The setting calculations are shown in Table 4.2. The zone 1 and zone 2 reaches are set to cover 80% and 120% of the line respectively in the forward direction, and zone3 covers zone 2 of the remote end with 20% margin of safety in the reverse direction. The directional angles were set appropriately to discriminate between forward and reverse faults. The phase selection function was also set accordingly to cover all protection zones with sufficient margin of safety as illustrated in the previous chapter.

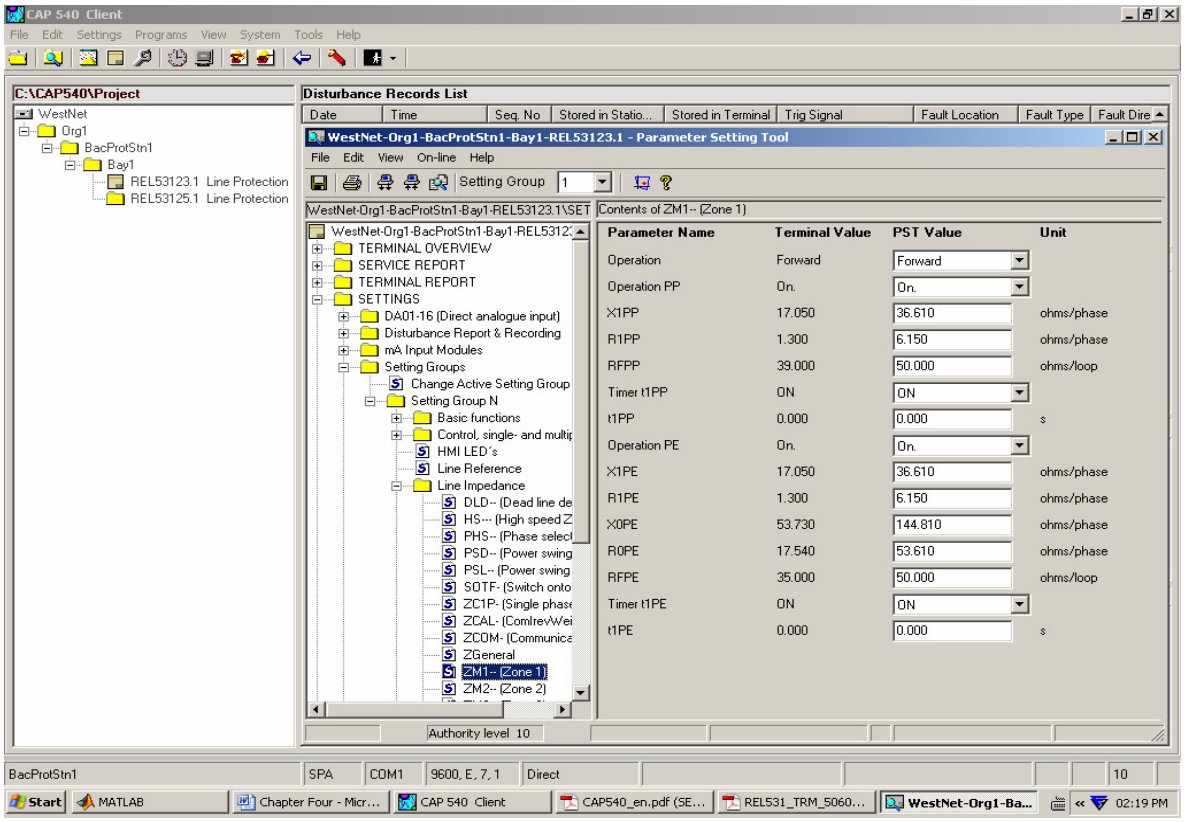

Figure 4.13: CAP 540 settings for REL531.

Table 4.2: The REL531 relay settings for the simple system without series capacitor.

Parameter	Zone 1	Zone 2	Unit	Description.
Operation	Forward	Forward	-	Operation Direction.
Operation PP	On.	On.	-	Operation phase-to-phase.
X1PP	36.61	54.92	ohms/phase	Positive sequence reactance, phase-to-phase.
R1PP	6.15	9.22	ohms/phase	Positive sequence resistance, phase-to-phase.
RFPP	26.40	33.00	ohms/loop	Fault resistance, phase-to-phase
Timer t1PP	ON	ON	-	Operation trip time delay, phase-to-phase.
t1PP	0.0	0.4	s	Trip time delay, phase-to-phase.
Operation PE	On.	On.	-	Operation phase-to-earth.
X1PE	36.61	54.92	ohms/phase	Positive sequence reactance phase-to-earth.
R1PE	6.15	9.22	ohms/phase	Positive sequence resistance phase-to-earth.
X0PE	144.81	217.21	ohms/phase	Zero sequence reactance phase-to-earth.
R0PE	53.61	80.42	ohms/phase	Zero sequence resistance phase-to-earth.
RFPE	26.40	33.00	ohms/loop	Fault resistance phase-to-earth.
Timer t1PE	ON	ON	-	Operation trip time delay phase-to-earth.
t1PE	0.0	0.4	s	Trip time delay phase-to-earth.

4.4.4 Hardware-in-loop real-time simulation testing

The previous results have shown the validity of the real-time simulation model of the relay under test. This section presents a summary of the actual relay performance operating in parallel with the real-time simulation model of the relay for a simple uncompensated transmission network of Figure 4.7.

A range of short-circuit faults that can be experienced in practice were simulated to evaluate the performance of the numerical distance protection relays under test. Every time a fault was initiated, each relay's performance was recorded. The fault records were uploaded from each relay and analyzed. Each such fault record contains six analogue signals and forty-eight digital signals as shown in Appendix B, Figure B1. Due to the large number of scenarios simulated, and the amount of data captured and analyzed, the results are presented in Table 4.3 in the form of a summary of the overall performance of the standard distance protection scheme combined with permissive overreaching scheme for internal three-phase faults. The faults were applied at different distances along the protected line from the relay 1 terminal up to the end of the line (relay 2 terminal) in steps of 10% of the line length. The fault inception angle of phase A was set to 90^{o}. More detailed information regarding the performance of selected output signals from the distance relay functions is tabulated in Appendix B, Table B1. The following performance indices were analyzed for each simulation: fault detection and clearance, faulted phase identification, directional selection, communication signals, fault location, single-pole trip and three-pole trip selection.

The relay performance for the uncompensated transmission line was satisfactory, with a maximum tripping time of 32 ms for faults in zone 1 and a maximum tripping time of 51 ms for communication assisted tripping. The REL531 relay operated correctly in terms of fault detection, faulted phase identification, fault direction, communication signaling, and pole tripping selection. The reactive coverage of zone 1 is quite satisfactory as effective coverage is 80% of the protected line as expected as shown in Table 4.3.

Table 4.3: Performance of the REL531 relays for three-phase faults (simple uncompensated line).

Fault position (%)	Relay 1 performance			Relay 2 performance		
	FLT LOC %	Trip signal	Trip time	FLT LOC %	Trip signal	Trip time
0	0	Zone 1	25	100	ZCOM	43
10	9.3	Zone 1	24	91	ZCOM	41
20	18.5	Zone 1	29	82.5	ZCOM	41
30	27.7	Zone 1	31	70.1	Zone 1	32
40	49.1	Zone 1	23	60.5	Zone 1	27
50	49.9	Zone 1	27	49.5	Zone 1	26
60	71.4	Zone 1	22	39.8	Zone 1	26
70	69.9	Zone 1	28	29.5	Zone 1	26
80	83.8	ZCOM	44	19.6	Zone 1	27
90	100	ZCOM	46	9.3	Zone 1	24
100	100	ZCOM	51	3.9	Zone 1	30

Figure 4.14 shows prefault and post-fault voltage and current waveforms obtained from the real-time simulation tests for the case of a three-phase to ground fault at 50% of the line length from relay 1. The voltage and current waveforms show the expected response and successful operation of REL531 relay under test. When the fault occurs, the three-phase busbar voltages behind the relays at each end of the line are pulled down until the circuit breakers are opened. The measured voltage is distorted by high frequency components while the current waveforms exhibit exponentially decaying dc components after fault inception. The current waveforms increase in magnitude when the fault is initiated and become zero when the relays operate the circuit breakers to clear the fault.

Figure 4.15 shows the fault initiation signal applied within the real-time simulation study, and the trip signals sent by the external hardware relays to operate the circuit breakers in the simulation in response to this fault. The results show that relay 1 and 2 issued three-phase trip signals 26 ms and 29.6 ms respectively after the fault inception. Each circuit breaker opened a few milliseconds later on the next zero crossing of the current waveform in each pole of the breaker.

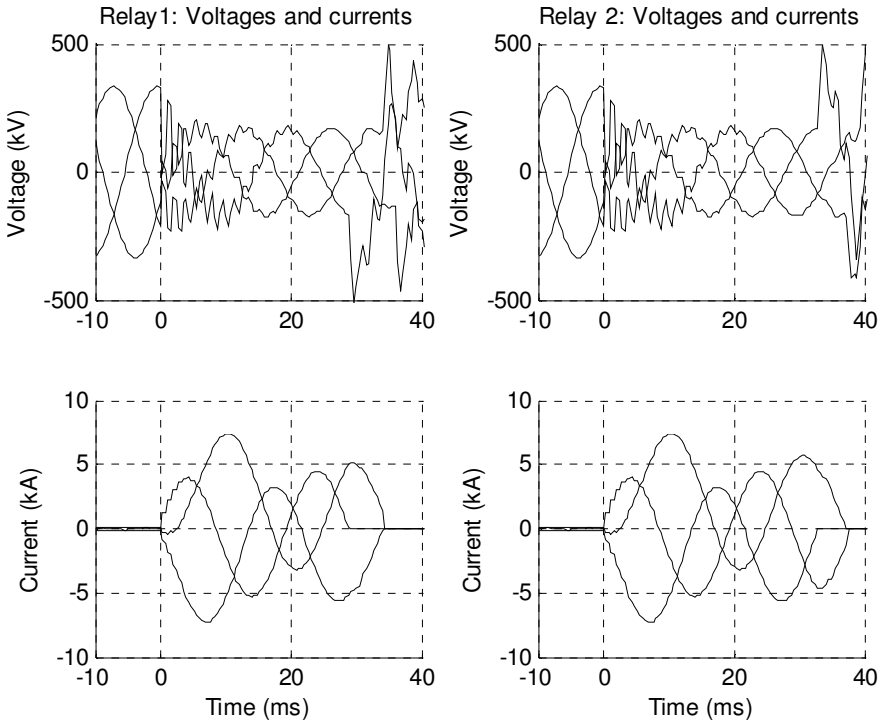

Figure 4.14: The voltages and currents at the relay location for a three-phase-to-ground fault at the middle of the transmission line.

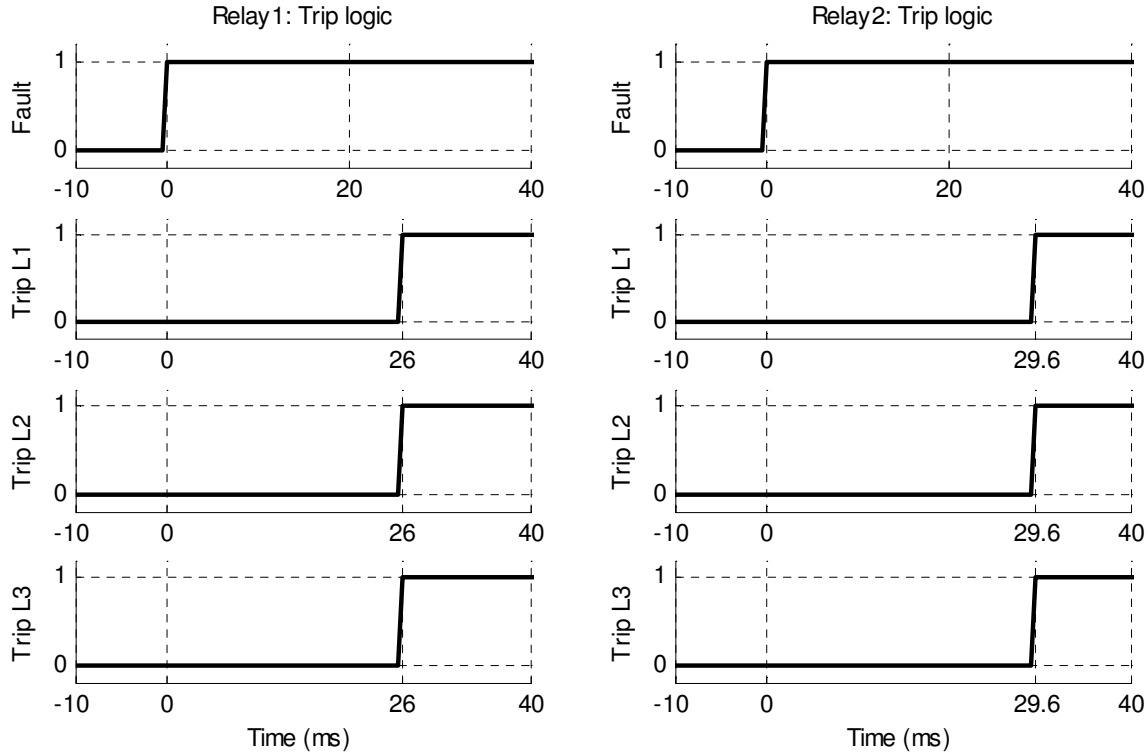

Figure 4.15: The REL531 relay trip signals for three-phase-to-ground fault at the middle of the protected line.

Figure 4.16 shows the impedance seen by the real-time relay 1 model for the same fault conditions as in Figures. 4.14 and 4.15. The relay zone 1 setting characteristic and transmission line impedance are also shown. The impedance locus is plotted only up to the point when the trip signals are issued by the external relay at the same end of the line. The impedance seen by the relay prior to trip signals being issued, is clearly visualized. Figure 4.16 shows that the real-time model of the actual relay sees the measured impedance inside zone 1 thus correctly explaining the behaviour of the actual relay, which issued a zone 1 trip. The impedance transition periods from prefault to fault state are also shown. The effect of the exponentially decaying dc component of the fault current is quite clear. The effect of the dc component is seen as an incomplete spiral around the fault location. The fault location can also be estimated from the plot. The center of the curve from t=20 ms to t=30 ms is the approximate position of the fault.

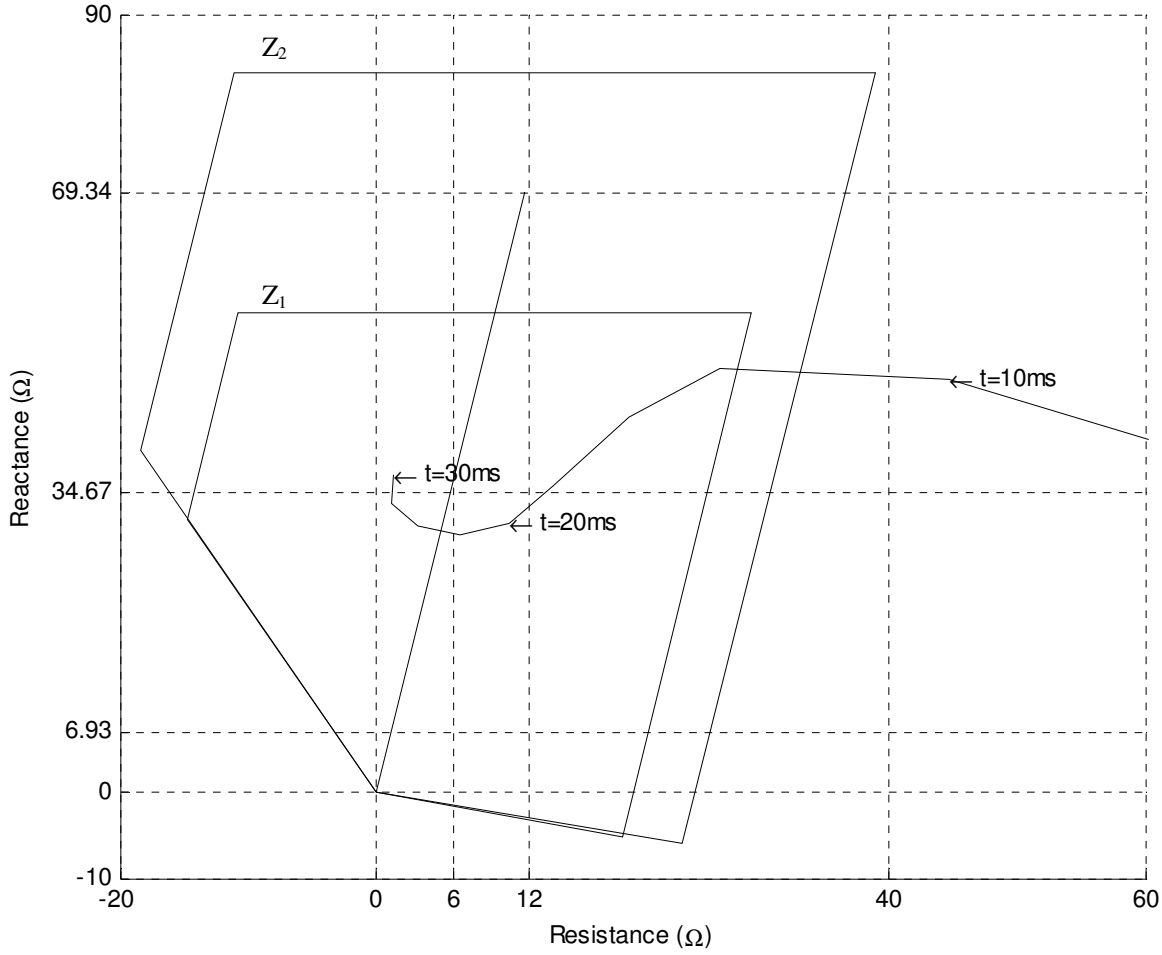

Figure 4.16: The impedance measurement loop BC of the real-time relay model for a fault location at 50% along the line.

Figure 4.17 shows the impedance seen by the real-time simulation model of the relay 1 for the corresponding 80% fault location in Table 4.3. The relay zone 1 and zone 2 setting characteristics and transmission line impedance are also shown. The impedance locus is plotted only up to the point when the trip signals are issued by the external relay at the same end of the line. The results in Table 4.3 show that the physical relay issued a communication assisted trip for this fault location, yet the fault is at the boundary of zone 1 protection. Figure 4.17 shows that the real-time impedance locus moves in and out of zone 1 due to the spiral associated with dc component in the current signals, hence zone 1 never picked up. As a result, the relay under reached this fault at the boundary of zone 1. If the impedance transition was slower, the relay could have picked up in zone 1.

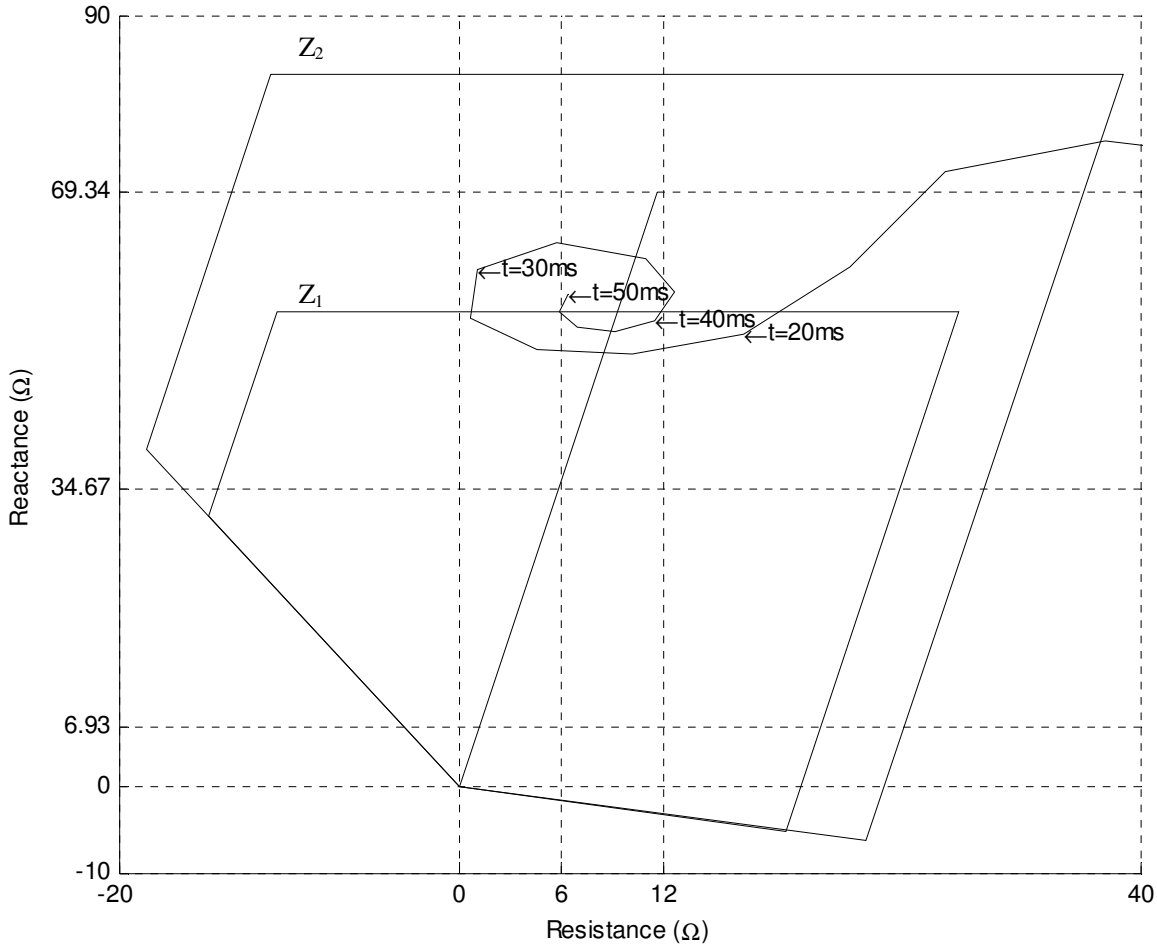

Figure 4.17: The impedance measurement loop BC of the real-time relay model for a fault location at 80% along the line.

Figure 4.18 presents impedance plots predicted by the real-time simulation model of the relay 1 for some selected faults shown in Table 4.3. The effect of the exponentially decaying dc component of the fault current on the impedance locus is more pronounced down the protected line with reference to relay 1. The impedance convergence to fault location is faster for close-up faults and slower for faults further down the line. The results also reveal one of the reasons for zone 1 being set with margin of safety to avoid overreaching faults at the end of the protected line and beyond due to transient characteristic of the impedance locus.

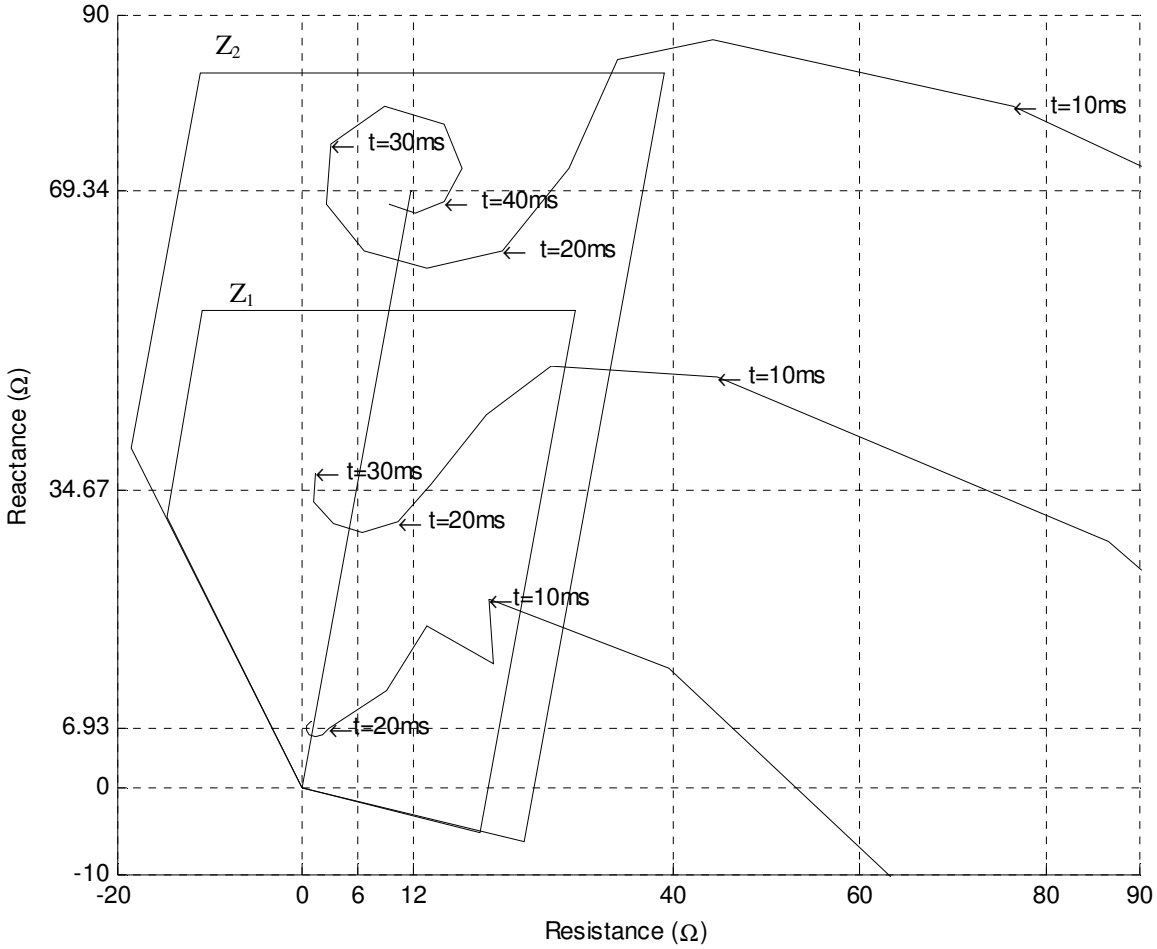

Figure 4.18: The impedance plots predicted by the real-time simulation model at 10%, 50% and 100% fault positions in Table 4.3.

4.5 Compensated transmission line simulation studies

The previous section has presented the performance of the real-time model of the relay against that of the actual REL531 relay in a simple transmission line without series capacitors. This section presents the performance of the real-time simulation model in parallel operation with actual relays in a series compensated transmission line.

In order to investigate the performance of the hybrid protection scheme in a simple series compensated transmission system, a 400 km transmission line with 60% series compensation at the mid-point of the protected line was considered. Figure 4.19 depicts the network under investigation. The parameters of this simple test system implemented on the real-time simulator are summarized in Table 4.4.

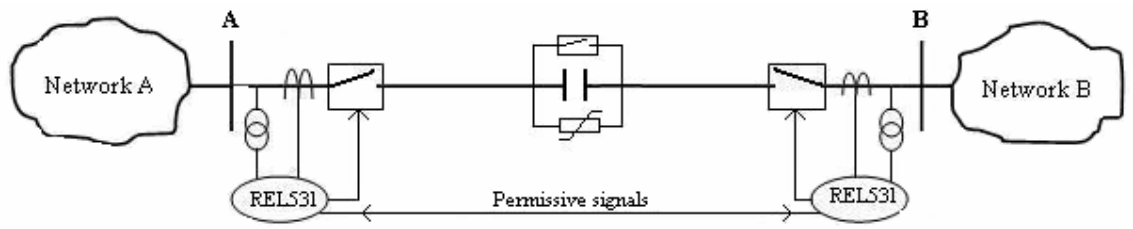

Figure 4.19: Power system model for verification of the real-time relay model: compensated line.

Table 4.4: Test system parameters (compensated line).

Parameter		Value	Units
Transmission line	Length	400	km
	Positive sequence reactance (XL)	0.3217	Ω/km
	Positive sequence resistance (RL)	0.0245	Ω/km
	Zero sequence reactance (X0)	0.5903	Ω/km
	Zero sequence resistance (R0)	0.3276	Ω/km
Source	Positive sequence impedance (Z1)	4.944 + j21.632	Ω
	Zero sequence impedance (Z0)	4.112 + j27.648	Ω
System voltage	Voltage	400	kV
Voltage Transformer	Primary voltage	400	kV
	Secondary voltage	110	V
Current Transformer	Primary current	1600	kA
	Secondary current	1	A
Series capacitance	Positive sequence capacitance	81	Ω
Metal Oxide Varistor	Discharge voltage @10 kA	398	kV
	Thermal energy limit	23	MJ

4.5.1 The impact of MOV protected series capacitor

A similar set of simulation studies to those conducted in section 4.4 were carried out on the series compensated transmission line in Figure 4.19 for various fault locations, fault types and at different fault inception angles to demonstrate the impact of the MOV protected series capacitor. The relay model was used initially without the physical relay connected to analyze the impact of the MOV protected series capacitor on the impedance seen by the relay. Figure 4.20 shows the voltages and currents at both terminals of the protected line for a single-phase-to-ground fault located immediately behind the series capacitor with reference to relay 1. The current waveforms at each end of the faulted line no longer exhibit the exponentially decaying dc component when the series capacitor is in the fault loop. Instead, in the presence of series capacitors, the measured voltages and currents are now distorted by subharmonic oscillations due to the damped natural frequency of the series RLC circuit in the fault loop.

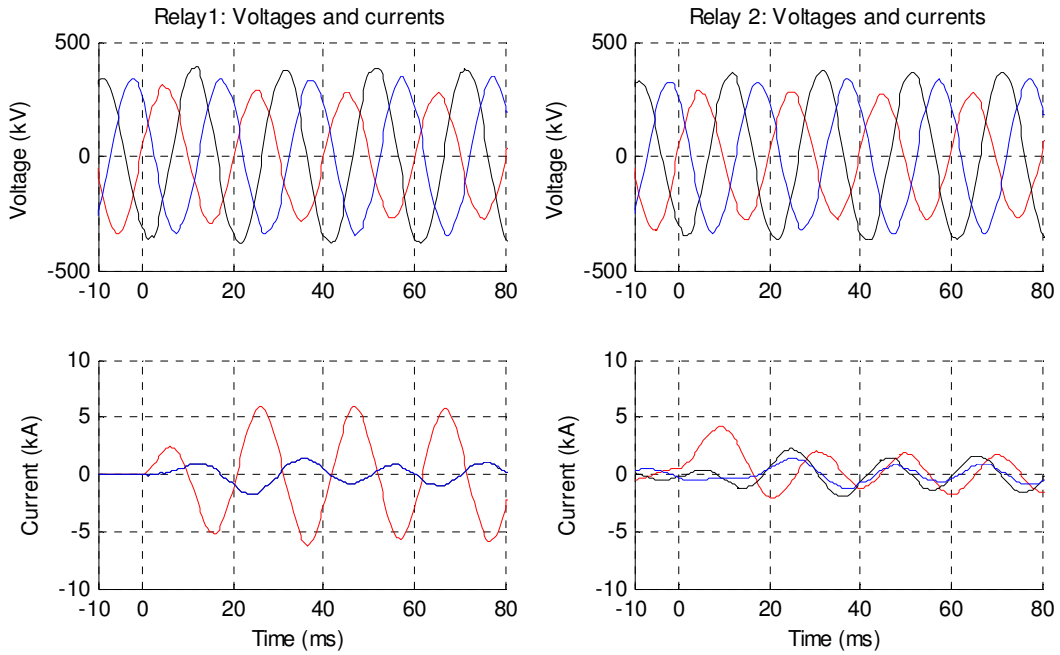

Figure 4.20: The voltages and currents at both terminals of the protected line for a single-phase-to-ground fault located immediately behind the series capacitor.

Figure 4.21 shows the behaviour of the MOV protected series capacitors for the single-phase to ground fault behind the series capacitor as obtained from the real-time simulation model of the studied system. The results show that because this fault is immediately behind the series capacitor, the MOV in the phase of the series capacitor bank carrying fault current is required to conduct in order to limit the voltage across that phase of the series capacitor to the protective level voltage of 398 kV. The results show that the series capacitor and MOV interchange conduction for approximately four ac cycles before the by-pass breaker is triggered by thermal MOV protection after fault inception. Figure 4.21 also shows that the

energy accumulated in the MOV of the faulted phase increases until it exceeds the allowable thermal limit of 23 MJ, at which point the bypass breaker is operated, thus removing the compensating impedance in the faulted phase.

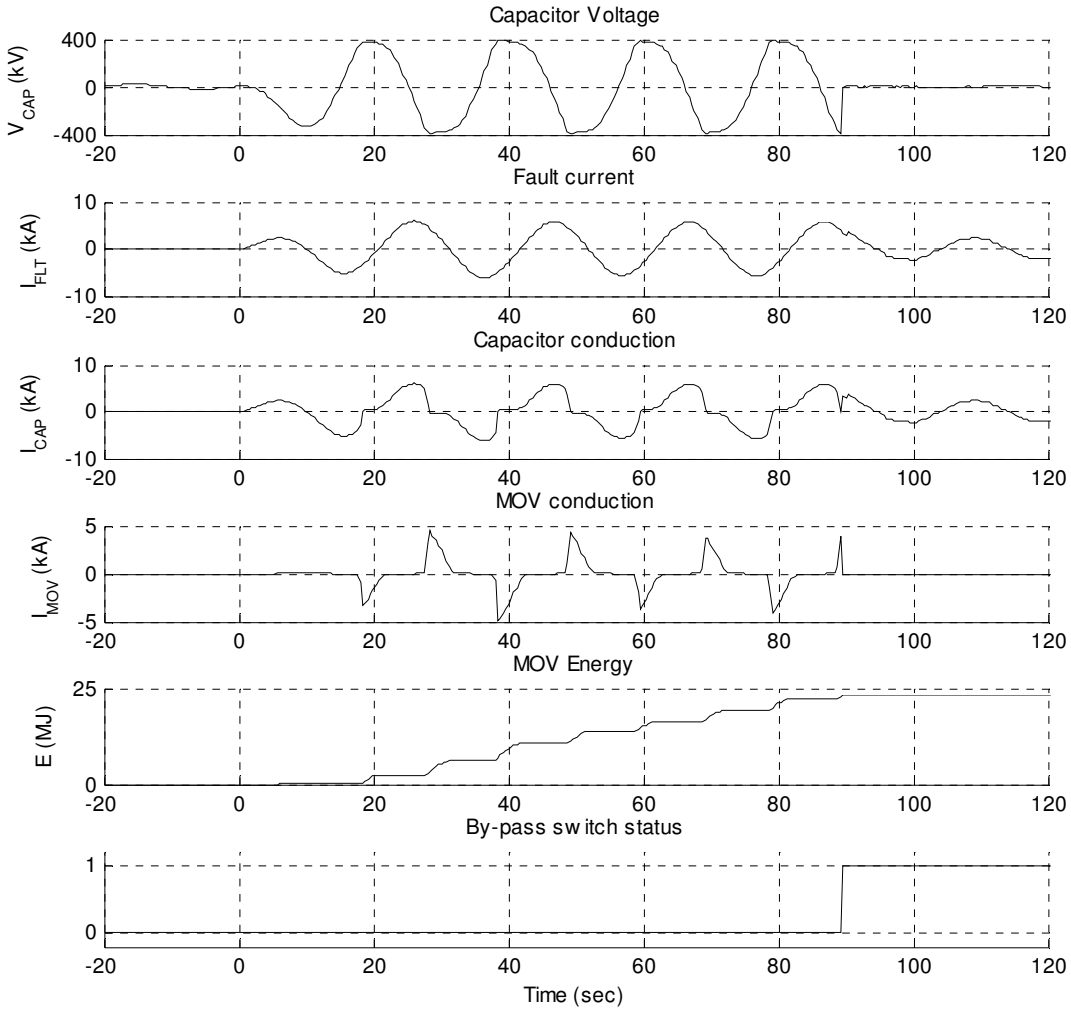

Figure 4.21: Behaviour of MOV protected series capacitor for single-phase-to-ground fault.

Figure 4.22 presents the prefault and postfault measured series capacitive reactance and series resistance of the MOV-SC conduction for the single-phase-to-ground fault. During MOV conduction the effective compensating reactance of the MOV-SC combination is reduced, with an additional resistive component as shown in Figure 4.22. Once the bypass breaker operates, shorting out MOV-SC, its series impedance becomes zero.

Figure 4.23 shows the impedance as seen by the real-time model of the distance relay with the series capacitor in the fault loop. The reactance seen by the relay first settles at 20 Ω, and then moves later to the actual fault location (at 64.67 Ω reactance) when the bypass breaker operates at time t = 90 ms after the fault inception.

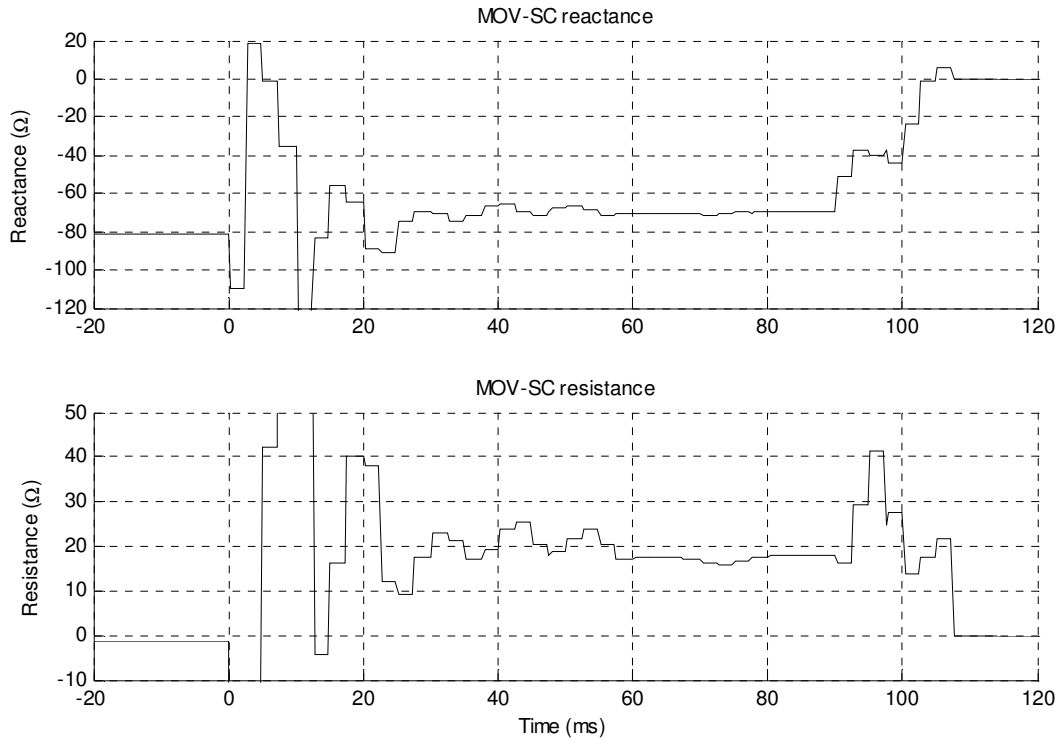

Figure 4.22: The MOV protected series capacitor's reactance and resistance during a single-phase-to-ground fault.

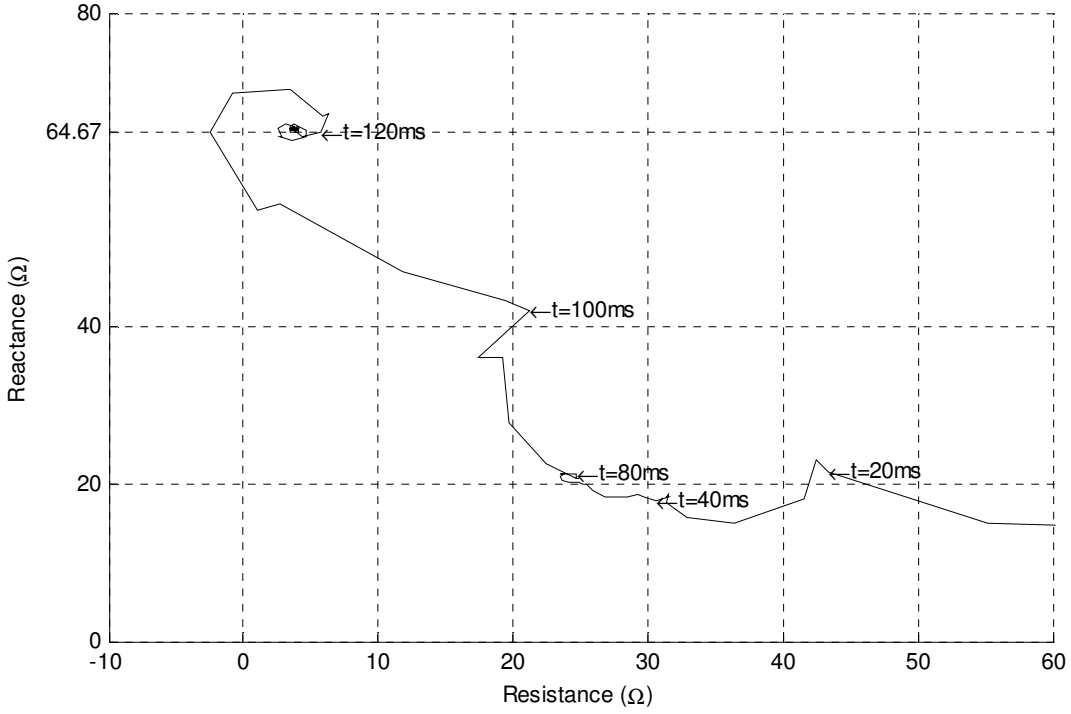

Figure 4.23: The impedance seen by the relay with series capacitor in the fault loop.

For comparison, Figure 4.24 shows the impedance convergence speed without the series capacitor in the fault loop for the same fault considered in Figure 4.23. It can be concluded from these two simulation studies that the impedance takes more time to converge to the true fault location when the series capacitor is in the fault loop. This would affect the speed of operation of the distance protection as the impedance trajectory progresses slowly to the fault location as a result of the dynamic behaviour of the MOV-SC combination.

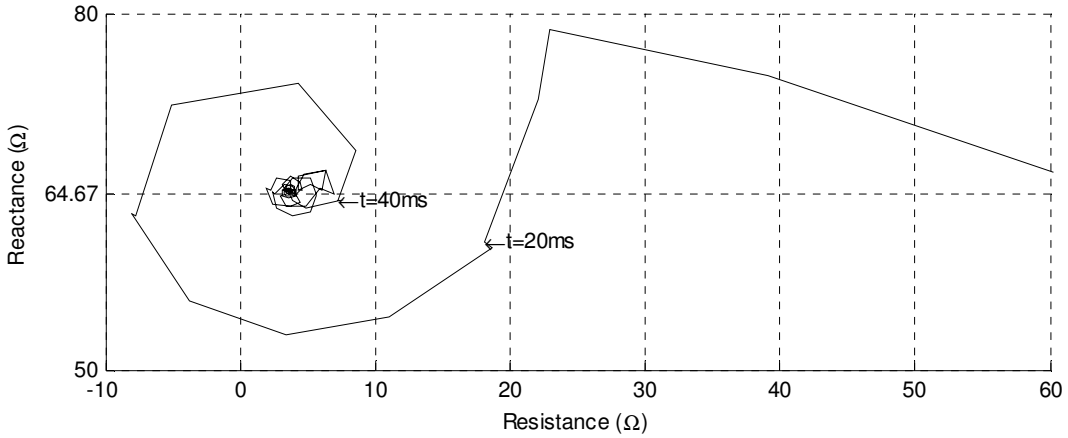

Figure 4.24: The impedance seen by the relay without series capacitor in the fault loop.

4.5.2 Hybrid protection scheme performance

Comprehensive simulations and testing of the actual REL531 relay's performances have been performed for various fault locations and fault inception angles (from 0º to 90º) using the real-time power system model shown in Figure 4.19. The REL531 hybrid protection scheme consists of a standard distance protection scheme in parallel combination with a high-speed distance protection scheme. The standard distance protection zone 1 was set to identify faults up to 80% of the compensated impedance of the protected line. The corresponding zone 2 was set to cover 120% of the uncompensated impedance of the transmission line. The underreaching zone 1 of the high-speed element was set to 50% of the uncompensated line impedance and the high-speed overreaching zone 2 covered 150% of the uncompensated impedance of the protected line.

The two relays have been analyzed simultaneously, as relay 1 sees the fault without the series capacitor in the fault loop while relay 2 sees the fault through the series capacitor. Table 4.5 presents statistical performance analysis as the fault position is varied from 5% to 45% of the protected line with reference to relay 1. The trip time is the average of ten shots in one fault location as the fault inception angle is varied from 0º to 90º in steps of 10º. The detailed test results are shown in Appendix B, Table B2.

Table 4.5: REL531 relay performances for single and three-phase faults.

Fault		Relay 1 performance			Relay 2 performance		
Position %	Type	FLT LOC %	Trip signal	Trip time	FLT LOC %	Trip signal	Trip time
5 (%)	AG	4.8	HS	16.7	36.1	ZCOM	39.7
	ABCG	7.1	HS	14.7	29.3	Z1	37.4
10 (%)	AG	9.4	HS	17.1	35.4	ZCOM	39.5
	ABCG	11.7	HS	15.3	25.1	Z1	35.0
20 (%)	AG	19.7	HS	18.3	25.5	ZCOM	41.2
	ABCG	22.2	HS	17.0	21.2	Z1	36.5
30 (%)	AG	28.4	HS	20.8	18.9	Z1	34.5
	ABCG	30.1	HS	15.6	18.1	Z1	36.1
45 (%)	AG	43.9	HS	26.7	7.8	Z1	35.0
	ABCG	46.1	HS	19.7	10.6	Z1	35.3

The high-speed protection scheme outperforms the standard distance protection scheme in terms of fault detection speed and secure protection coverage. The high-speed communication scheme reduced the relay trip time on the protected line to two cycles of the fundamental power frequency irrespective of series capacitor in the fault loop. The standard distance protection zone 1 requires further reduction in coverage due to subharmonic oscillations to maintain protection security of the scheme. The detailed simulation results also show that standard distance protection elements require more time after fault inception if the MOV protected series capacitor is in the fault loop. This slow response was predicted by the real-time simulation model, where the impedance transition from the normal load impedance to the impedance associated with the true fault location was observed to be slow when the series capacitor is in the fault loop.

The impedance seen by the relay has been monitored with the real-time relay simulation model throughout. Figure 4.25 shows the dynamic impedance seen by the real-time simulation model of the relay after a single-phase-to-ground fault at 50% of the protected line. The impedance locus is plotted only up to the point when the physical relay under test issued trip signals. The graph (a) in Figure 4.25 shows the impedance seen by the relay without the series capacitor in the fault loop while graph (b) shows the impedance seen by the relay with series capacitor in the fault loop. From the graphs, it is clear that faults occurring behind the series capacitor appear electrically closer than their physical location. Hence the relay zone 1 protection overreaches faults behind the series capacitor, which jeopardizes the security of hybrid protection scheme. Additional zone 1 security tests were conducted by applying a short-circuit fault at the ends of the protected line behind the remote relay. During these tests, the remote relay never tripped, as expected, since the fault was behind it. However, the relay looking into the fault tripped in zone 1 under certain fault applications during the statistical evaluation. This indicates that further reduction of zone 1 is necessary to avoid overreaching due to subharmonic oscillations.

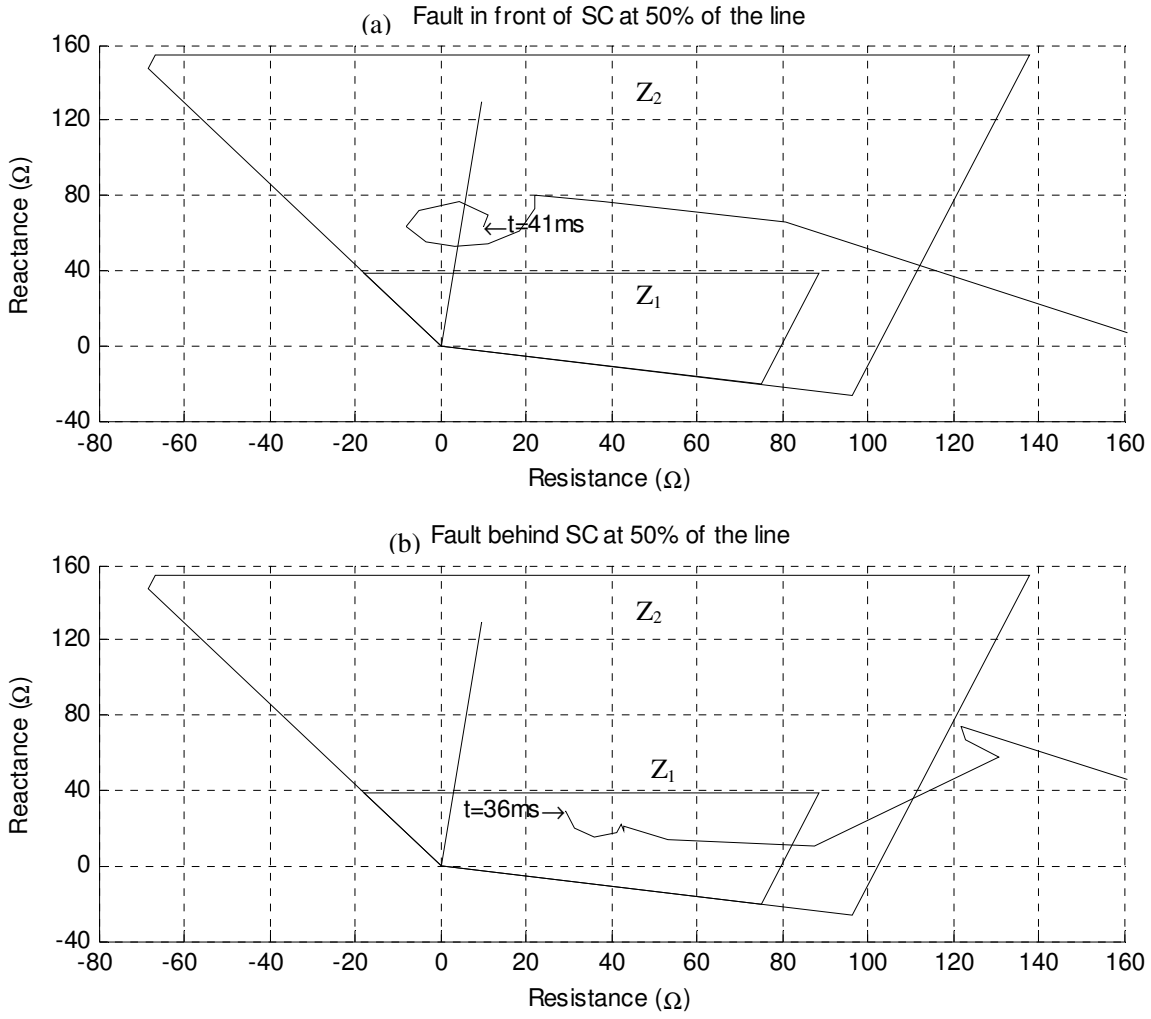

Figure 4.25: The impedance seen by the real-time model of the relay for faults immediately in front of and behind the series capacitor.

4.6 Conclusion

This chapter has presented detailed closed-loop testing of the distance relays with the RTDS simulator on a relatively simple power system model. A real-time model of a distance relay has also been developed and used to evaluate the performance of the physical relays under test for non-compensated and series capacitor compensated transmission line protection. The simulation results showed the benefits of combining closed-loop testing of physical relays in parallel with a detailed relay model, which enables the extent of the distance protection challenges to be better quantified and explained. The REL531 relay setting parameters and their performance testing results have been presented and explained. The impact of the MOV-SC response on the relay operation has also been highlighted.

Chapter Five presents a real-time model of the Western Cape transmission network for the RTDS simulator. This network will be used in subsequent chapters for dynamic performance testing of the REL531 numerical distance protection relays under more detailed network conditions found in practice.

CHAPTER 5

REAL-TIME SIMULATION OF A HEAVILY SERIES COMPENSATED NETWORK

5.1 Introduction

The previous chapter has introduced closed-loop testing of advanced numerical distance relays with a real-time simulation model of a simple power system. A detailed real-time model of the relays under study has also been developed, verified and used to run in parallel with the actual numerical distance relays under test. The dynamic performance of the numerical distance protection relays in a simple non-compensated transmission line as well as a simple compensated transmission line was presented. The impact of the MOV protected series capacitor has also been presented.

This chapter describes a real-time simulation model of Eskom's heavily series compensated Western Cape transmission network that includes detailed dynamic models of the non-linear metal oxide varistor characteristics, control logic of the series capacitor protection and bypass breakers at each series compensation station. This detailed dynamic simulation model is used in subsequent chapters to study the performance of distance protection schemes for specific lines in this network using the actual numerical distance relays that are used in the field, connected in closed-loop with the real-time power system model. The detailed model of the relays themselves developed in the previous chapter has been arranged to run in parallel with the actual relays under study, in order to gain a better insight into the reasons for their response to particular fault scenarios.

5.2 Eskom 400 kV Western Cape transmission network

In the transmission networks of South Africa, a significant programme of network strengthening has been undertaken initially to address power transfer capacity constraints. In large countries like South Africa where generating stations are several hundreds of kilometers away from load centers, series capacitor compensation is extensively utilized to enhance power transfer capacity and power system stability. The main generating stations (coal-fired) are concentrated in the north-eastern part of the country, and a small nuclear power station is located in the south-western part of the country. The transmission network spans long distances to the load centers in the rest of the country. The study in this thesis focuses on the heavily series compensated Eskom transmission network in the Western Cape region of the country.

Figure 5.1 shows the topology of the full system under study. The system forms part of the main transmission system in the Western Cape (as shown in Appendix C, Figure C1), and comprises a number of long, 400 kV transmission lines, most of which are series compensated. The entire transmission system in Figure 5.1 has been modelled on the real-time digital simulator, with each transmission line represented using a distributed-parameter, travelling-wave model, and with the series capacitors in all the lines

represented explicitly. In addition, the models of the series capacitors near the relays of interest in the study also include detailed representations of their MOVs and bypass breakers, with the actual parameters and bypass breaker logic used in these models closely representative of conditions in the field. The protection in the Mul-Bac and Bac-Dro lines in this study made use of the actual ABB REL-531 [20] distance relays described earlier in the thesis, with each such relay connected in a hardware-in-loop arrangement with the real-time simulator model of the system. In this way, the physical relays are fed with amplified versions of the live, real-time simulation model outputs, and their trip signals operate the circuit breakers in the respective lines of the real-time model.

The focus of the studies is the area of the network shown in expanded view in Figure 5.2, in particular the two long (400 km) lines connecting substations Bac and Dro, and the relatively short line from Mul to Bac (110 km). The substations at Mul and Bac are electrically close to two power stations at K and P. By contrast, the substation at H (which is itself some 250 km from Dro) is fed from a relatively weak source. The series compensation in the Bac-Dro line has recently been increased to 60% of that line's impedance; the Mul-Bac line has no series compensation.

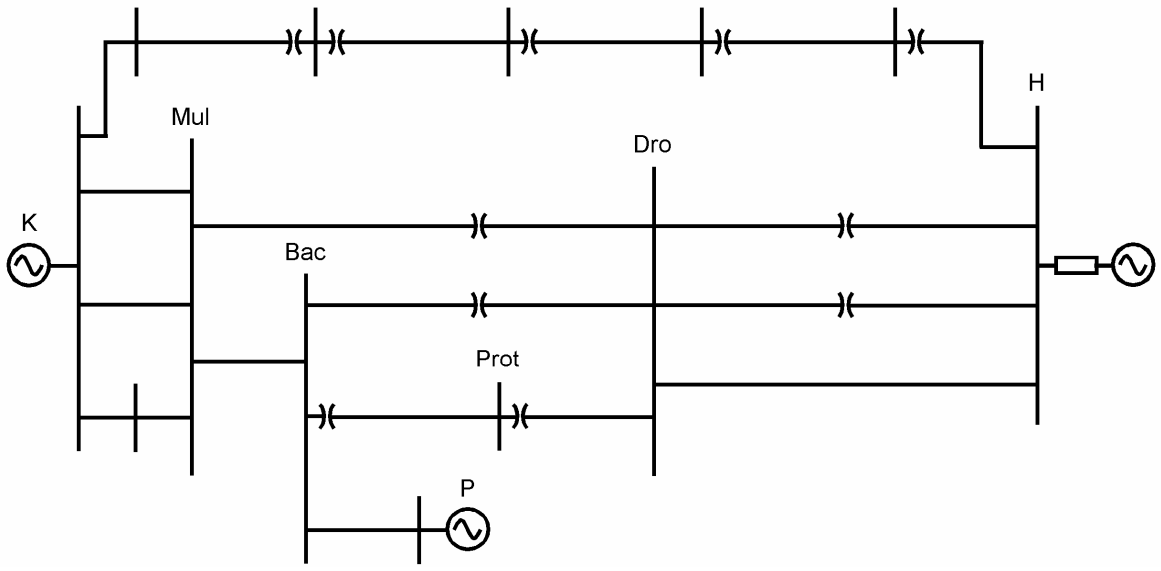

Figure 5.1: Network topology of the full study system [42].

As in the initial tests in Chapter Four, the mathematical model of these relays' impedance measurement algorithms and zone reaches was also included as a part of the real-time simulation model; these real-time relay models were not used to operate the circuit breakers in any of the studies, but rather were run in parallel with the actual hardware relays being tested so as to provide greater insight into the reasons for the real relays' responses to each fault scenario.

The real-time model of the Western Cape transmission network used in this thesis had already been developed and tested prior to the work reported here [47], and hence it does not form part of the work of the thesis. However, in order to conduct the studies described in subsequent chapters, it has been necessary to interface the REL531 relays to this real-time model, and to add to it the parallel real-time model of the two relays themselves, as well as to include a number of additional measurement and visualization models in order to analyse the dynamic performance of the hardware-in-loop relays under test. Thus, the existing real-time model of the Western Cape network shown in Figures 5.1 and 5.2 has been extended and enhanced as part of the work of this thesis.

The following subsection summarises the tests and simulation studies to be presented in subsequent chapters using this extended real-time model of the Western Cape network.

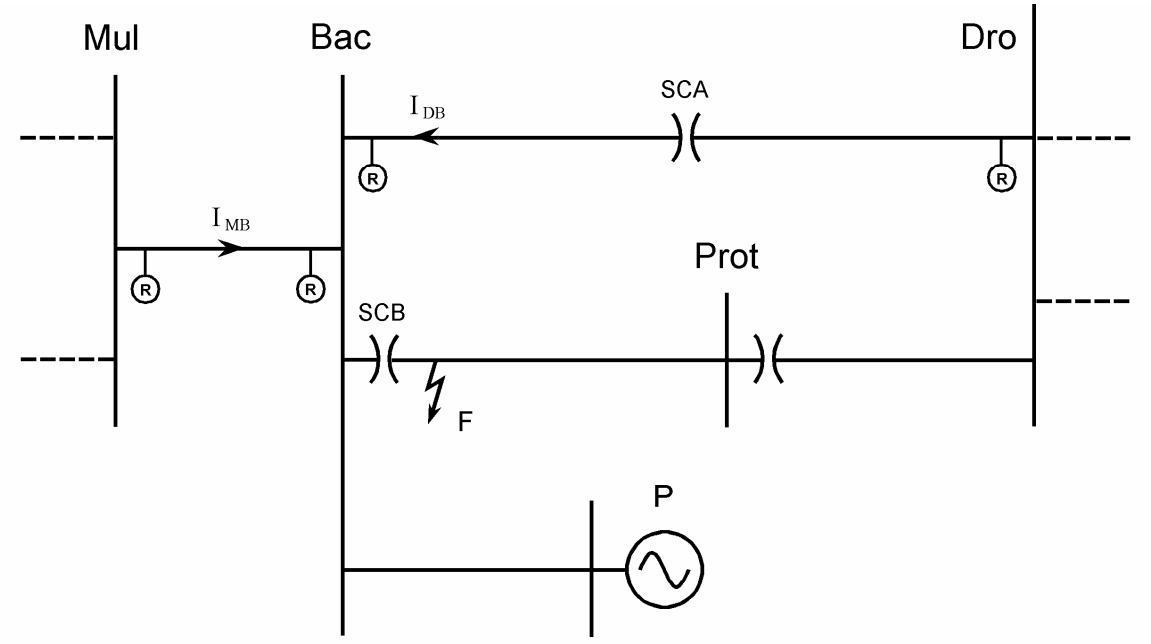

Figure 5.2: Network topology of the expanded view of the area containing the relays under investigation [42]

5.3 Fault scenarios and relay setting considerations

Studies were first conducted to determine the appropriate zone 1 reach settings for the relays on the Mul-Bac and Bac-Dro lines, in order to ensure that faults behind series capacitors on adjacent lines do not appear in zone 1 of either the Mul-Bac or Bac-Dro lines, hence preventing incorrect high-speed tripping. In order to determine the appropriate zone 1 reaches for the relays in the Mul-Bac and Bac-Dro lines, the performance of these relays was analysed by applying faults at point F in the real-time model, just behind the series capacitor bank SCB in the adjacent Bac-Prot line. For a fault located at this point F, the relays on the Mul-Bac and Bac-Dro lines are not supposed to operate; however, such a fault could appear in zone 1 of the relay at either Mul or Dro if the net capacitive reactance between the busbar at Bac and the

point of the fault F is sufficiently large. A calculation based solely on the parameters of the Mul-Bac and Bac-Dro lines and the steady-state capacitive reactance of the capacitors at SCB indicated that not only does such a possibility exist, but that the fault would appear *behind* the relay at Mul. However, a detailed simulation study was required to determine the effective impedance of the series capacitors at SCB under *dynamic* fault conditions.

In the initial studies, the relays in each line were first set without concern for the effects of the series capacitors in other lines. In the case of the Mul-Bac line, this meant that the zone 1 reach of the relays was set to 80% of the line length. In the case of the Bac-Dro line, the zone 1 reach had to be reduced in order to cater for the 60% series compensation in the middle of this line itself (at SCA); in this line the zone 1 reach of the relays was set to 80% of the line impedance after deducting the reactance of the series compensation, which equates to a reach of 32% of the physical (uncompensated) Bac-Dro line reactance. The extent of any over-reaching for external faults was then determined to decide on adjusted zone 1 settings at each of the relays at Mul and Dro. Subsequently, further fault studies were carried out to consider the effect of both fault arc resistance and the status of the generators (connected or off-line) at power station P on the over-reaching of the relays.

5.4 Conclusion

This chapter has described the real-time simulation model of Eskom's heavily series compensated Western Cape transmission network, including detailed dynamic models of the non-linear metal oxide varistor characteristics, control logic of the series capacitor protection and bypass breakers at each series compensated station of interest. This detailed dynamic simulation model is used in the following chapters to study the performance of distance protection schemes for the lines in this network using the actual numerical distance relays that are used in the field, connected in closed-loop with the real-time power system model.

Chapter Six presents comprehensive results of detailed real-time simulator testing of distance relays, using both physical relays and real-time models of the relay algorithms, to determine the performance of, and appropriate settings for these relays when used to protect a particular series capacitor compensated line (the Bac-Dro line) within this heavily series capacitor compensated network.

Chapter Seven also presents comprehensive results of detailed real-time simulator testing of distance relays, using both physical relays and real-time models of the relay algorithms, to determine the performance of, and appropriate settings for these relays when used to protect an uncompensated line (the Mul-Bac line) adjacent to heavily series capacitor compensated lines in this network.

CHAPTER 6

THE REL531 RELAY PERFORMANCE ANALYSIS IN A HEAVILY SERIES COMPENSATED NETWORK: BAC-DRO CASE STUDY

6.1 Introduction

The previous chapter described the real-time simulation model of Eskom's heavily series compensated Western Cape transmission network, including detailed dynamic models of the non-linear metal oxide varistor characteristics, control logic of the series capacitor protection and bypass breakers at each series compensated station of interest. This detailed dynamic simulation model is used in this chapter to study the performance of distance protection schemes for a particular series compensated line in this network, the Bac-Dro line, using the actual numerical distance relays that are used in the field, connected in closed-loop with the real-time power system model. The detailed model of the relays themselves developed in Chapter 4 has been arranged to run in parallel with the actual relays under study, in order to gain a better insight into the reasons for their response to particular fault scenarios.

This chapter presents comprehensive results of detailed real-time simulator testing of distance relays, using both physical relays and real-time models of the relay algorithms, to determine the performance of, and appropriate settings for these relays when used to protect the Bac-Dro series capacitor compensated line within a heavily series compensated network.

6.2 Initial zone 1 setting considerations for the Bac-Dro line

The protection of a series capacitor compensated transmission network requires special care when setting advanced numerical relays due to the effect of series capacitors in the fault loop. The distance relay's performance is affected by both internal series capacitors in the protected line and external series capacitors within the neighborhood of the protected line. There is a risk that zone 1 may underreach or overreach a fault beyond the protected line depending on the fault current level, series capacitor protection status and subsynchronous oscillations. The series capacitor maybe in service, out of service (bypassed) or partly bypassed as illustrated in Figures 6.1 and 6.2.

A number of simulations were carried out to verify the zone 1 reach setting in the Bac-Dro series capacitor compensated line for the conventional zone 1 setting (Z1 = 0.8ZL). The series capacitor, located in the middle of the Bac-Dro line, brings a fault at the far end of the line into the protected zone 1 reach as shown in Figure 6.1. Hence, the zone 1 protection overreaches the remote busbar faults.

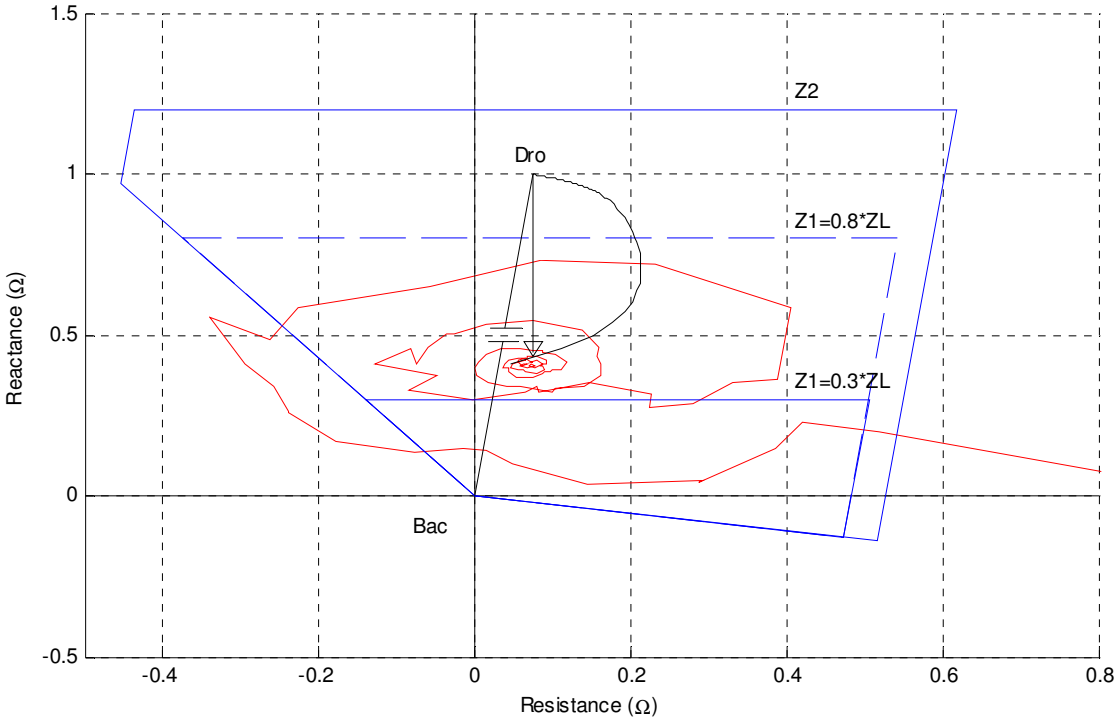

Figure 6.1: The effect of fully in service series capacitor on the impedance seen by the relay at Bac for a three-phase fault at the Dro Busbar.

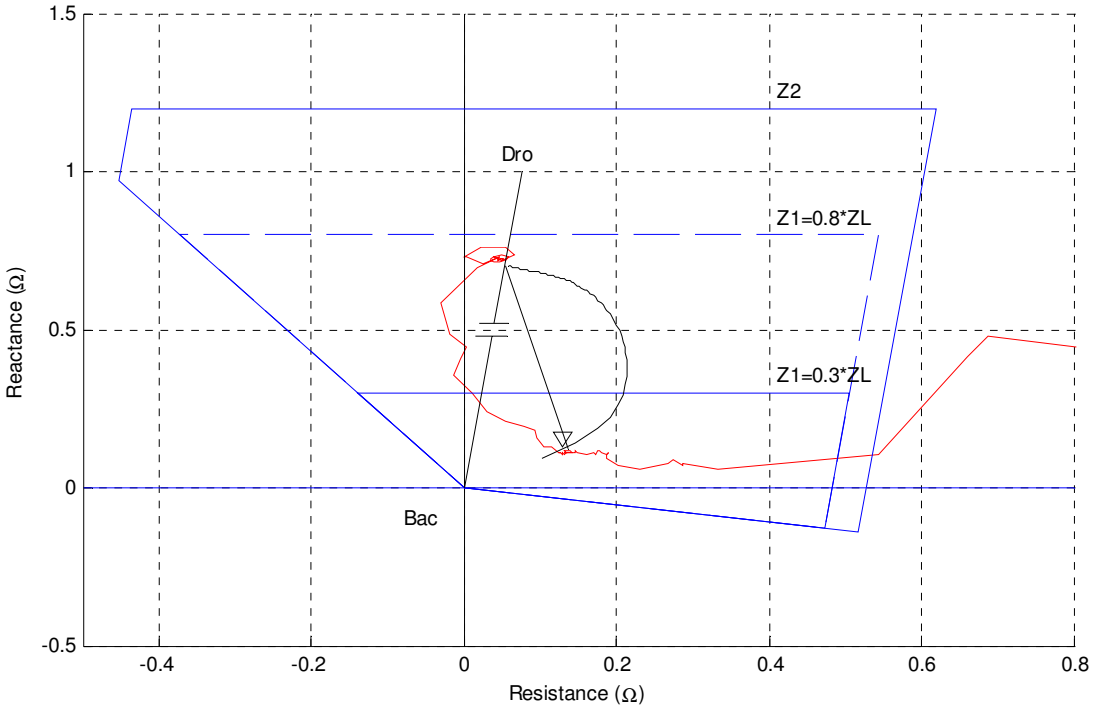

Figure 6.2: The effect of MOV conduction followed by series capacitor bypass on the impedance seen by the relay at Bac for a three-phase fault at 70% along the Bac-Dro line from Bac.

Further simulations were carried out with the series capacitor taken into consideration, and zone 1 set to cover 80% of the compensated impedance, ie. $Z1=0.8(Z_L-jX_C)$. The relay was found to still overreach remote faults due to subsynchronous oscillations. The impedance oscillations are quite large and must be considered during relay settings optimization. Further reduction of the zone 1 reach setting, taking into consideration subsynchronous oscillations according to the approach recommended in the REL531 relay manual, was carried out, but a study of the impedance loci showed that there are no compromise zone 1 settings for this line that ensured security for external faults. Consequently, the final decision regarding the zone 1 settings on the Bac-Dro line was that they had to be turned off.

Figure 6.2 further illustrates that the conduction of the series capacitors' MOVs cannot be relied on to take the faults out of the protected zone 1. For most fault scenarios, the relay issues a trip signal before the series capacitor is bypassed. The results also show that the MOV conduction suppresses the subsynchronous oscillations. The zone 1 reduction must be large enough to avoid overreaching produced by voltage reversal and subsynchronous oscillations. Due to the complexity of the analytical approach to visualize the combined effect of pre-fault load flow, fault resistance, and MOV protected series capacitor dynamics, a number of simulation studies have been conducted to find the appropriate zone 1 reach setting for the Bac-Dro line.

6.3 REL531 relay performance analysis for internal faults

The fact that the zone 1 reach settings have effectively had to be reduced to zero (as discussed in the previous section) increases the dependency on communication assisted tripping for fast fault clearance in the Bac-Dro line. A range of internal faults on the protected line were therefore simulated, and the correct operation of the physical relay was evaluated. The phrase internal faults as used here refers to faults on the protected line itself, i.e. in this case faults located anywhere between Bac and Dro. The simulation of the faulted power system is shown in expanded view in Figure 6.3, in particular the mid-point series capacitor compensated line (Bac-Dro) in parallel with two series single-end compensated lines (Bac-Prot and Prot-Dro lines). The models of the series capacitors in the protected line and both of the parallel lines included detailed representations of their MOVs and bypass breakers, with the actual parameters and bypass logic closely representative of conditions in the field. The protection in the Bac-Dro line made use of the REL531 relays connected hardware-in-loop with the real-time simulation model of the network. The REL531 relay is equipped with the full distance protection scheme and special settings for compensated line protection in particular, memory voltages for correct directional determination under voltage reversal conditions.

In order to evaluate the dependability of the protection scheme, the performance of these relays was analyzed by applying an internal fault F1 at various positions from the Bac busbar towards the midpoint series capacitor, and then an internal fault F2 at various positions from behind the midpoint series

capacitor towards the Dro busbar. The simulation studies considered various fault locations, fault types and different fault inception angles to expose the protection relays to a realistic range of conditions expected in the field. The purpose of these tests was to validate the REL531 relay settings and to evaluate the effectiveness of the internal fault clearance with each relays' zone 1 turned off. The two relays were tested simultaneously to analyze the correct operation of the communication assisted tripping, permissive overreaching scheme. The tripping times, phase selection, directional selection, and pole trip selection obtained from these studies are presented in Table 6.1 for the two REL531 relays installed at each end of the Bac-Dro line for the particular case of single-phase-to-ground faults.

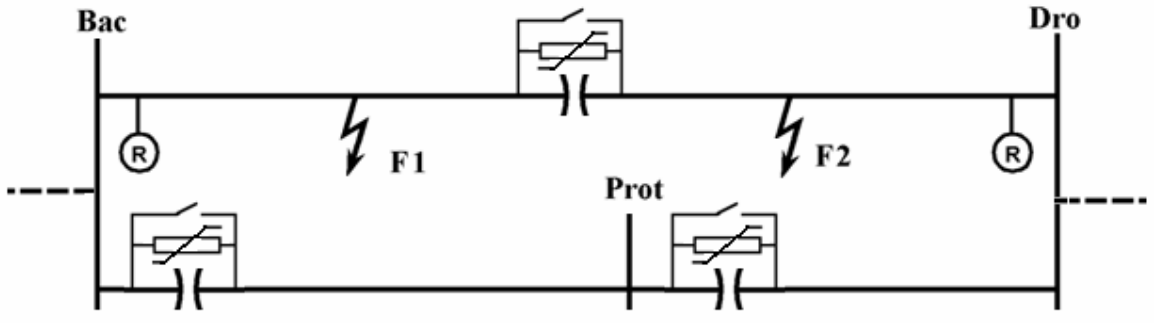

Figure 6.3: Expanded view of the area containing the relays under investigation for internal faults on the Bac-Dro line.

Table 6.1: The results of the dependability tests for the Bac-Dro line protection for single-phase-to-ground faults.

Flt type and loc	Ang	R_F (Ω)	Bac relay				Dro relay			
			Phase trip	Flt Loc %	Trip signal	Trip time (ms)	Phase trip	Flt Loc %	Trip signal	Trip time (ms)
AG 0%	0°	0	1P	0	zcom	51	3P	27.3	zcom	44
		40	3P	0	Z2	425	1P	0.0	zcom	471
	90°	0	1P	0	zcom	49	3P	42.4	zcom	43
		40	3P	0	Z2	427	1P	0.0	zcom	470
AG 20%	0°	0	1P	20	zcom	50	3P	16.4	zcom	38
		40	1P	34.8	zcom	65	1P	20.2	zcom	42
	90°	0	1P	21.7	zcom	41	3P	15.9	zcom	42
		40	1P	29.8	zcom	68	1P	22.2	zcom	46
AG 35%	0°	0	1P	34.5	zcom	51	3P	67.3	zcom	45
		40	1P	72.3	zcom	61	3P	0.6	zcom	43
	90°	0	1P	34.9	zcom	44	3P	94.9	zcom	40
		40	1P	61.9	zcom	56	3P	0.0	zcom	37
AG 50%	0°	0	1P	48.4	zcom	40	3P	49.5	zcom	40
		40	1P	100	zcom	42	3P	53.4	zcom	43
	90°	0	1P	49.7	zcom	44	3P	73.6	zcom	43
		40	1P	53.2	zcom	42	3P	0.0	zcom	49

The performance of the REL531 relays for internal fault clearance was found to be satisfactory. Both relays saw internal faults correctly in the forward direction irrespective of the series capacitor in the fault loop. The trip times were acceptable even for the highest value of fault resistance of 40 Ω expected in the Eskom transmission network. From the stability point of view, all faults were cleared before the power system became unstable. However, longer tripping times (greater than 50 ms) can be attributed to the failure of relay 1 and the remote relay (relay 2) to detect high resistive faults fast. These longer tripping times can be mitigated by advanced relaying algorithms such as weak end infeed logic in the REL531 relay, but further investigation of this issue lay outside the scope of this study.

For the fault scenarios in Table 6.1 in which relay 1 tripped in zone 2 (Z2) and relay 2 tripped via communication assisted tripping (zcom), the actual tripping sequences of relay 1 and relay 2, downloaded from the two relays, are shown in Figures 6.4 and 6.5 respectively.

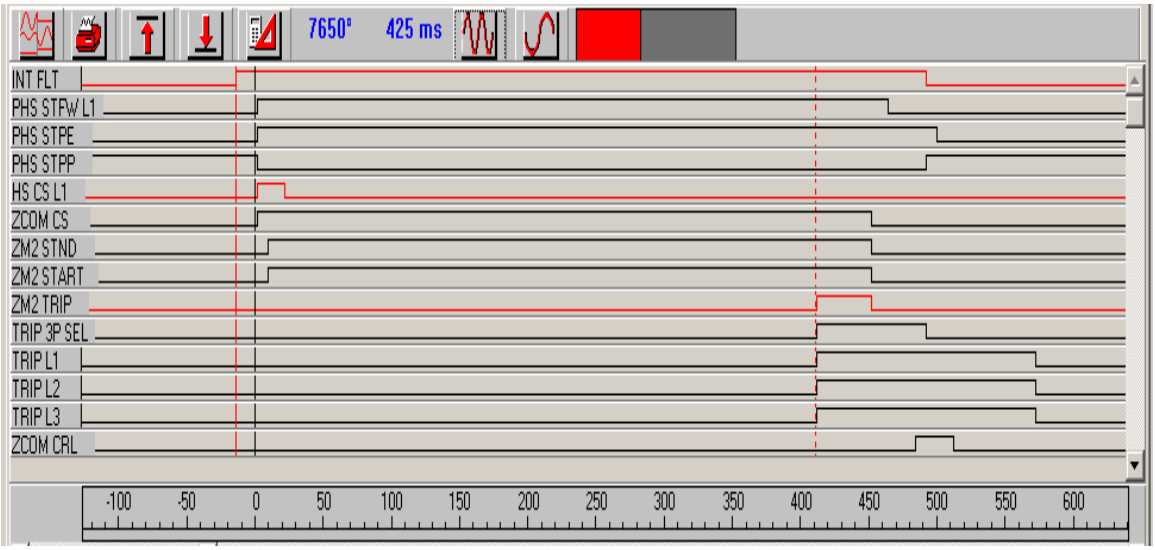

Figure 6.4: Relay 1 trip sequence for single-phase fault at 0% of Bac-Dro line, 0^{0} inception angle and 40 Ω fault resistance.

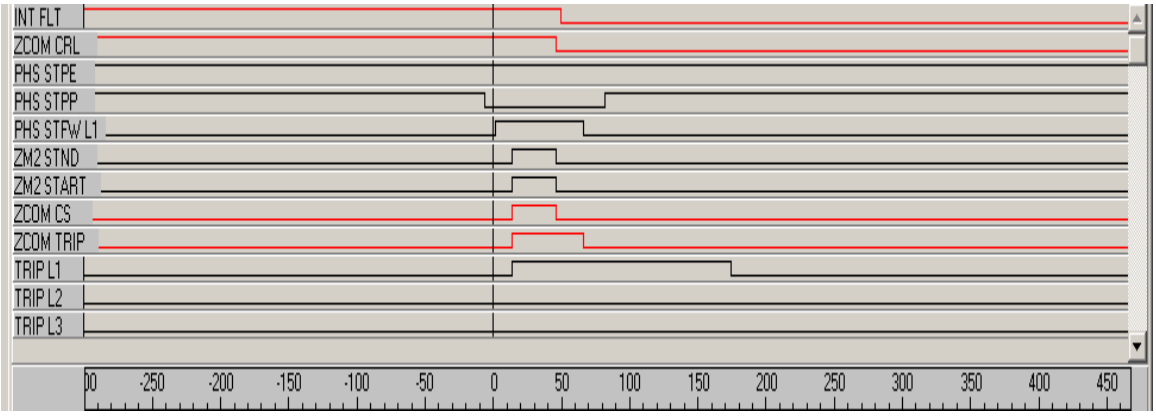

Figure 6.5: Relay 2 trip sequence for single-phase fault at 0% of Bac-Dro line, 0^{0} inception angle and 40 Ω fault resistance.

The results above are best explained by considering the impedances seen by the real-time relay models operating in parallel with the real relays at both Bac and Dro. Figures 6.6 and 6.7 show the impedances measured by the parallel relay models at Bac and Dro respectively during the 400 ms following the inception of the fault, when both line end breakers are still closed. Figure 6.6 shows that relay 1 at Bac sees the fault impedance locus in its permissive zone of protection (zone 2) and sends a permissive signal to the relay 2 at Dro as captured in Figure 6.4. However, Figure 6.7 shows that relay 2 at Dro cannot trip even with receipt of this communication assisted trip signal during the 400 ms following the fault: due to weak infeed fault current, the impedance locus in Figure 6.7 remained outside the relay's permissive zone 2 protection during this period. Consequently, relay 1 at Bac could also not operate via communication assisted tripping, because it never received a permissive signal from the relay 2 at Dro. Hence relay 1 at Bac issues a zone 2 trip and opens the circuit breakers at Bac only 400 ms after the fault.

Figure 6.8 then shows that once the circuit breakers are opened by relay 1 at Bac, the impedance measured by relay 2 at Dro jumps into the permissive zone 2 of protection of relay 2, such that relay 2 sends a permissive signal to relay 1 only after it has already tripped in zone 2 as captured in Figures 6.4 and 6.5. Relay 2 at Dro then issues a trip signal via communication assisted tripping, because its permissive signal (received earlier from relay 1) is still active. This long sequential tripping can be accelerated by weak end infeed logic.

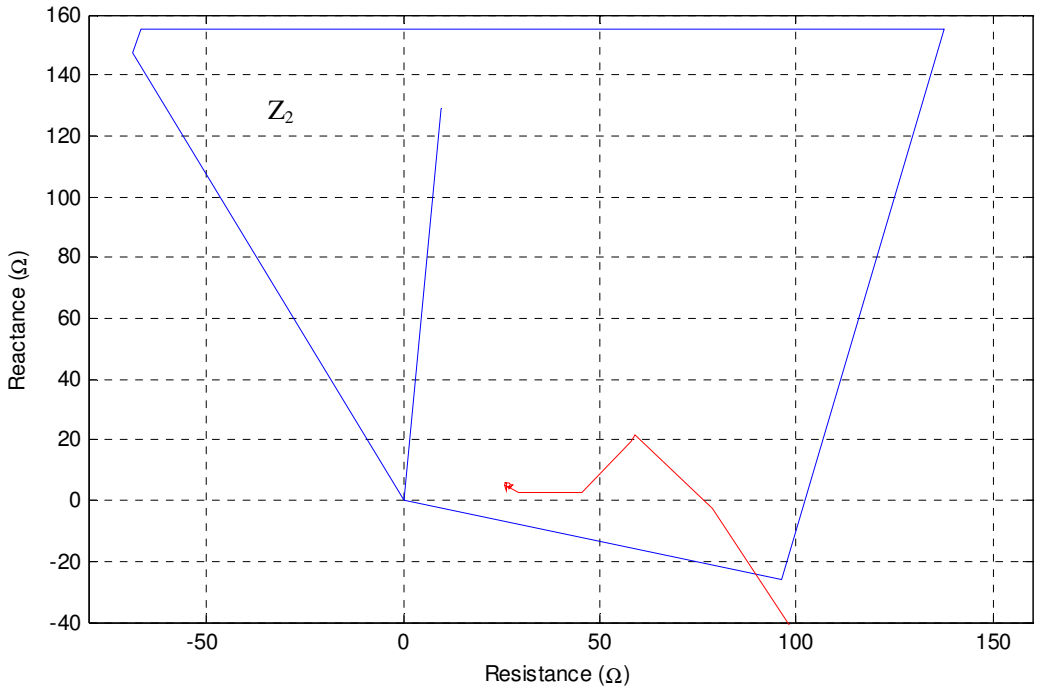

Figure 6.6: The impedance seen by the parallel real time model of the relay at Bac for a single-phase fault, with 40 Ω fault resistance, directly in front of the Bac relay; first 400 ms following fault inception, before the zone 2 trip.

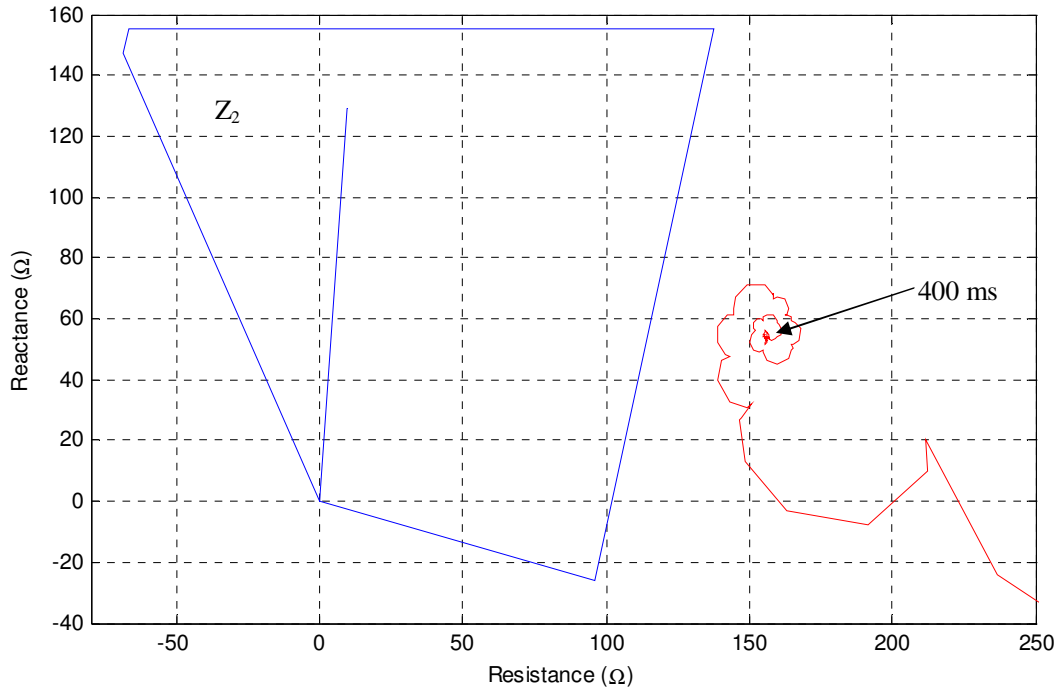

Figure 6.7: The impedance seen by the parallel real time model of the relay at Dro for a single-phase fault, with 40 Ω fault resistance, directly in front of the Bac relay; first 400 ms following fault inception, before the zone 2 trip.

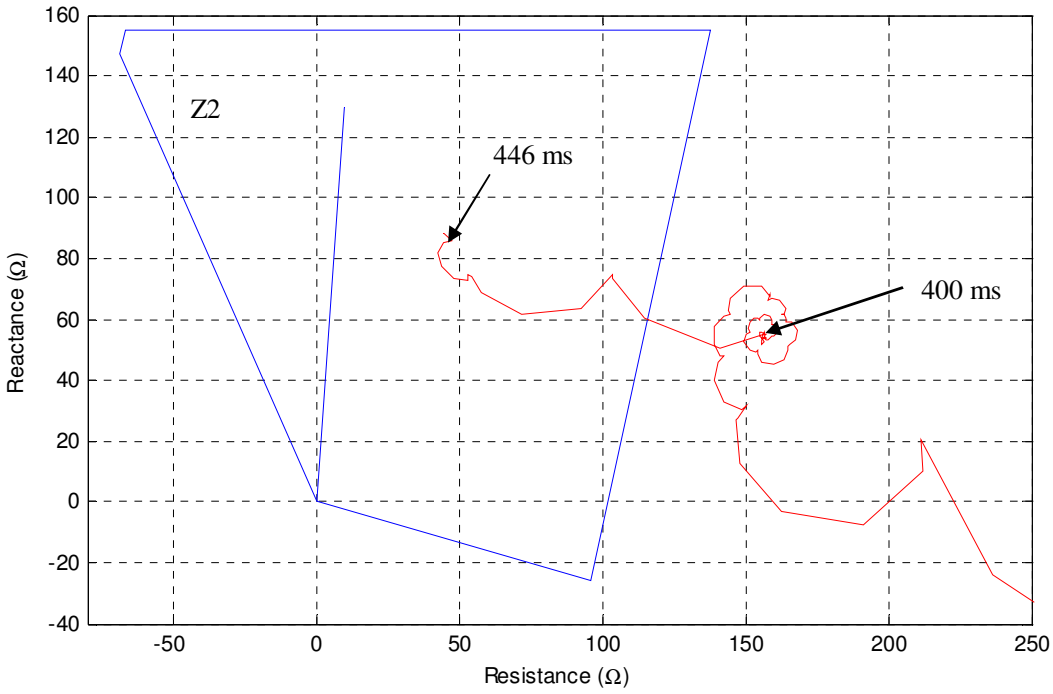

Figure 6.8: The impedance seen by the parallel real time model of the relay at Dro for a single-phase fault, with 40 Ω fault resistance, directly in front of the Bac relay; first 400 ms following fault inception, and subsequent 46 ms until relay at Dro operates via communication assisted tripping.

The results in Table 6.1 also indicate a three-pole (3P) trip by the relays for single-phase-to-ground faults when the series capacitor is in the fault loop. The REL531 relay digital fault records downloaded from the two relays for one such case are shown in Figures 6.9 and 6.10 respectively. Relay 1 at Bac correctly identified the faulted phase and issued a single-pole trip, while relay 2 at Dro initially identified the faulted phase correctly and later malfunctioned by picking up in phase L3. This resulted in two faulted phases being identified and sent to the trip logic. This problem can be mitigated by redesign of the relay protection philosophy, in particular a redesign of the relay configuration logic. However, this issue lay outside the scope of this research work.

The series capacitor and its protection equipment have a negative impact on the phase selection function for single-phase-to-ground fault identification. The REL531 relay "sees" single-phase-to-ground faults as multiphase faults. The phase selection accuracy is paramount for single-pole tripping and single-phase auto-reclosing applications. However, the failure of the REL531 relay to distinguish single-phase-to-ground faults from multiphase faults is not critical for the system under study, because the Eskom network is meshed, and single-pole tripping is not the only way to maintain power transfer and generator synchronism within the power system during single-phase-to-ground faults. In single-pole tripping and auto-reclosing applications, for persistent single-phase-to-ground faults, a subsequent action is to trip three-pole after failure of single-phase auto-reclosing.

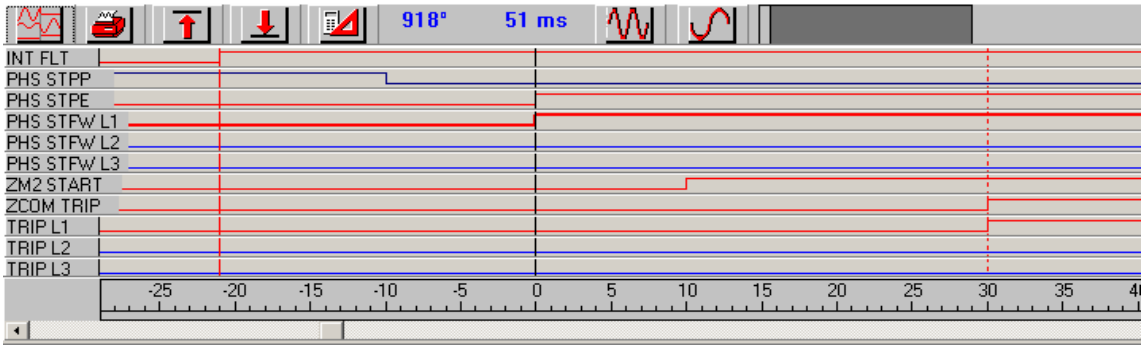

Figure 6.9: Relay 1 trip sequence for single-phase fault at 35% of Bac-Dro line, 0^{0} inception angle and 0 Ω fault resistance.

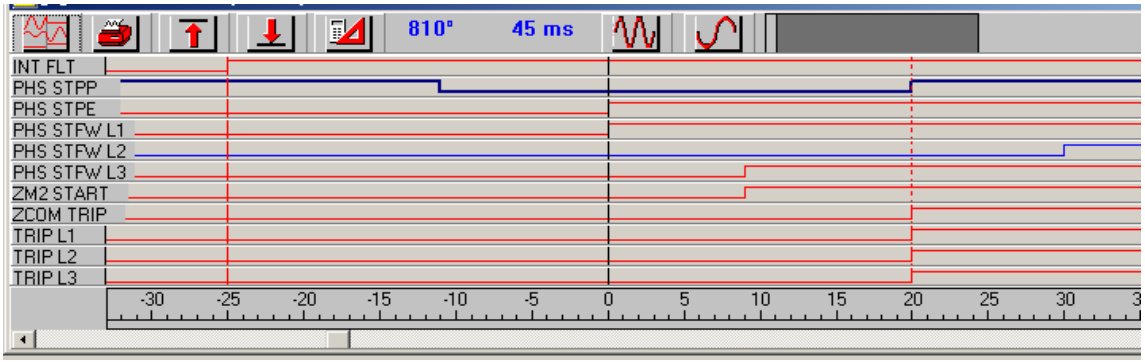

Figure 6.10: Relay 2 trip sequence for single-phase fault at 35% of Bac-Dro line, 0^{0} inception angle and 0 Ω fault resistance.

6.4 REL531 relay performance analysis for external faults

In order to ensure high protection security level, the performance of the relays on the Bac-Dro line were analysed by applying external faults at point F3 in the real-time simulation model, just behind the series capacitor bank B in the parallel Bac-Prot line as shown in Figure 6.11. Point F3 is a critical fault location for which relays on adjacent lines may operate incorrectly if this external series capacitor is not taken into consideration when setting such relays. The relays on the Bac-Dro line are not supposed to operate for a fault located at F3; however, such faults could appear in zone 1 of the relay at Bac and Dro if the net capacitive reactance between the busbar at Bac and the point of the fault F3 is sufficiently large. Hence, a detailed simulation study was required to determine the effective impedance of the series capacitor bank B under *dynamic* fault conditions.

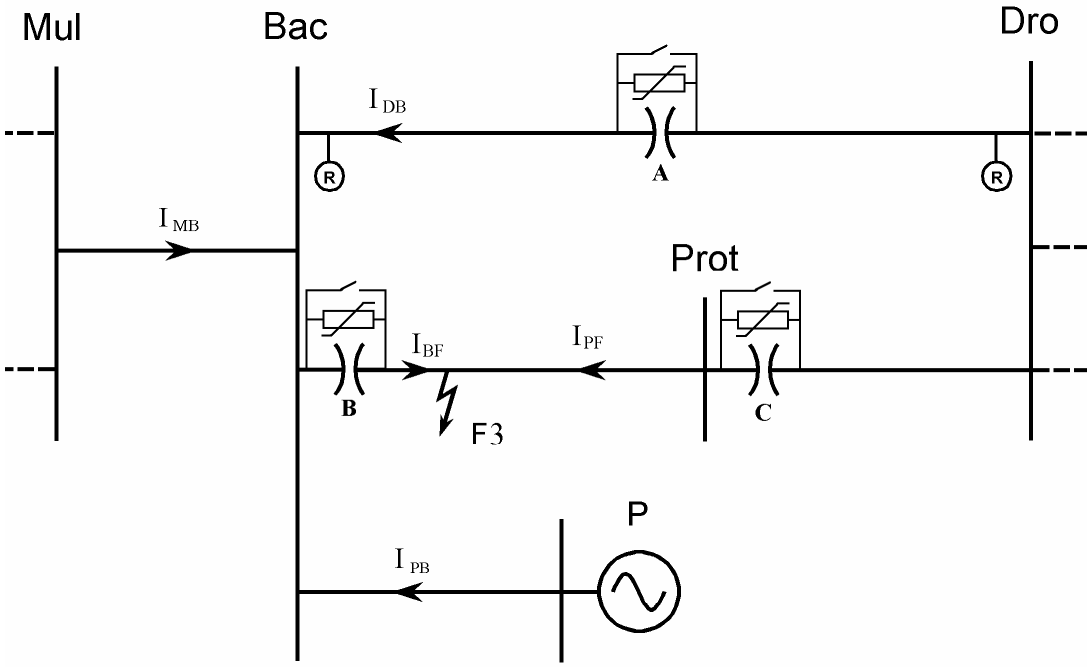

Figure 6.11: Expanded view of the area containing the relays under investigation for external faults.

In the initial studies, the relays in the protected line (Bac-Dro) were first set without concern for the effects of the series capacitors in other lines. This meant that the zone 1 reach of the relays were set to 80% of the compensated impedance of the line, (which equates to a reach of 30% of the physical Bac-Dro line reactance) in order to cater for the 60% series compensation in the middle of this line itself (series capacitor bank A). The extent of any over-reaching for external faults was then determined to decide on fine tuning zone 1 settings of the relays at Dro. (Note, even though the analysis for internal fault security in section 6.2 has already shown that zone 1 had to be turned off in the Bac-Dro line relays, this approach for considering settings security for external faults was adopted so as to be able to study each issue independently).

6.4.1 The response of the series capacitor bank B

Figure 6.12 shows the behaviour of the series capacitor bank B in the Bac-Prot line, as well as of the MOVs of this capacitor bank, for both a single-phase-to-ground fault and a three-phase fault at F3, as obtained from the real-time simulation model of the studied system. The results show that because this fault is immediately behind the series capacitor bank B, the MOVs in all phases of the series capacitor bank that carry fault current are required to conduct in order to limit the voltages across the series capacitor in those phases to 157 kV.

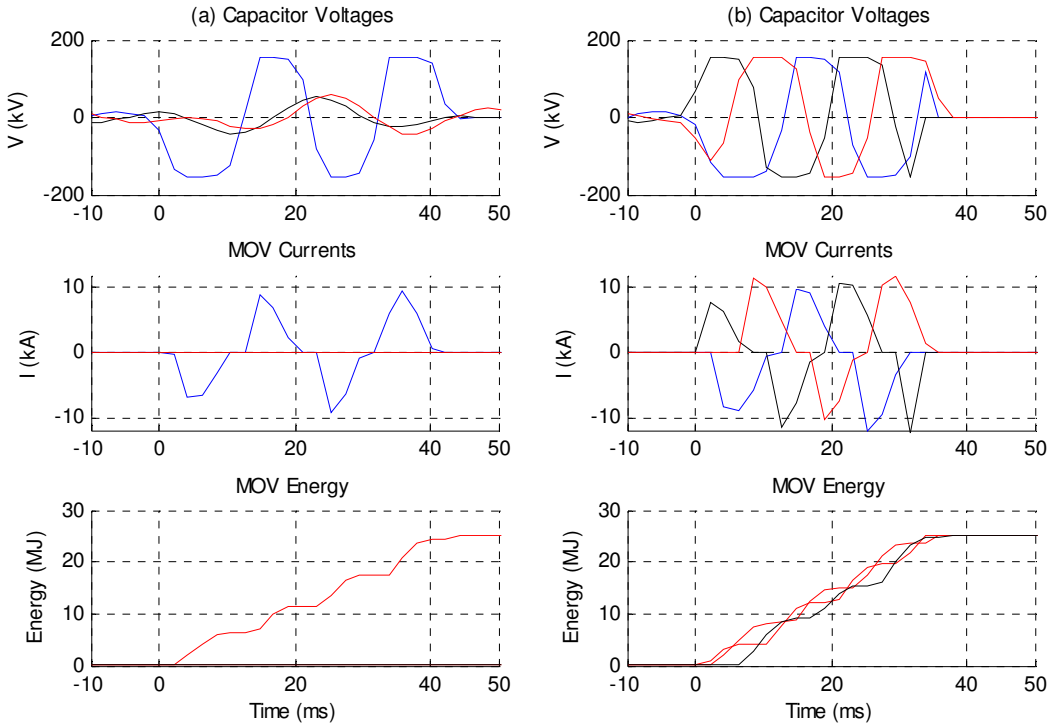

Figure 6.12: Behaviour of series capacitor bank B for: (a) a single-phase fault; (b) a three-phase fault at F3.

The results show that the MOVs conduct for approximately two ac cycles and during this period the effective compensating reactance of the SC-MOV combination at B will be reduced, with an additional resistive component introduced into the impedance as a result of the MOV conduction. Figure 6.12 also shows that the energy accumulated in the MOV of each faulted phase increases until it exceeds the allowable threshold of 23 MJ, at which point the bypass breaker is operated, thus reducing the compensating impedance at B to zero in the faulted phase. In this test it was found that despite the immediate conduction of the MOVs in the series capacitor bank B, and the subsequent removal of the series capacitors by their bypass breakers after two cycles, the relays connected hardware-in-loop with the real-time model at Dro tripped incorrectly, indicating that the fault at F3 had resulted in significant over-reaching of these relays; this was found to be the case for both phase-to-ground and phase-to-phase faults.

6.4.2 Response of the relays at Dro

In order to verify the reasons for the incorrect tripping of the REL531 relays in the adjacent lines, the parallel real-time models of the affected relays were analyzed, firstly for the relay at Dro. Figure 6.13 shows the dynamic impedance seen by the parallel real-time model of the relay at Dro for a single-phase-to-ground fault at F3, while Figure 6.14 shows the impedance seen by this parallel relay model for a three-phase fault at F3. The results in Figures 6.13 and 6.14 confirm that for both fault types at F3, the impedance enters zone 1 of the relay characteristic at Dro, despite the reduction in reach of this zone to cater for the series capacitor bank at A in the Bac-Dro line. The combination of the Bac-Dro line's own 60% series compensation, and the presence of the series capacitors at the end of the adjacent line means that the zone 1 elements of this line's relays cannot simply be reduced in reach, but rather that they must be turned off to prevent incorrect tripping for faults behind series capacitor banks in the adjacent lines, in particular behind the Bac-Prot series capacitor bank at B.

Thus, in the case of the zone 1 reaches of the relays in the Bac-Dro line, the same conclusion has been reached (zone 1s must be turned off) by considering independently, the security of operation of the relays in the Bac-Dro line for both internal and external faults.

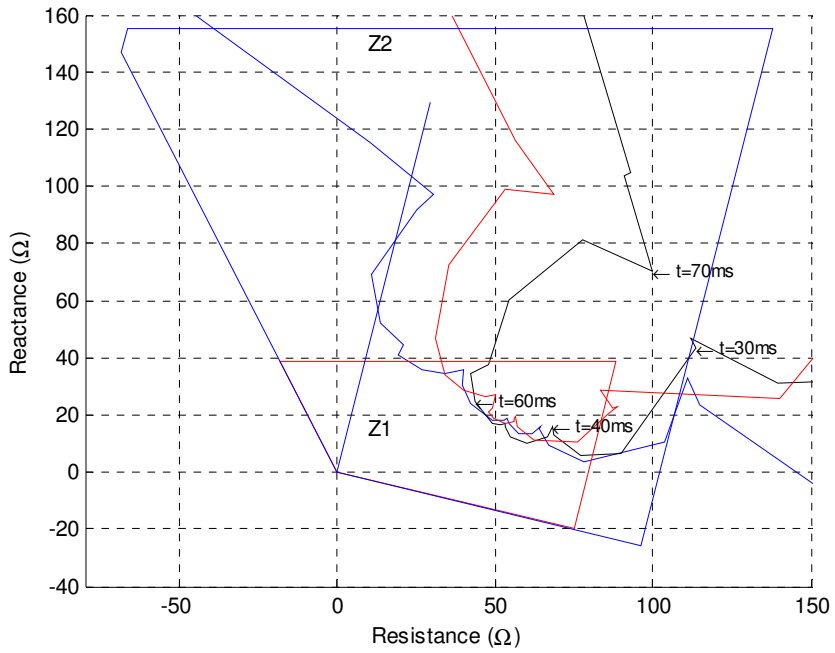

Figure 6.13: Impedance seen by the parallel real-time model of the relay at Dro for a single-phase fault at F3.

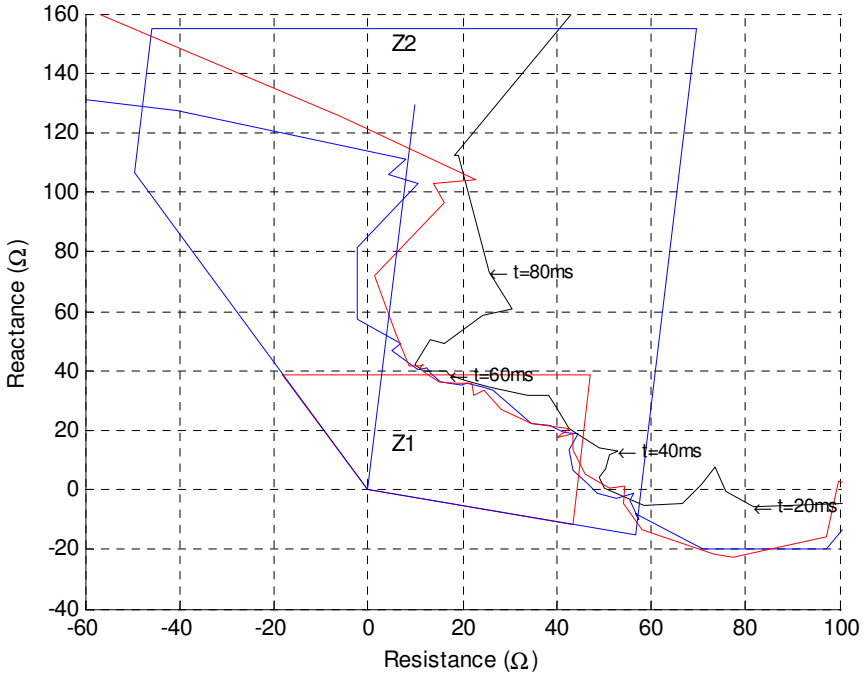

Figure 6.14: Impedance seen by the parallel real-time model of the relay at Dro for a three-phase fault at F3.

6.4.3 The effect of infeed currents on the seen impedance of the external series capacitor bank.

In order to confirm (and then explain) this observation, further analytical calculations were carried out within the real-time simulation model to determine the impedance actually presented by the series capacitor bank B in the Bac-Prot line during the faults examined in the previous studies, as well as the effective impedance of this series capacitor bank that is seen from within the protected line under study. In order to understand why such calculations are of interest, it is necessary to briefly return to the single-line diagram of the study system to explain why the impedance of the capacitor bank B may appear different when observed by the relays in the adjacent protected lines.

Consider once again in Figure 6.11: because each of the lines that feeds current into the fault at F3 contributes only a fraction of the total fault current I_{BF} flowing through the series capacitor bank B, the effective impedance of this capacitor is amplified when seen by the relays within each of these adjacent lines. The extent to which such amplification of the effective impedance of the series capacitor occurs in a particular line is governed by the ratio of the total fault current I_{BF} to the fault current contributed by that line. The amplification factor from the Dro-Bac line is given by eqn. 6.1.

$$\frac{I_{BF}}{I_{DB}} = \frac{I_{DB} + I_{MB} + I_{PB}}{I_{DB}} \qquad (6.1)$$

In effect, this means that for a fault at F3, there is likely to be a greater amplification of the "seen" impedance of the series capacitor at B (over its actual impedance) for a relay located at a weaker part of the system than is the case for a relay located at a stronger part of the system, because the fraction of the total current contributed from a weaker part of the system will be lower.

Figure 6.15 shows the actual dynamic impedance measured across phase A of the series capacitor bank and MOV combination at B during a single-phase-to-ground fault and during a three-phase fault; this impedance was calculated within the real-time model during the fault using the voltage measured at Bac and the actual fault current (I_{BF}) flowing through the series capacitor and MOV combination (in other words, it represents the combined impedance of the capacitor bank and MOV in phase A during each fault study).

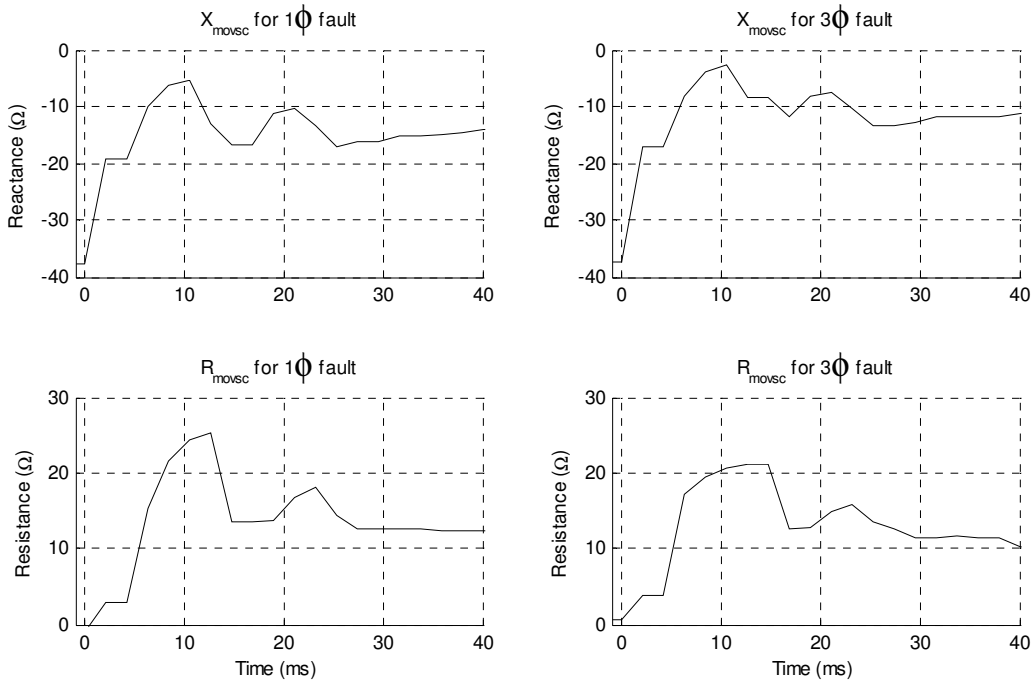

Figure 6.15: The impedance measured across one phase of the series capacitor bank B during a single-phase fault and a three-phase fault at F3.

The results in Figure 6.15 show that in the 20 ms following the application of the fault there is a noticeable difference between the amount of capacitive compensating reactance presented by series capacitor bank B for phase-to-ground and phase-to-phase faults. The reason for this difference lies in the fact that the amplitude of the current in a three-phase fault is larger than that in a single-phase fault at the same location: the larger current in the three-phase fault at F3 forces the MOVs to conduct more current, and to do so for longer durations on each half cycle, than is the case for the single-phase fault at F3, which in turn results in a greater reduction in the effective compensating reactance of the series capacitor by the MOVs during the three-phase fault (see. Figure 6.12).

Figure 6.16 shows the impedance of phase A of the series capacitor bank B as seen from the neighbouring Bac-Dro line during the same single-phase and three-phase faults considered above. The impedance seen by the relay at Dro was calculated using the voltage measured at Bac (the remote end of the Bac-Dro line from the over-reaching relay at Dro) and the measured fault current (I_{DB}) flowing into Bac down the Bac-Dro line.

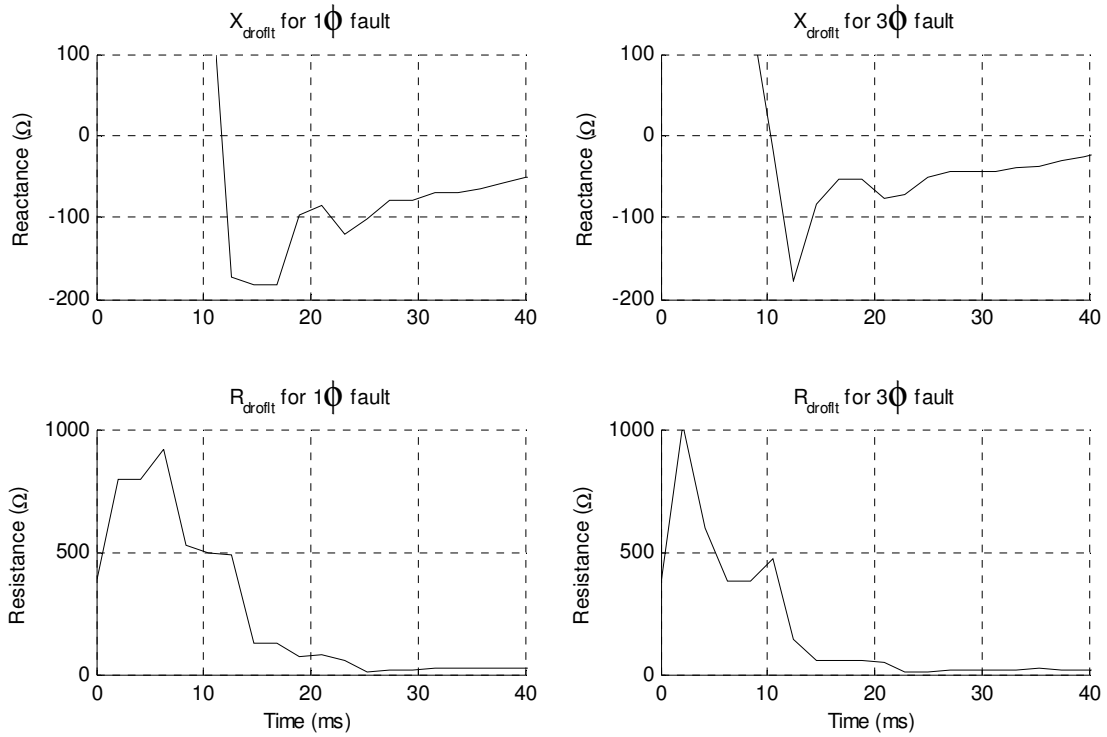

Figure 6.16: Effective impedance of one phase of the series capacitor bank B, during single-phase and three-phase faults at F3, as seen from the Bac-Dro line**.**

Comparison of these impedances seen by the relay for single-phase and three-phase faults in Figure 6.16, with the actual impedances presented by the series capacitor bank B during the same faults (in Figure 6.15) confirms that the seen impedance is indeed magnified over the actual impedance of the series capacitor bank and MOV combination under dynamic fault conditions. This finding is consistent with the measured response of the REL531 relays at Dro, and with the behaviour of the real-time models of the relay (Figures 6.13 and 6.14), which have both shown far greater over-reaching for single-phase-to-ground and three-phase faults at F3 for the case of the relay at Dro, hence instantaneous zone 1 elements must be turned off.

As described earlier, this amplification of the actual reactance of the series capacitor bank B, as seen by the relay at Dro for external faults, can be explained by the fact that this relay is located at a relatively weak end of the system. As final confirmation of this reasoning, Figure 6.17 shows the ratios between the actual fault current I_{BF} through the series capacitors at B and the fault currents contributed by the Bac-Dro line for the single-phase fault and three-phase fault at F3. These fault current ratios were calculated using

instantaneous currents obtained from the real-time simulation studies, but with the trip signals from the hardware relays blocked. The results confirm that for most of the 20 ms period following the application of the fault (i.e. during the period that the zone 1 elements of the relays at Dro take the decision to operate when not blocked) the amplification factor for a three-phase fault is smaller than the amplification factor for a single-phase fault. Thus the different amplifications of the effective impedance of the series capacitor MOV combination in the Bac-Prot line can in fact be explained by the differences in fault current magnitudes for different types of faults.

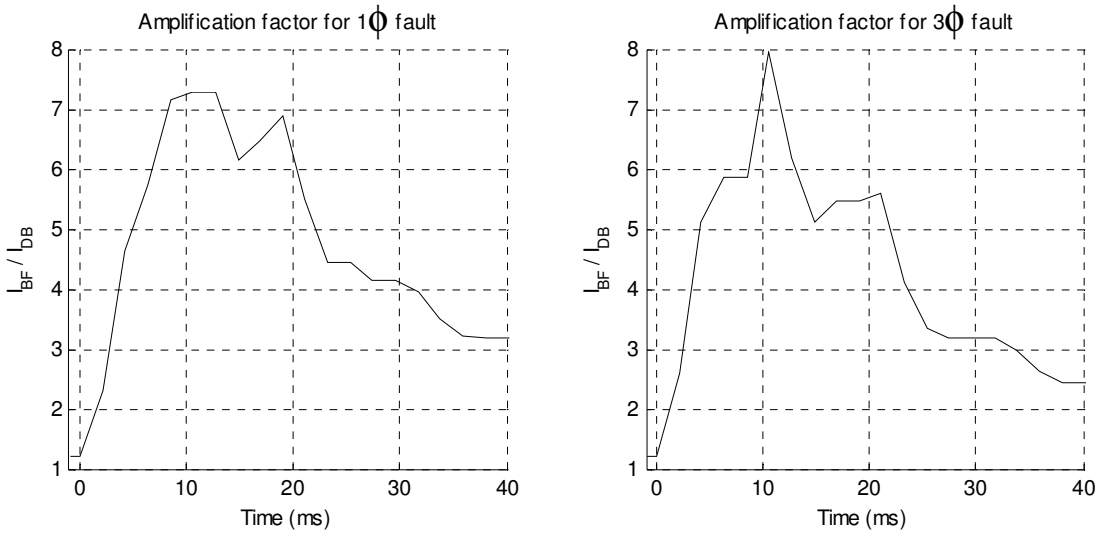

Figure 6.17: Amplification factors, I_{BF} / I_{DB} for single-phase and three-phase faults at F3.

6.4.4 The impact of fault resistance and status of generators at power station P

The power station at P is a pump storage station, so that its generators can be operating either in generating mode, motoring mode or be completely disconnected depending on system requirements. Subsequently, further fault studies were carried out to consider the effect of both fault arc resistance and the status of the generators at power station P on the over-reaching of the relays.

The previous tests were all conducted for zero-resistance faults, with the generators at power station P in service. Those results have shown that the effective impedance of the series capacitor bank at B as seen by the relay in the Bac-Dro line depends on the actual impedance of the SC-MOV combination at B during the fault (which in turn depends on the fault current through series capacitor bank B), and the extent of the amplification of this impedance within the protected line (which depends on the percentage contribution of the fault current at F3 from Bac-Dro line). The presence of resistance in the fault at F3 will reduce the amplitude of the through-fault current at B to some extent, and if the generators at P are not in service, the percentage contribution to this fault current from each adjacent line will be considerably higher; hence each of these factors is likely to influence the effective impedance of the

series capacitor bank at B as seen by the relay at Dro, and hence the extent to which the zone 1 reaches of the relays in the Bac-Dro line may require alternative settings. For this reason, additional tests were carried out using the real-time simulation model for various values of non-zero fault resistance, with and without the generators at P in service.

The study of the effect of disconnecting the generators at P on the impedance seen during faults behind series capacitor bank B will not change the conclusions already reached regarding the relay at Dro's zone 1 settings, since it has already been shown that with the generators in service the zone 1 elements at Dro need to be turned off (ie. the most conservative possible reduction of the zone 1 reach is already indicated for this relay). However, it is still of interest to note that with the originally-calculated zone 1 settings for this relay at Dro (ie. with the zone 1 reach reduced to 30% to cater only for the internal capacitor bank A) the disconnection of the generators at P marginally reduces the over-reaching of zone 1 at Dro for ground faults behind series capacitor bank B, but significantly increases the over-reaching for phase faults behind series capacitor bank B. Thus the relay at Dro sees phase faults located behind the external capacitor bank at B appearing significantly nearer when the generators at P are disconnected.

Figures 6.18 and 6.19 show the dynamic impedances seen by the parallel real-time relay model at Dro for single-phase and three-phase faults of varying fault resistance at F3, with the generators at P in service and out of service respectively. As the fault resistance increases, the impedance seen by the real-time relay model at Dro has progressively lower reactance, but also progressively higher resistance. The lower seen reactance is due to the reduced fault current and hence reduced extent of MOV conduction during the fault as the fault resistance increases. The larger seen resistance is because of the infeed of additional current through the fault resistance that is not seen by the relay at Dro (ie. amplification of the seen resistance at the fault itself).

Figures 6.20 and 6.21 show the dynamic impedance of the series capacitor bank B during single-phase and three-phase faults of varying fault resistance at F3, with the generators at P in service and out of service respectively. The results show that the capacitive reactance of the MOV-SC combination is higher with the generators at P out of service. This is to be expected, as the total fault current through the series capacitor at B, and hence the extent of the MOV conduction at B, is lower with no generators connected at P. Figures 6.22 and 6.23 show the dynamic impedances of the series capacitors at B as seen from the Dro-Bac line during the same fault conditions. The actual impedances presented by the series capacitor bank B (in Figures 6.20 and 6.21) during the faults confirm that in all cases the seen impedance is amplified.

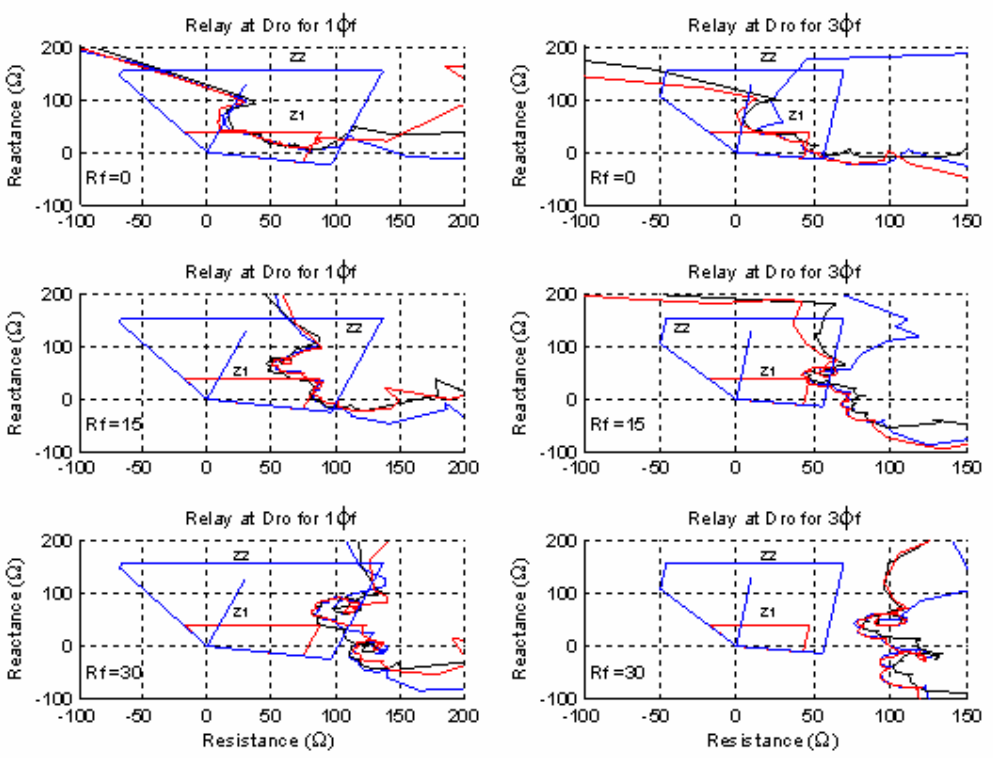

Figure 6.18: Impedances measured by the parallel relay model at Dro for single-phase and three-phase faults at F3 of varying fault resistance: generators at power station P in service.

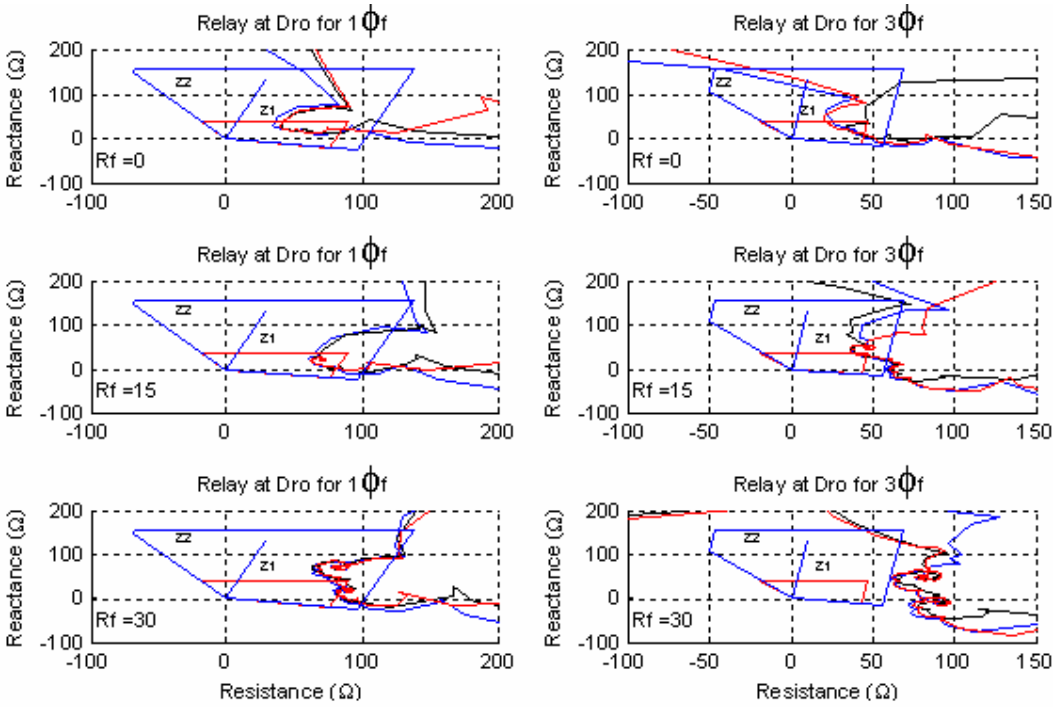

Figure 6.19: Impedances measured by the parallel relay model at Dro for single-phase and three-phase faults at F3 of varying fault resistance: generators at power station P disconnected.

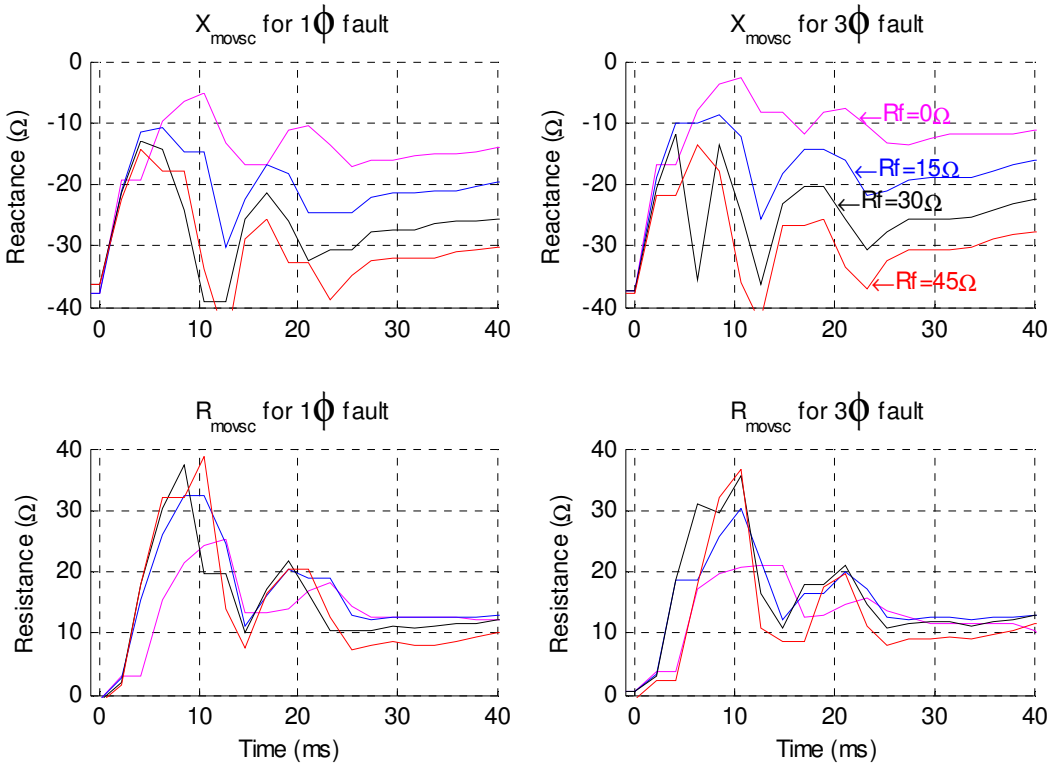

Figure 6.20: Impedances in one phase of the series capacitor bank B for single-phase and three-phase faults at F3 of varying fault resistance: generators at power station P in service.

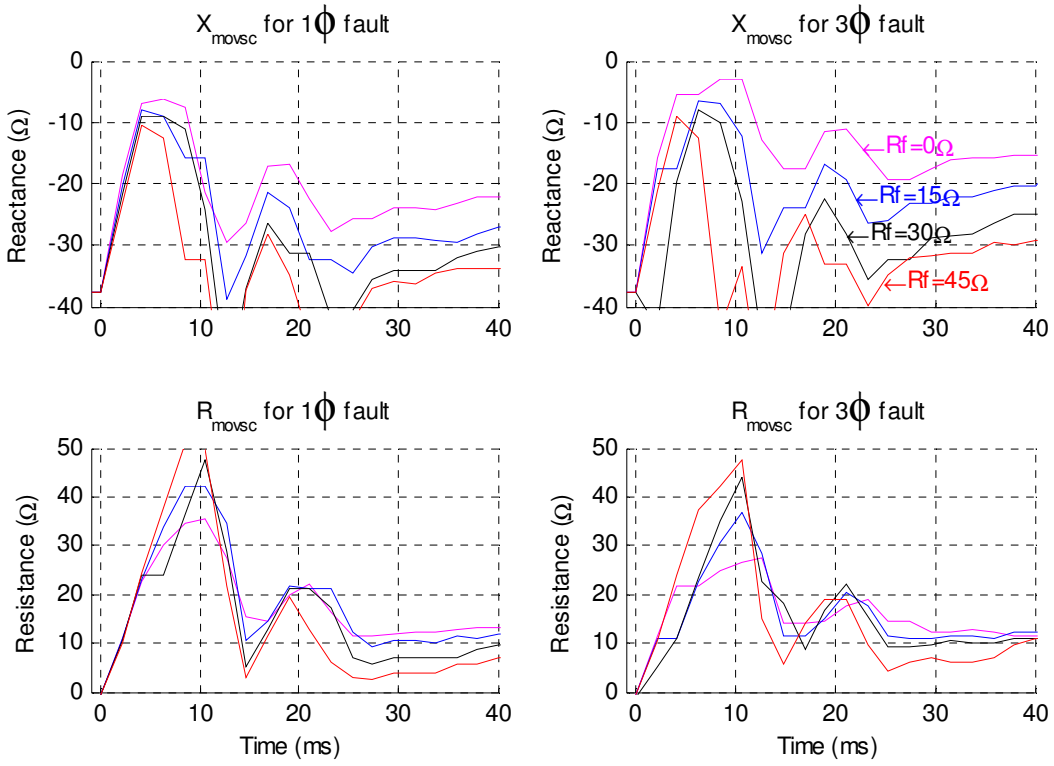

Figure 6.21: Impedances in one phase of the series capacitor bank B for single-phase and three-phase faults at F3 of varying fault resistance: generators at power station P disconnected.

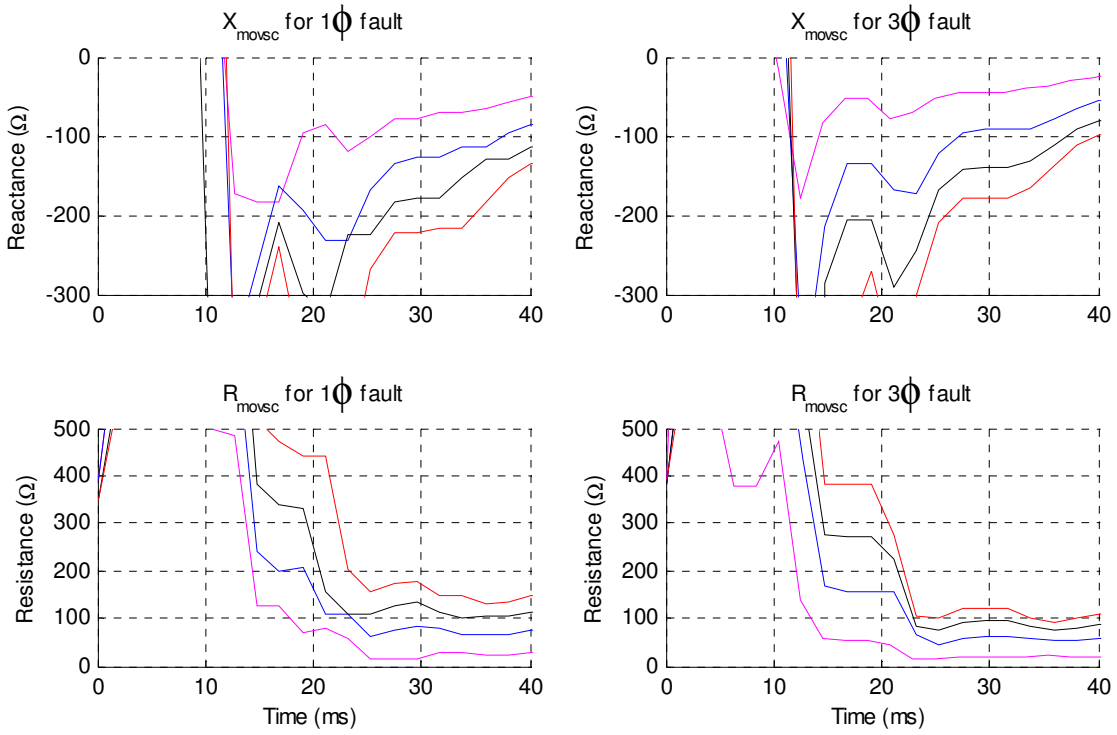

Figure 6.22: Effective impedances as seen from the Bac-Dro line of one phase of the series capacitor bank B for single-phase and three-phase faults at F3 of varying fault resistance: generators at power station P in service.

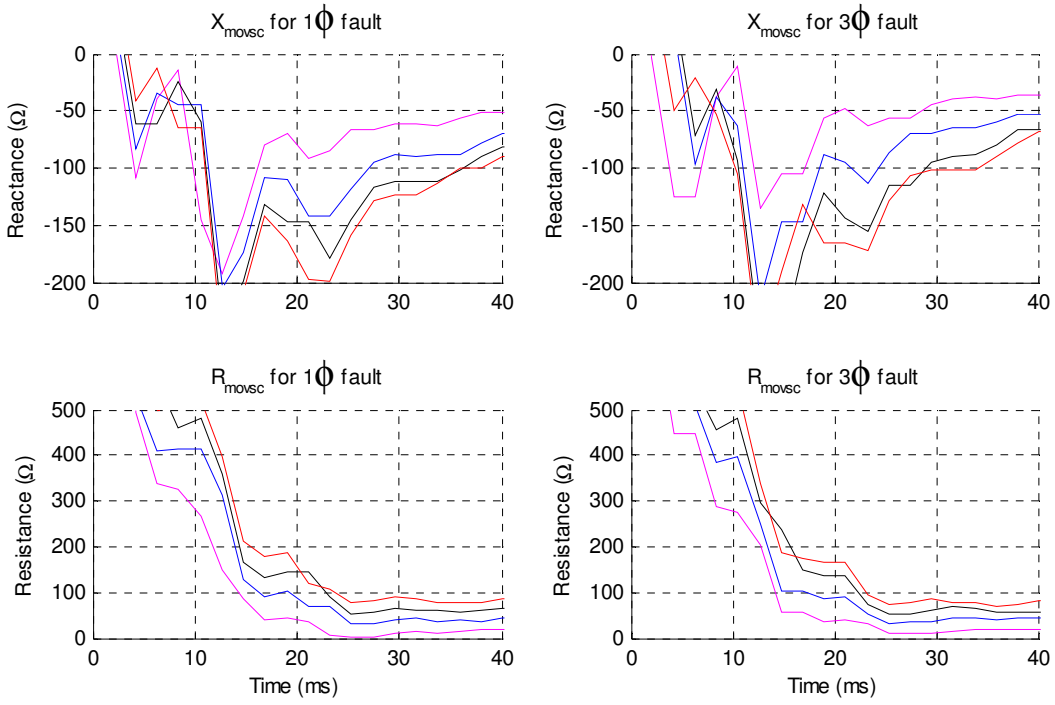

Figure 6.23: Effective impedances as seen from the Bac-Dro line of one phase of the series capacitor bank B for single-phase and three-phase faults at F3 of varying fault resistance: generators at power station P disconnected.

The amplification factors due to infeed currents through the series capacitor bank B are shown in Figure 6.24. The amplification factor (I_{BF}/I_{DB}) is lower without generators at P in service. The lower amplification factor dominates the higher capacitive reactance of the MOV-SC at B during the fault when the generators at P are disconnected, resulting in lower seen reactance, but higher seen resistance from the Bac-Dro line. The fault resistance itself is further amplified due to infeed currents (I_{PF}) from Prot to the fault location. So despite the reduced amplification factor of the seen capacitive reactance, when the generators at P are offline, the problem is that the fault appears much closer towards the relay at Dro along the resistive boundary of the impedance chart for the case when the generators at P are offline. Hence further reduction of the zone 1 resistive coverage is necessary. However, the earlier studies have already shown that for the case of Dro-Bac line, the relays' zone 1 must be turned off to ensure security for external short-circuit faults.

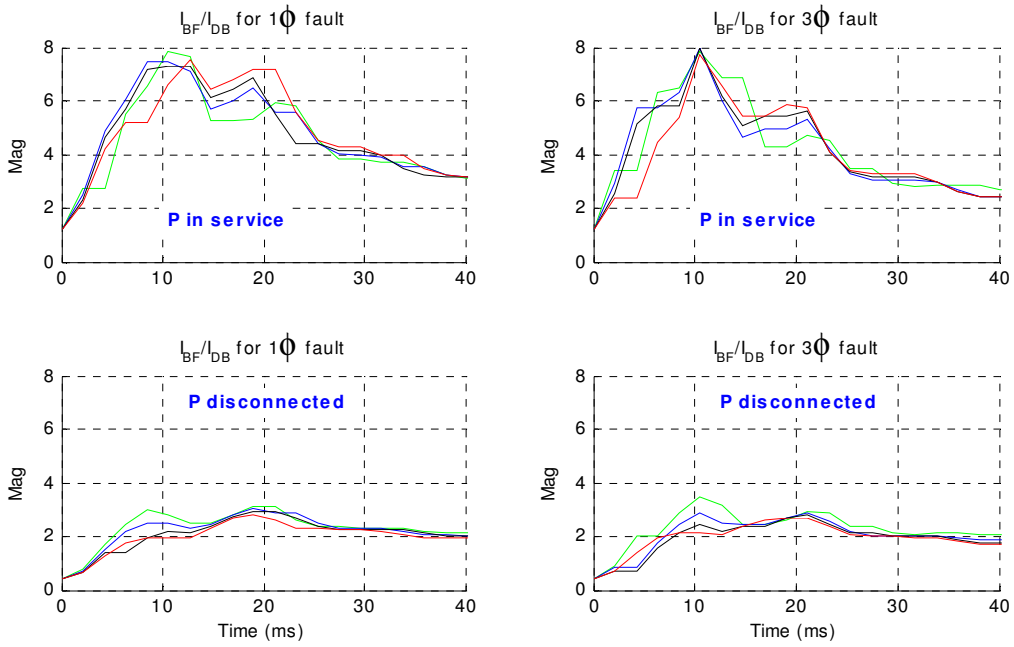

Figure 6.24: Amplification factors I_{BF} / I_{DB} for single-phase and three-phase faults at F3 of varying fault resistance: generators at power station P in service and disconnected respectively.

In the initial stage of this research work, a suggestion was received from utility protection engineers to investigate the feasibility of leaving the zone 1 ground elements turned on (with restricted reach) on the basis that the zero sequence impedance of the protected line may be sufficiently large to push the impedance seen by a relay during ground faults, even in the presence of the series capacitors, outside the restricted zone 1 reach. This idea initiated further testing of the physical relay at Dro to determine the extent of the overreaching of its zone 1 element for external phase versus ground faults. Zero-resistance faults (both single-phase and three-phase) were applied at increasing distances down the Bac-Prot line, starting immediately behind series capacitor bank B and moving towards Prot. These tests showed that, with the originally-calculated zone 1 reach at Dro, its zone 1 element stops tripping for ground faults

located further than 10% down the Bac-Prot line behind the series capacitor bank B when the generators at P are connected, but stops tripping for phase-to-ground faults located further than 6% down the Bac-Prot line when the generators at P are out of service. By contrast, for phase-to-phase faults, the zone 1 element at Dro stops tripping for faults located further than 10% down the Bac-Prot line when the generators at P are connected, but only stops tripping for faults further than 33% down the Bac-Prot line when the generators at P are out of service.

These tests confirmed that, for phase faults in particular, the potential for over-reaching of the relay at Dro is worse when the generators at P are disconnected. They have also shown that it is incorrect to assume that the extent of overreaching for grounds faults is less than that for phase faults: in other words, despite the increased zero sequence impedance of a transmission line, the extent of the overreaching due to grounds faults in series compensated networks may well be worse than that for phase faults, and is dependent on the system operating conditions.

6.5 Conclusion

The performance of the REL531 relays, aided with a permissive overreaching scheme, were evaluated for a particular series compensated line in the wider heavily series compensated Eskom transmission network of the Western Cape. A comprehensive simulation study has been performed to validate REL531 relays' settings and only selected results for internal and external faults were presented and discussed. The REL531 relay protection scheme has been tested and validated using both dynamic models of the relaying algorithms and the practical relays connected hardware-in-loop. When using such relays in a heavily series capacitor compensated network, they must have a high level of security with regard to operation of their instantaneous tripping zone 1s.

This chapter has presented the results of detailed dynamic studies, using a real-time simulator and hardware-in-loop relay testing configuration. The results have shown that by using actual relays for testing, in combination with a detailed real-time model of the relaying algorithms, it is possible to determine with greater confidence, when to reduce the reach of high-speed distance elements, and when it is genuinely not possible to use such elements. As a result of these studies it has also been possible to identify important system properties that impact on the extent to which series capacitors result in over-reaching in distance relays and to show that detailed dynamic studies are required if such relays are to be set with confidence.

Chapter Seven presents comprehensive simulation results of detailed real-time simulator testing of distance relays, using both physical relays and real-time models of the relay algorithms, to determine the performance of, and appropriate settings for these relays when used to protect an uncompensated line adjacent to heavily series capacitor compensated lines in this Eskom network.

CHAPTER 7

THE REL531 RELAY PERFORMANCE ANALYSIS FOR UNCOMPENSATED LINE WITHIN A HEAVILY SERIES COMPENSATED NETWORK: MUL-BAC CASE STUDY

7.1 Introduction

The previous chapter presented the results of detailed dynamic studies for the Bac-Dro series capacitor compensated line within a heavily series compensated network, using a real-time simulator and hardware-in-loop relay testing configuration. This chapter considers the effect of external series compensating capacitors on an uncompensated line's protection in a heavily series compensated network.

In this chapter, the detailed dynamic simulation model is used to study the performance of a distance protection scheme for the Mul-Bac line in the network using the actual numerical distance relays, connected in closed-loop with the real-time power system model. The real-time model of the relays is once again run in parallel with the actual relays under study, in order to gain a better insight into the reasons for their response to particular fault scenarios.

This chapter presents comprehensive results of detailed real-time simulator testing of distance relays, using both physical relays and real-time models of the relay algorithms, to determine the performance of, and appropriate settings for these relays when used to protect the Mul-Bac uncompensated line within a heavily series compensated network.

7.2 Voltage reversal effects on measured impedance in the uncompensated Mul-Bac line

Series compensating capacitors significantly affect compensated lines' protection as well as uncompensated lines' protection within Eskom's series compensated network. The voltage reversal phenomenon explained earlier has spread into uncompensated lines to the extent that zone 1 elements in a number of transmission lines are turned off. The distribution of the voltage reversal depends on the network topology, series capacitor locations and degree of compensation. The Mul-Bac uncompensated transmission line is one of the critical lines affected by series compensating capacitors on adjacent lines (see Figure 7.1). The Mul-Bac line is electrically close to two strong sources (generation at power stations K and P) and is electrically far from a weaker source at H (see Figure 5.1). The Mul-Bac line is relatively short (110 km) and is adjacent to long parallel compensated lines (400 km) from Dro to Bac. Figure 7.2 shows the normalized Mul-Bac line impedance, series capacitor bank B reactance and combined MOV-SC impedance. It is obvious that the resultant negative reactance during short-circuit faults behind the series capacitor bank at B would affect relay settings of the Mul-Bac line and adjacent lines.

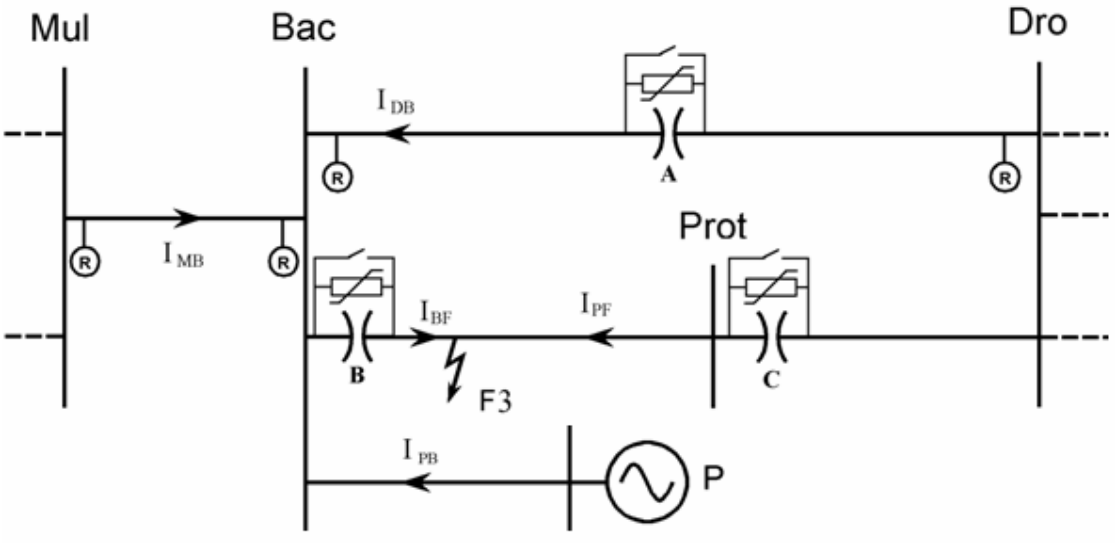

Figure 7.1: The expanded view of the area containing the relays under investigation for external faults.

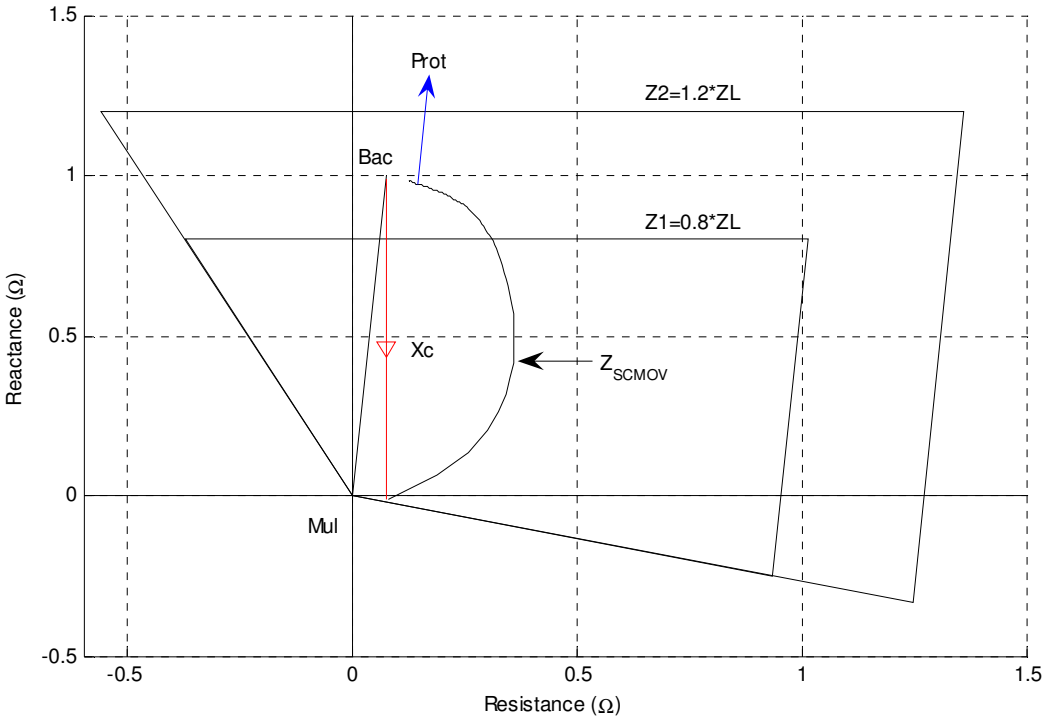

Figure 7.2: The effect of MOV series capacitor combination on the impedance seen by the relay at Mul for a fault behind series capacitor bank B.

It is also obvious that series capacitor bank B would cause voltage reversal at the Bac bus-bar during short-circuit faults behind the series capacitor terminals. Due to infeed fault currents, the voltage reversal would extend to the Mul bus-bar. In order to determine the appropriate zone 1 reaches for the relays in the Mul-Bac line, the performance of these relays were analyzed by applying faults at point F3 in the real-time model of Figure 7.1, just behind the series capacitor bank B in the adjacent Bac-Prot line. For a fault

located at this point F3, the relays on the Mul-Bac line are not supposed to operate; however, such a fault could appear in zone 1 of the relay at Mul if the net capacitive reactance between the busbar at Bac and the point of the fault F3 is sufficiently large. A calculation based solely on the parameters of the Mul-Bac line and the steady-state capacitive reactance of the series capacitor bank B indicated that not only does such a possibility exist, but that the fault would appear *behind* the relay at Mul. However, a detailed simulation study was required to determine the effective impedance of the series capacitors B under *dynamic* fault conditions as seen from Mul-Bac line.

In the initial studies, the relays in the Mul-Bac line were first set without concern for the effects of the series capacitors in adjacent lines. This meant that the zone 1 reach of the relays was set to 80% of the Mul-Bac line length. The extent of any over-reaching for external faults was then determined to decide on adjusted zone 1 settings of the relays at Mul. Subsequently, further fault studies were carried out to consider the effect of both fault arc resistance and the status (connected or off-line) of the generators at power station P on the over-reaching of the relays in the Mul-Bac line.

7.2.1 Response of the relays at Mul

In the initial studies of the REL531 relay performance in the Mul-Bac line, it was found that despite the immediate conduction of the MOVs in parallel with the series capacitors at B, and the subsequent removal of the series capacitor bank by their bypass breakers, the REL531 relay at Mul tripped incorrectly, indicating that the fault at F3 had resulted in significant over-reaching. In order to verify the reasons for the incorrect tripping of the REL531 relays at Mul, the parallel real-time models of the affected relays were analysed. Figures 7.3 and 7.4 show the dynamic impedance calculated by the parallel real-time model of the relay at Mul for a single-phase-to-ground fault and a three-phase fault at F3. The results show that the impedance seen by this parallel relay model in all three phases enters the zone 1 quadrilateral polygon characteristic, confirming that the zone 1 reach of 80% of line reactance is not appropriate for the Mul-Bac line. In other words, even though there is no series compensation in the Mul-Bac line itself, it is still necessary to reduce the zone 1 reach of its relays to prevent over-reaching as a result of the series capacitors in the adjacent Bac-Prot line. In case of the single-phase fault, Figure 7.3 shows that the impedance seen by the parallel relay model enters the zone 1 characteristic. The results therefore confirm that for the relay at Mul, reduction of the zone 1 reach of the ground elements is required. Figure 7.3 indicates that a reduction of the reactive reach to 56% (~ 20 Ω) would be sufficient, at least under these system operating conditions.

As for the three-phase fault, Figure 7.4 indicates that a quite substantial reduction in the reactive reach of zone 1 to 30% of line reactance (~ 10 Ω) is necessary in this line, under these operating conditions. However, the results also indicate that it is still possible to operate with a high-speed zone 1 element in the relays protecting this line (albeit with reduced reach) despite the fact that, as described earlier, simple

steady-state calculations would incorrectly point to more severe under-reaching and the need to turn off the zone 1 elements in this case. Comparison of the results of similar tests in Chapter Six for the relay at Dro (Figures 6.13 and 6.14) with those at Mul (Figures 7.3 and 7.4) suggests that the extent of the over-reaching phenomenon is far more pronounced in the relay at Dro than is the case for the relay at Mul, despite the fact that in each case the over-reaching is actually caused by the same external series capacitor bank B.

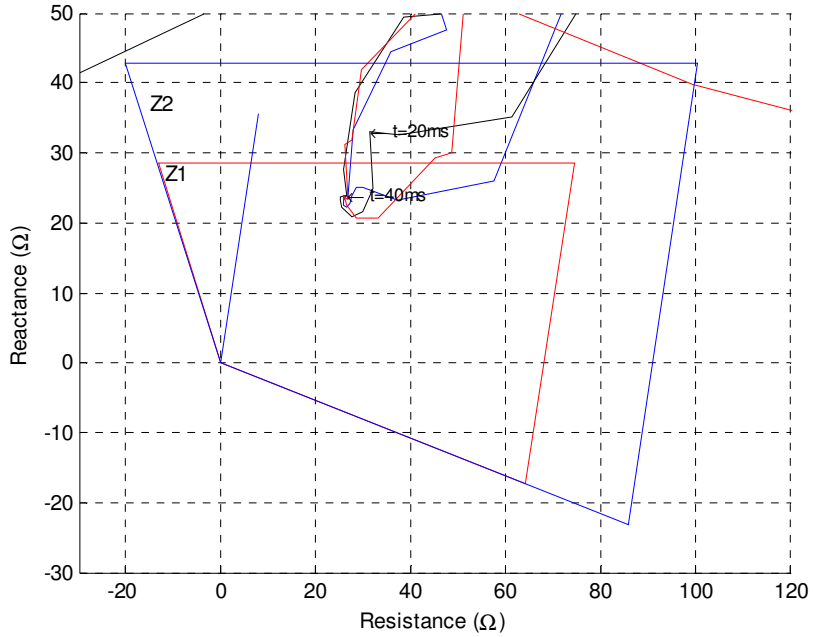

Figure 7.3: Impedance seen by the real-time model of the relay at Mul for a single-phase fault at F3.

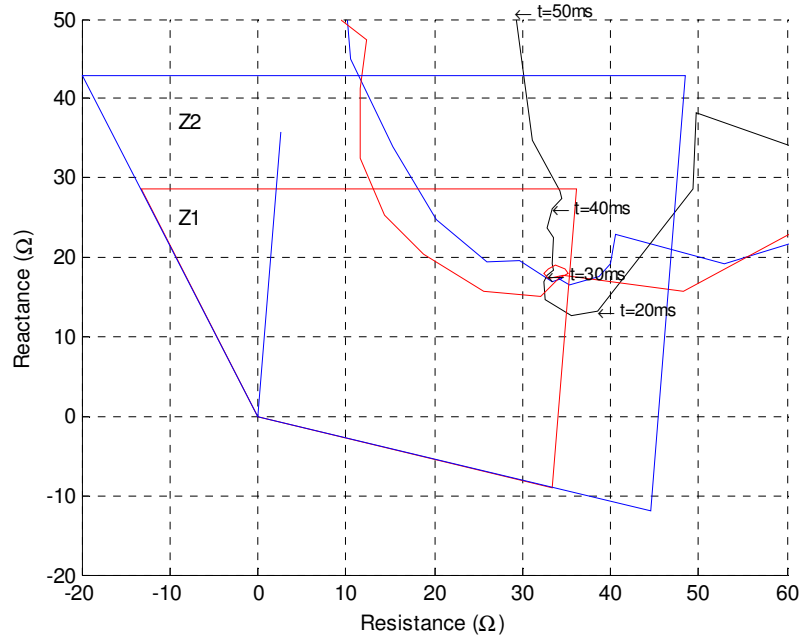

Figure 7.4: Impedance seen by the real-time model of the relay at Mul for a three-phase fault at F3.

7.3 The effect of infeed currents on seen impedance of external series capacitor bank

In order to confirm and then explain the overreaching problem, further analytical calculations were carried out within the real-time simulation model to determine the impedance actually presented by the series capacitor bank B during the faults examined in the previous studies, as well as the effective impedance of this series capacitor bank B that is seen from within the Mul-Bac line.

Consider, once again, the single-line diagram in Figure 7.1. Due to the different system strengths on either side of the busbar at Bac, for a fault located at F3 the individual fault currents contributed by the Mul-Bac and Bac-Dro lines are quite different: the current I_{MB} contributed to the fault by the Mul-Bac line is somewhat larger than the current I_{DB} contributed by the Bac-Dro line. Because each of the lines that feeds current into the fault at F3 contributes only a fraction of the total fault current I_{BF} flowing through the series capacitor bank B, the effective impedance of this capacitor is amplified when seen by the relays within each of these lines. The extent to which such amplification of the effective impedance of series capacitor bank B occurs in a particular line is governed by the ratio of the total fault current I_{BF} to the fault current contributed by that line. In effect, this means that for a fault at F3, there is likely to be a lower amplification of the "seen" impedance of series capacitor bank B (over its actual impedance) at the relay located at the stronger end of the system (Mul) than is the case at the relay located at the weaker end of the system (Dro). The amplification factors for the Dro-Bac line and Mul-Bac line are given by eqns.7.1 and 7.2 respectively.

$$\frac{I_{BF}}{I_{DB}} = \frac{I_{DB} + I_{MB} + I_{PB}}{I_{DB}} \tag{7.1}$$

$$\frac{I_{BF}}{I_{MB}} = \frac{I_{DB} + I_{MB} + I_{PB}}{I_{MB}} \tag{7.2}$$

Figure 7.5 shows the impedance in one phase of the series capacitor bank B as seen from the Mul-Bac and Dro-Bac lines during a single-phase and a three-phase fault at F3. It should be noted that for the purposes of this and the remaining studies, the trip signals from the hardware relays were deliberately blocked. Figure 7.5 (c) shows the dynamic impedance of phase A of the series capacitor bank B and its MOV during a phase-to-ground fault and a three-phase fault; it represents the actual impedance of the capacitor bank B and MOV in phase A during each fault study. Figures 7.5 (a) and (b) show the impedances in phase A of the series capacitor bank B as seen from each of the neighbouring lines Mul-Bac and Bac-Dro during the same ground and phase faults considered previously. In the case of the Mul-Bac line, this impedance was calculated within the real-time model using the voltage at Bac (i.e. the voltage at the remote end of the Mul-Bac line from the over-reaching relay at Mul) and the current flowing into Bac down the Mul-Bac line. Similarly, the impedance seen by the relay at Dro was

calculated using the voltage at Bac (the remote end of the Bac-Dro line from the over-reaching relay at Dro) and the current flowing into Bac down the Bac-Dro line.

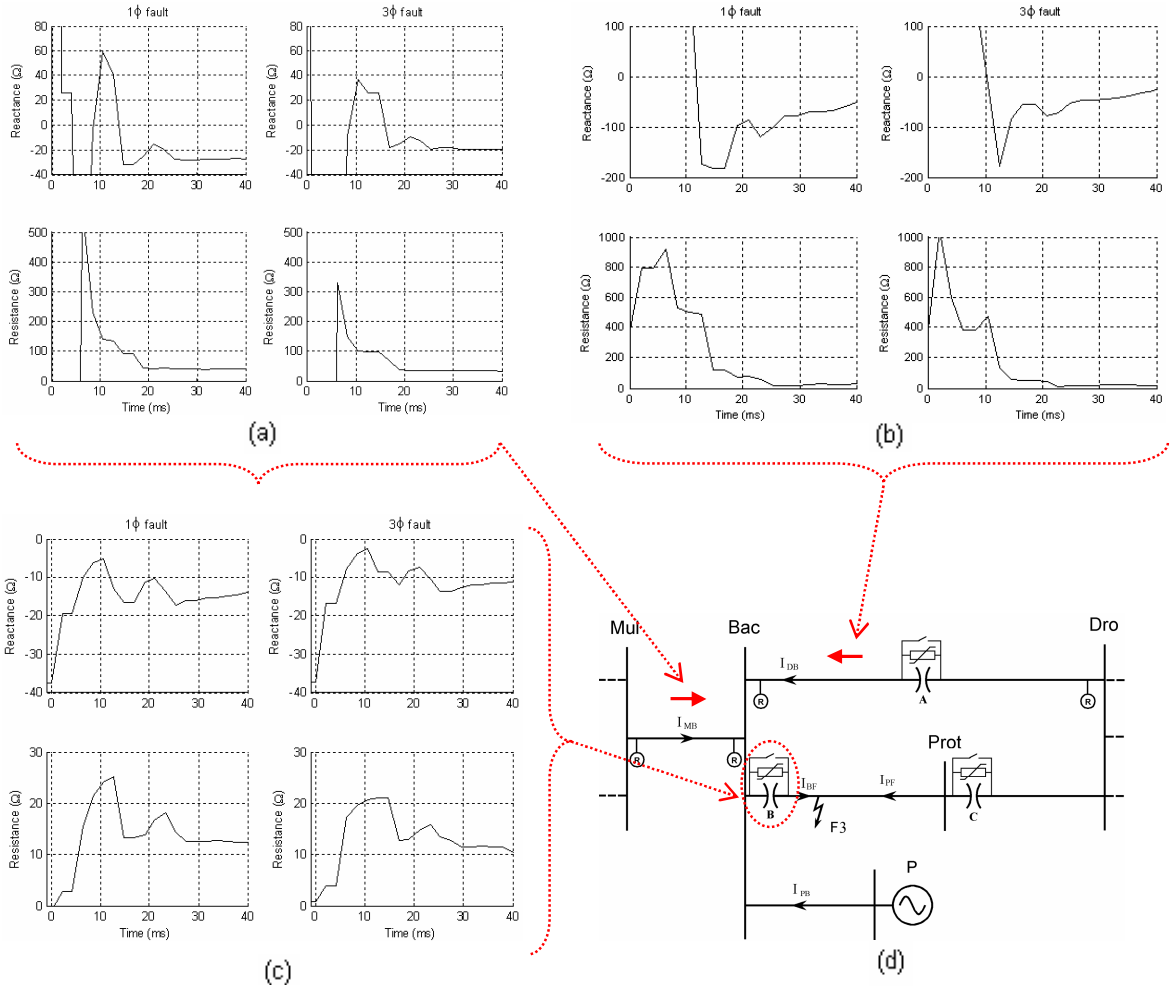

Figure 7.5: The impedance in one phase of the series capacitor bank B as seen from Mul-Bac and Dro-Bac lines during single-phase and three-phase faults at F3.

The results show that in the 20 ms following the application of the fault at F3 (i.e. during the period that the zone 1 elements of the relays at Mul and Dro take the decision to operate when not blocked) there is a noticeable difference between the amount of capacitive compensating reactance presented by series capacitor bank B for phase-to-ground and phase-to-phase faults. The reason for this difference lies in the fact that the amplitude of the current in a three-phase fault is larger than that in a single-phase fault at the same location: the larger current in the three-phase fault at F3 forces the MOVs to conduct more current, and to do so for longer durations on each half cycle, than is the case for the single-phase fault at F3, which in turn results in a greater reduction in the effective compensating reactance of the series capacitor by the MOVs during the three-phase fault.

Comparison of these impedances seen by the two relays at their respective line ends for phase-to-ground and phase-to-phase faults in Figures 7.5 (a) and (b), with the actual impedances presented by the series capacitor bank B during the same faults (Figure 7.5 (c)) confirms that in all cases the seen impedance is indeed magnified over the actual impedance of the series capacitor bank B and MOV combination under dynamic fault conditions. However, the comparisons also show that the extent of the amplification of the seen impedance over the actual impedance is considerably greater (for both phase-to-ground and phase-to-phase faults) for the relay at Dro than is the case for the relay at Mul. This finding is consistent with the measured response of the actual hardware relays at Mul and Dro, and with the behaviour of the parallel real-time models of these two relays, which have both shown far greater over-reaching for phase-to-ground and phase-to-phase faults at F3 for the case of the relay at Dro (see Figures 6.13 and 6.14).

As described earlier, this greater amplification of the reactance of the series capacitor bank B for external faults seen by the relay at Dro can be explained by the fact that this relay is located at the weaker of the two ends of the system. As final confirmation of this reasoning, Figure 7.6 shows the ratios between the actual fault current I_{BF} in the series capacitor bank B and the individual fault currents contributed by the Mul-Bac and Bac-Dro lines for the phase-to-ground and phase-to-phase faults at F3. These fault current ratios were calculated using instantaneous currents obtained from the real-time simulation studies, but with the trip signals from the hardware relays again blocked. The results confirm that in the 20 ms following the application of the fault (i.e. during the period that the zone 1 elements of the relays at Mul and Dro take the decision to operate when not blocked) the fault current ratio I_{BF} / I_{MB} experienced at Mul is noticeably smaller than the fault current ratio I_{BF} / I_{DB} at Dro for both ground and phase faults. Thus the different amplifications of the effective impedance of the series capacitor bank and MOV combination at B can in fact be explained by the differences in fault current magnitudes contributed by the two adjacent lines.

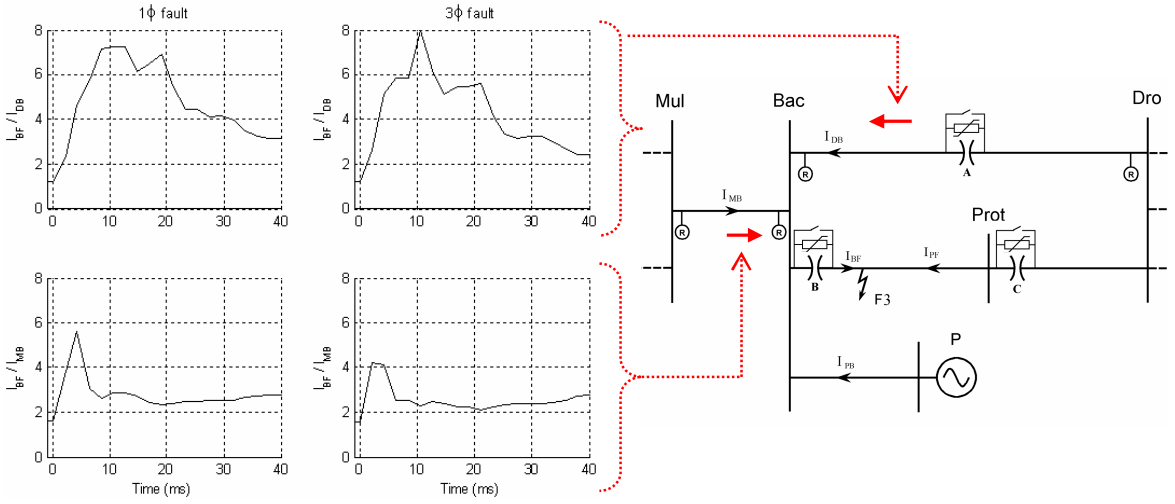

Figure 7.6: Amplification factors I_{BF} / I_{MB} and I_{BF} / I_{DB} for single-phase and three-phase faults at F3.

7.4 The impact of fault resistance and status of generators at power station P

The previous tests were all conducted for zero-resistance faults, with the generators at power station P in service. Those results have shown that the effective impedance of the series capacitor bank B seen by the relays in each adjacent line depends on the actual impedance of the SC-MOV combination during the fault (which in turn depends on the fault current through series capacitor bank B), and the extent of the amplification of this impedance in each adjacent line (which depends on the percentage contribution of the fault current at F3 from that adjacent line). The presence of resistance in the fault at F3 will reduce the amplitude of the through-fault current at series capacitor bank B to some extent, and if the generators at power station P are not in service, the percentage contribution to this fault current from the Mul-Bac line will be considerably higher; hence each of these factors is likely to influence the effective impedance of the series capacitor bank B seen by the relays at Mul and Dro, and hence the extent to which their zone 1 reaches may require further reduction. For this reason, additional tests were carried out using the real-time simulation model for various values of non-zero fault resistance, with and without the generators at P in service.

Figures 7.7 and 7.8 show the dynamic impedances seen by the relay at Mul for single-phase-to-ground and three-phase faults of varying resistance at F3, with the generators at P in service and disconnected respectively. In both Figures 7.7 and 7.8 (ie. with or without generators connected at power station P), as the fault resistance increases, the impedance seen by the relay at Mul has progressively lower reactance, but also progressively higher resistance: the lower seen reactance is due to the reduced fault current, and hence reduced extent of MOV conduction at series capacitor bank B during the fault, as the resistance of the fault increases; the larger seen resistance is due to the increased MOV resistance associated with its own reduced conduction at higher fault resistances, as well as the higher fault resistance itself adding to the impedance seen by the relay. However, comparison between Figures 7.7 and 7.8 shows that the encroachment of the seen impedance towards the zone 1 polygon of the relay at Mul is marginally worse for ground faults when the generators at power station P are out of service, but the impedance comes noticeably closer to zone 1 at Mul for phase faults when the generators at power station P are disconnected.

A study of the actual impedance of the MOV-SC combination at series capacitor bank B in Figures 7.9 and 7.10 and that seen by the relay at Mul in Figures 7.11 and 7.12 shows two competing effects when the generators at power station P are disconnected: with no generators at power station P the fault current at F3 is lower, meaning reduced MOV conduction and hence larger effective capacitive reactance at series capacitor bank B during the fault; however, with no fault current contributed by the generators at power station P, a larger portion of this reduced fault current at F3 comes from the Mul-Bac line, hence there is less amplification of the actual impedance of the capacitor bank B during the fault (see amplification factors in Figure 7.13). In the case of phase faults in particular, the increased effective capacitive

reactance at series capacitor bank B during the fault outweighs the reduced amplification factor at Mul when the generators at power station P are disconnected, so that there is *greater* over-reaching of the phase elements at Mul for a fault at F3 when the generators at power station P are disconnected. Also of interest in Figure 7.13 are the short-duration but higher-amplitude values of amplification factor that are observed between zero and 10 ms when the generators at P are connected, but which are not present when the generators at P are disconnected; these initial transients in the amplification factor might be the result of fast-decaying subtransient components in the fault current that would only be present when the electrically-close generators at P are in service.

This understanding was confirmed by conducting a further test to determine the extent of the over-reaching of the zone 1 element in the relay at Mul. Zero-resistance faults (both single-phase and three-phase faults) were applied at increasing distances down the Bac-Prot line, starting immediately behind series capacitor bank B and moving towards Prot. These tests showed that, with the originally-calculated zone 1 reach at Mul, its zone 1 element stops tripping for ground faults located further than 8% down the Bac-Prot line behind SCB when the generators at power station P are connected, but stops tripping for phase-to-ground faults located further than 10% down the Bac-Prot line when the generators at power station P are out of service. By contrast, for phase-to-phase faults, the zone 1 element at Mul stops tripping for faults located further than 10% down the Bac-Prot line when the generators at power station P are connected, but only stops tripping for faults further than 21% down the Bac-Prot line when the generators at power station P are out of service. These tests confirmed that, for phase faults in particular, the potential for over-reaching of the relay at Mul is worse when the generators at power station P are disconnected.

Thus both the relays at Mul and Dro see phase-to-phase faults located behind the external series capacitor bank B appearing significantly nearer to their respective locations when the generators at power station P are disconnected; by contrast, when the generators at power station P are disconnected, the relay at Mul sees phase-to-ground faults located behind series capacitor bank B appearing marginally closer to its location, whereas the relay at Dro sees such faults appearing marginally further from its location.

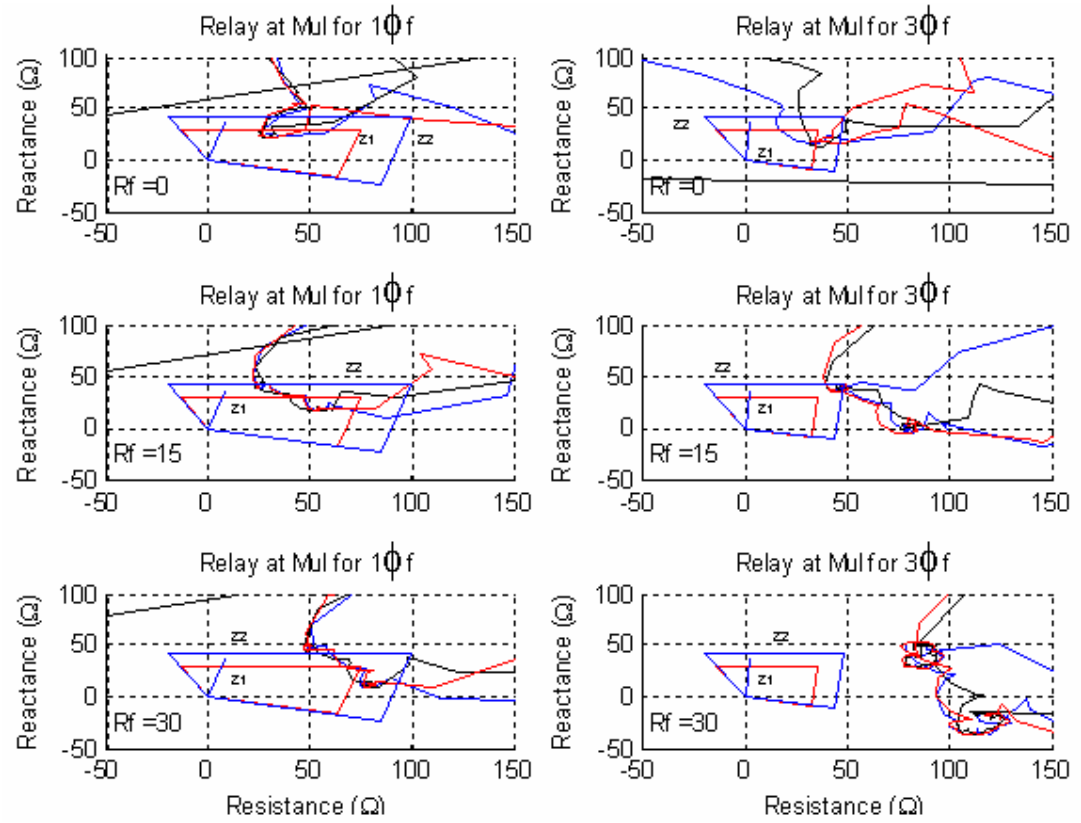

Figure 7.7: Impedances measured by relay at Mul for single-phase and three-phase faults at F3 of varying fault resistance: generators at power station P in service.

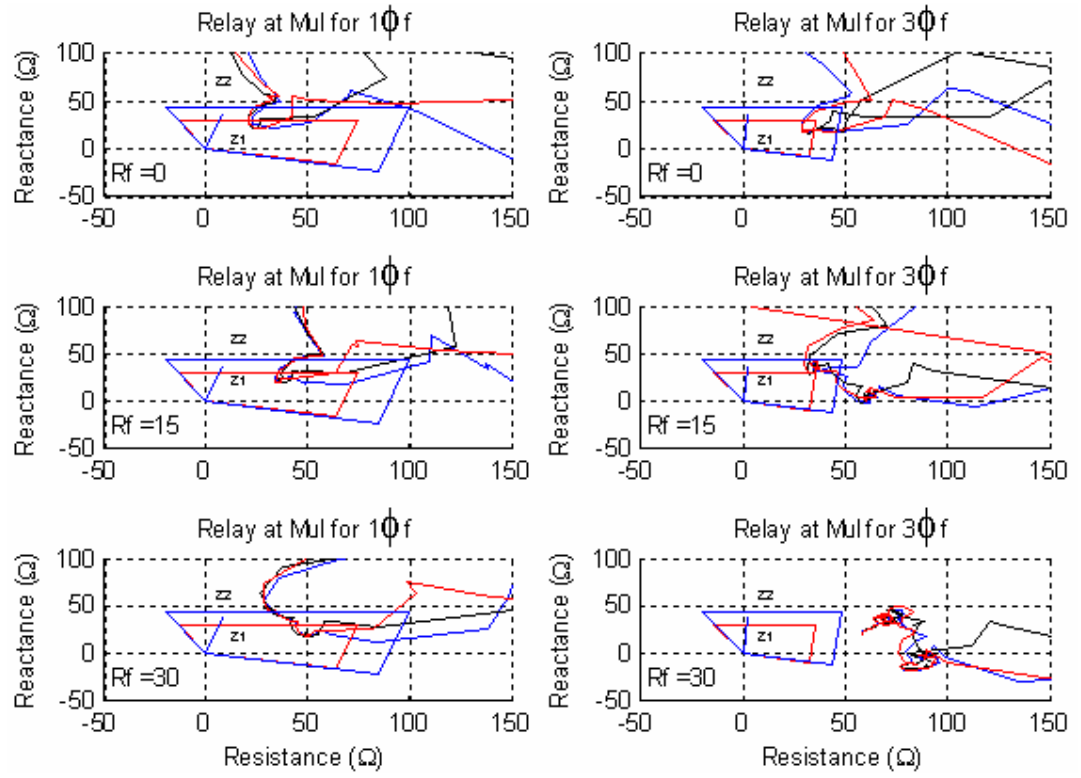

Figure 7.8: Impedances measured by relay at Mul for single-phase and three-phase faults at F3 of varying fault resistance: generators at power station P disconnected.

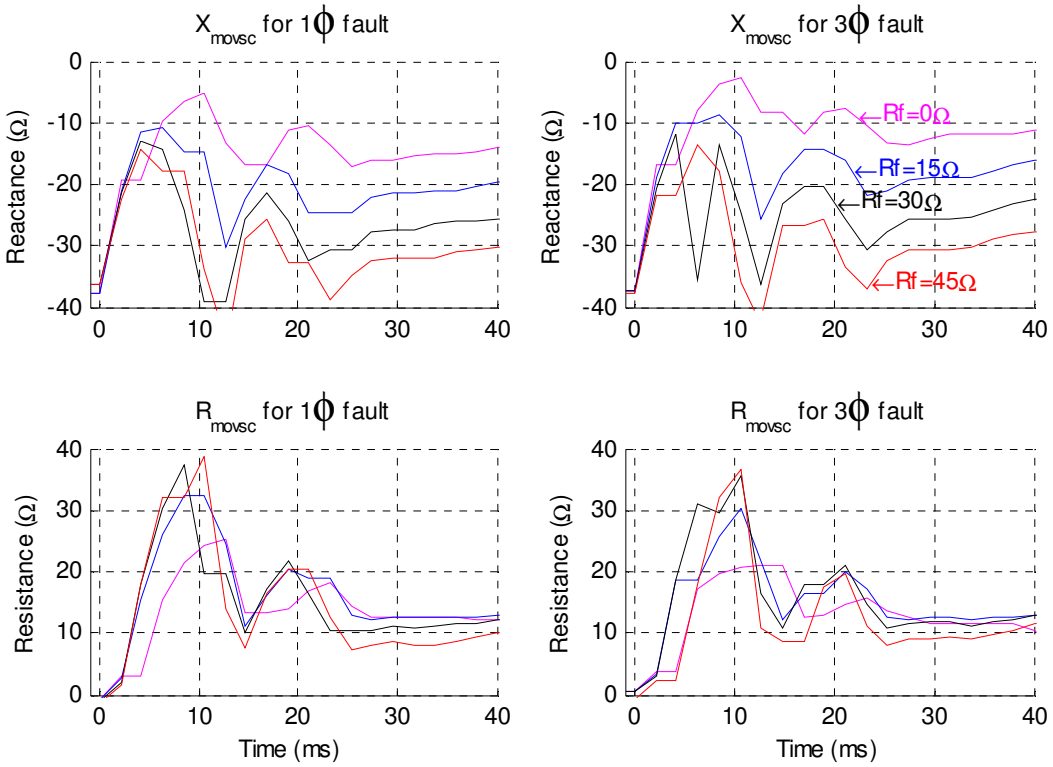

Figure 7.9: Impedances in one phase of the series capacitor bank B for single-phase and three-phase faults at F3 of varying fault resistance: generators at power station P in service.

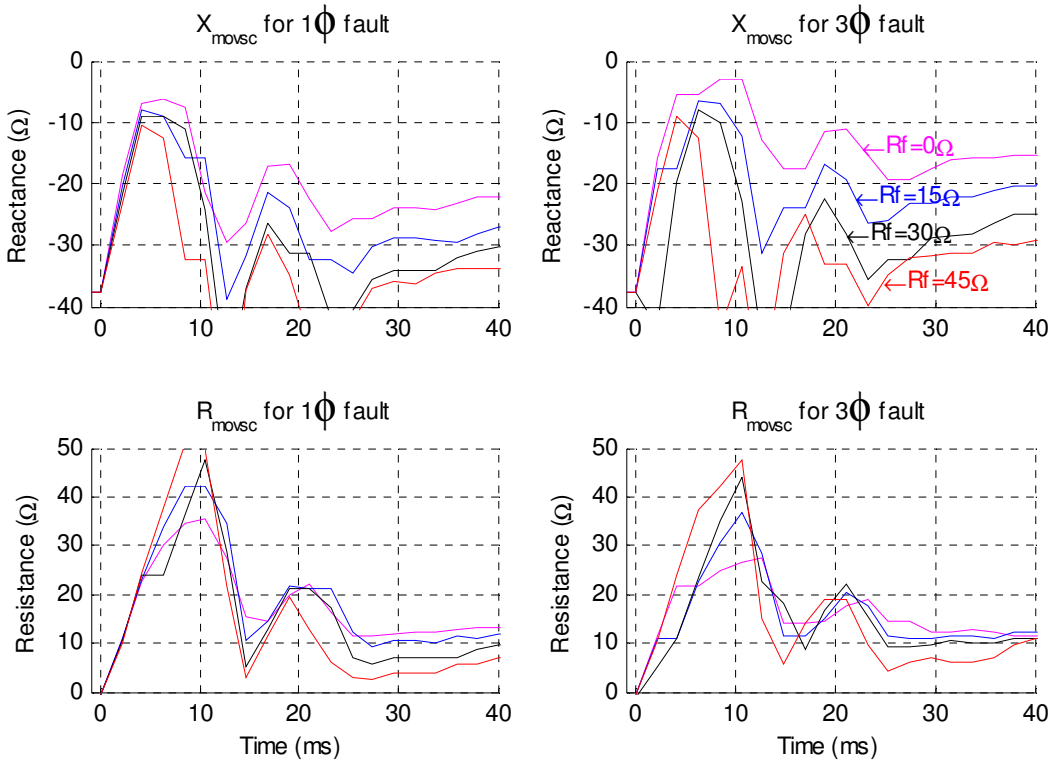

Figure 7.10: Impedances in one phase of the series capacitor bank B for single-phase and three-phase faults at F3 of varying fault resistance: generators at P disconnected.

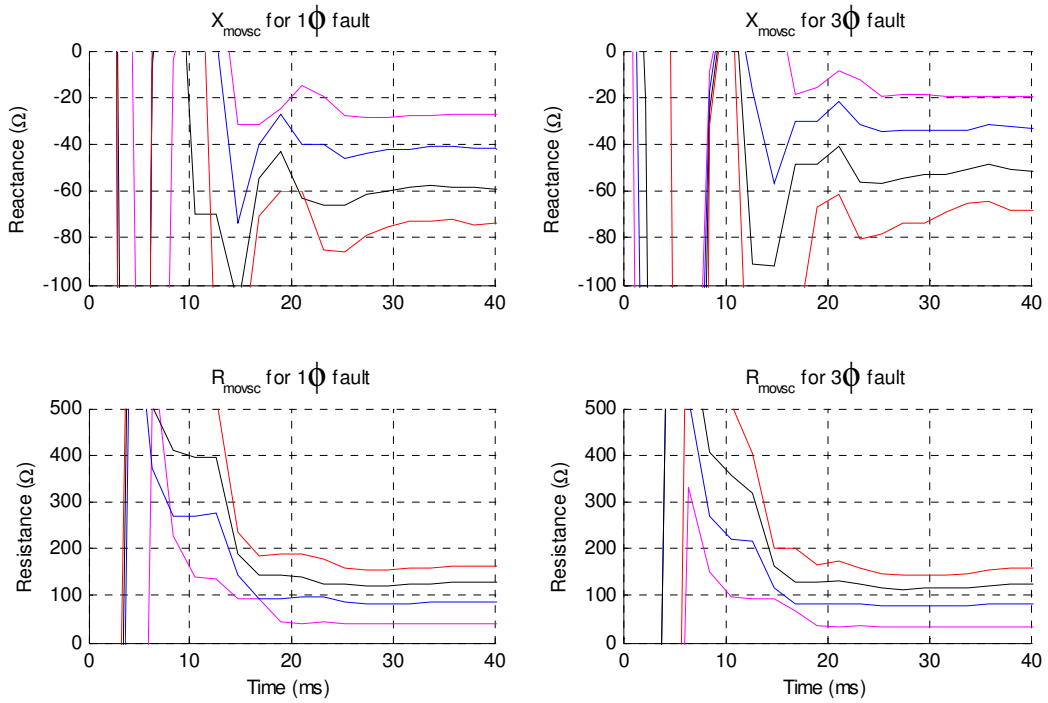

Figure 7.11: Effective impedances as seen from the Mul-Bac line of one phase of the series capacitor bank B for single-phase and three-phase faults at F3 of varying fault resistance: generators at power station P in service.

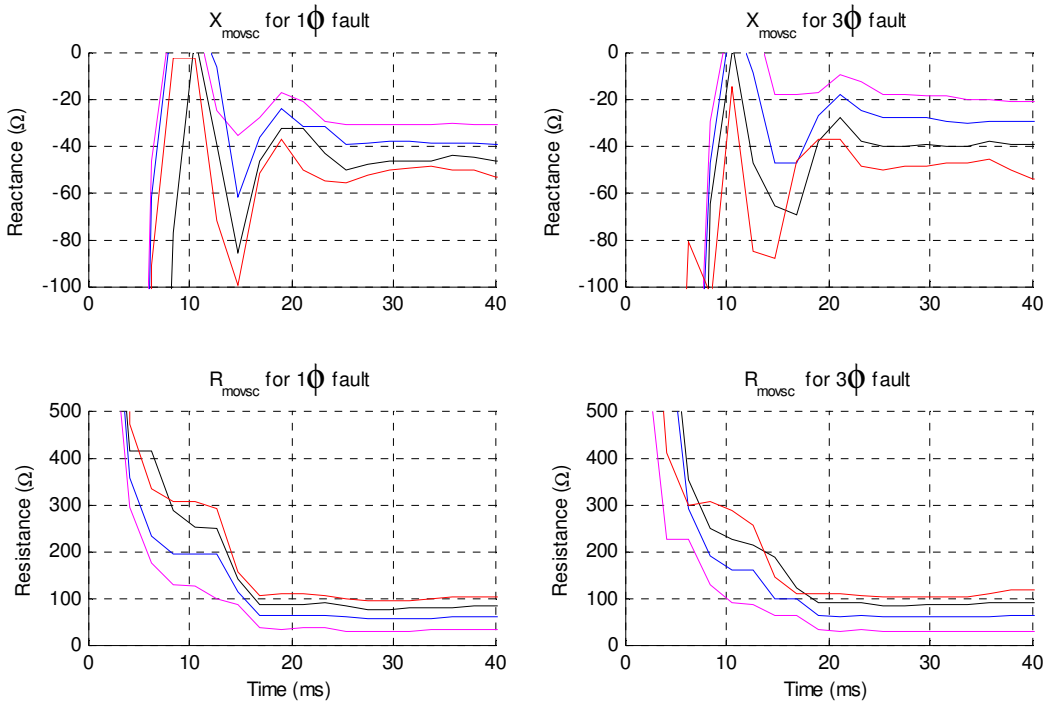

Figure 7.12: Effective impedances as seen from the Mul-Bac line of one phase of the series capacitor bank B for single-phase and three-phase faults at F3 of varying fault resistance: generators at power station P disconnected.

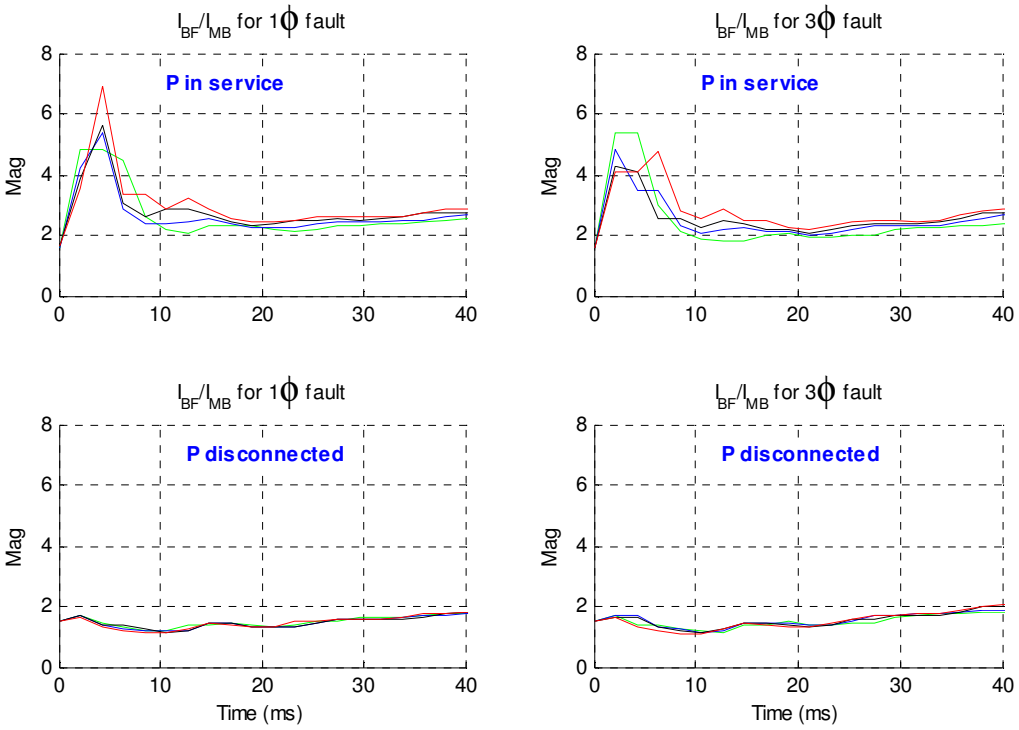

Figure 7.13: Amplification factors I_{BF} / I_{MB} for single-phase and three-phase faults at F3 of varying fault resistance: generators at power station P in service and disconnected respectively.

7.5 Conclusion

This chapter has presented the results of detailed dynamic studies, using a real-time simulator and hardware-in-loop relays, to determine appropriate settings for REL531 distance relays installed in an uncompensated line in the heavily series compensated network of the Western Cape. The results have shown that by using actual relays for testing, in combination with a detailed real-time model of the relaying algorithms, it is possible to determine with greater confidence, the extent to which the reach of high-speed distance elements needs to be reduced in such lines and the factors that influence this reduction in reach needed. As a result of these studies it has also been possible to identify important system operating conditions that impact on the extent to which series capacitors in adjacent lines result in over-reaching in distance relays and to show that detailed dynamic studies are required if such relays are to be set with confidence under different operating conditions. The practical simulation results have also shown that the optimum setting of distance relays depends on network topology, fault resistance, amount of infeed current and general system operating conditions.

Chapter Eight presents the conclusions drawn from the research work presented in this thesis and finally suggests further research work that could be undertaken in this area.

CHAPTER 8

CONCLUSION AND SUGGESTION FOR FURTHER RESEARCH

8.1 Introduction

This thesis has examined the performance of distance protection schemes in Eskom's heavily series compensated Western Cape transmission network, under a wide range of practical fault scenarios, using the actual numerical distance relays that are used in the field, connected in closed-loop configuration with a real-time power system model. The investigations have shown that using this approach, it will be possible to evaluate many more of the features of these modern numerical relays under realistic test conditions in the future. This chapter presents the conclusions of this thesis, chapter by chapter, and finally suggests further research studies that could be undertaken as extensions of this thesis.

8.2 Conclusions

The introductory chapter (Chapter One) explained that the main objective of series compensating capacitors in Eskom transmission lines is to increase power transfer capacity. Chapter One also highlighted protection challenges presented by series compensating capacitors. Then a brief review of relaying technology development was considered and advanced numerical relays were identified as suitable for series compensated transmission line protection. However, protection relay application in series compensated networks is not straight forward, hence careful analysis, evaluation and testing has been emphasized.

The literature review in Chapter Two provided the background theory and the initial review carried out into the technical challenges presented when designing distance protection schemes and setting advanced numerical distance protection relays in the presence of series compensating capacitors. The chapter reviewed the fundamentals of protection philosophies with more emphasis placed on protection of series compensated lines. The review also highlighted protection challenges, proposed solutions and their drawbacks. These solutions are not all thoroughly evaluated and tested nor accepted by electrical utilities and relay manufacturers [30].

Chapter Three has described the particular numerical distance protection relay, the REL531, that has been used in this research work. This particular relay is designed for use in series compensated networks and is currently used in all new protection schemes at transmission voltage levels by the national electricity utility in South Africa.

The installation of series capacitors in a transmission network complicates the design and setting of protection relays in the neighborhood of the series capacitors. Chapter Three considered the application of the fast hybrid protection scheme within the REL531 relay, which combines the high-speed protection

scheme in parallel operation with the modified standard distance protection scheme to cope with voltage reversal. The chapter also included a detailed description of setting philosophies for uncompensated lines and extended this discussion to series compensated lines.

Chapter Four presented detailed closed-loop testing of the REL531 distance relays with an RTDS real-time simulator on a relatively simple power system model. The real-time simulation model of a simple series capacitor compensated transmission line was developed, including detailed dynamic models of the non-linear characteristics and control logic of the series capacitors' metal oxide varistors (MOVs) and bypass breakers. The impact of the MOV protected series capacitor and bypass breaker during short-circuit faults was simulated and explained. This dynamic model was used to study the performance of the distance protection scheme using the actual numerical relays, connected in a closed-loop configuration with the real-time power system model.

A real-time model of a distance relay has also been developed and used to evaluate the performance of the physical relays under test for non-compensated and series capacitor compensated transmission lines. The relay setting parameters and their performance test results have been presented and explained. The initial simulation results in Chapter Four of this thesis showed the benefits of combining closed-loop testing of physical relays in parallel with a detailed relay model, which enabled the extent of the distance protection challenges to be better quantified and explained.

Chapter Five described a real-time simulation model of Eskom's heavily series compensated Western Cape transmission network that includes detailed dynamic models of the non-linear metal oxide varistor characteristics, control logic of the series capacitor protection and bypass breakers at each series compensation station. This detailed dynamic simulation model was used in Chapter Six and Seven to study the performance of distance protection schemes for specific lines in this network using the actual numerical distance relays that are used in this network, connected in closed-loop with the real-time power system model. The detailed model of the relays themselves developed in Chapter Four was arranged to run in parallel with the actual relays under study, in order to gain a better insight into the reasons for their response to particular fault scenarios. The steady-state analysis of the Western Cape transmission network indicated critical external fault locations for which relays on adjacent lines may operate incorrectly if external series capacitors are not taken into consideration when setting such relays.

Chapter Six presented comprehensive results of detailed real-time simulator testing of distance relays, using both physical relays and real-time models of the relay algorithms, to determine the performance of, and appropriate settings for these relays when used to protect the Bac-Dro series capacitor compensated line within the heavily series compensated Western Cape transmission network.

The performance of the REL531 relays, aided with a permissive overreaching logic scheme, were evaluated for the Bac-Dro series compensated transmission line in the wider heavily series compensated Eskom transmission network of the Western Cape. A comprehensive simulation study has been performed to validate REL531 relays' settings and only selected results for internal and external faults were presented and discussed. The REL531 relay protection scheme has been tested and validated using both dynamic real-time models of the relaying algorithms and the practical relays connected in a hardware-in-loop configuration. When using such relays in a heavily series capacitor compensated network, they must have a high level of security with regard to operation of their instantaneous tripping zone 1s.

Chapter Seven considered the effect of external series compensating capacitors on an uncompensated line's protection in the heavily series compensated Western Cape network. Chapter Seven also used the detailed dynamic simulation model to study the performance of a distance protection scheme for the Mul-Bac line in the network using the actual numerical distance relays, connected in closed-loop with the real-time power system model. The real-time model of the relays was once again run in parallel with the actual relays under study, in order to gain a better insight into the reasons for their response to particular fault scenarios. Chapter Seven presented comprehensive results of detailed real-time simulator testing of distance relays, using both physical relays and real-time models of the relay algorithms, to determine the performance of, and appropriate settings for these relays when used to protect the Mul-Bac uncompensated line within the heavily series compensated Western Cape network.

The simulation results have shown that by using actual relays for testing, in combination with a detailed real-time model of the relaying algorithms, it is possible to determine with greater confidence, when to reduce the reach of high-speed distance elements, and when it is genuinely not possible to use such elements. As a result of these studies it has also been possible to identify important system properties and system operating conditions that impact on the extent to which series capacitors result in over-reaching in distance relays and to show that detailed dynamic studies are required if such relays are to be set with confidence. The practical simulation results have also shown that the optimum setting of distance relays depends on the network topology, fault resistance, amount of infeed current and general system operating conditions.

The settings of a distance protection scheme in a heavily series compensated network remain a challenge. It is very difficult to calculate optimum distance protection settings by following relay setting manuals and standard practice in a large complicated network. Network-specific dynamic simulations, with the series capacitor protection modelled in detail, are practically necessary for fine tuning distance protection settings. It is difficult to foresee the impact of dynamic behavior of the series capacitor compensated transmission network when setting distance protection schemes. The setting of distance protection

schemes through relay manuals and standard practice is not adequate, without a knowledge and understanding of the behavior of the protected network itself. The real-time closed-loop testing approach enables relay setting optimization and provides assurance of a more reliable protection scheme. The closed-loop testing of distance relays with a real-time digital simulator (RTDS) is done in real time so as to be able to re-create their operation under actual power system conditions.

Finally the author recommends further research studies that could be undertaken as extension of this thesis.

8.3 Suggestion for further studies

This thesis has made use of actual numerical distance relays, in parallel operation with a detailed real-time model of the relays' algorithms to study the dynamic performance of such relays in heavily series compensated networks. Although some important distance protection aspects have been addressed, it has not been the objective of this thesis to cover every aspect of series compensated line protection. The results obtained from this research work have identified certain issues which require further studies. Therefore, specific issues which require further research are recommended as follows.

This research work did not consider the following applications to enhance series compensated line protection:

(a) Weak-end infeed logic;
(b) Current reversal logic;
(c) Power swing logic;
(d) Switch onto fault logic.

Detailed dynamic studies are required if such applications are to be implemented with confidence and maintain adequate performance in the presence of series capacitors and their protective equipment (MOV and bypass switch). The investigation could also be extended to examine the transient effects on distance protection when an MOV-protected series capacitor bank is re-inserted.

The real-time relay model developed in this thesis could be further extended and refined. Once the real-time relay model is modified to include more of the advanced features of the actual relay, the real-time model could be very useful for further studies and research in its own right.

The REL531 relay's algorithms do not monitor series capacitor status, hence their decision to trip or not to trip is based solely on the measurements at the relay locations. Therefore, much scope exists for further research in this area.

APPENDIX A

HARDWARE-IN-LOOP TESTING OF THE REL531 RELAYS USING THE RTDS

The RTDS simulator performs power system simulations in real time. When conducting real-time closed-loop testing of distance relays, the simulator provides continuous real time outputs of breaker status, voltages and currents of the simulated power system to the external REL531 relays being tested. The REL531 relays directly control the breakers of the simulated power system in the RTDS hardware. Since the power system is being simulated in real-time, all types of short-circuit faults experienced by the actual power system can easily be studied so as to evaluate the performance of the REL531 numerical distance protection relays connected in closed-loop configuration with the RTDS hardware.

Figure A1: Hardware-in-loop testing of the REL531 relays using the RTDS.

APPENDIX B

DETAILED REAL-TIME CLOSED-LOOP TESTING FOR REL531 RELAY VERIFICATION

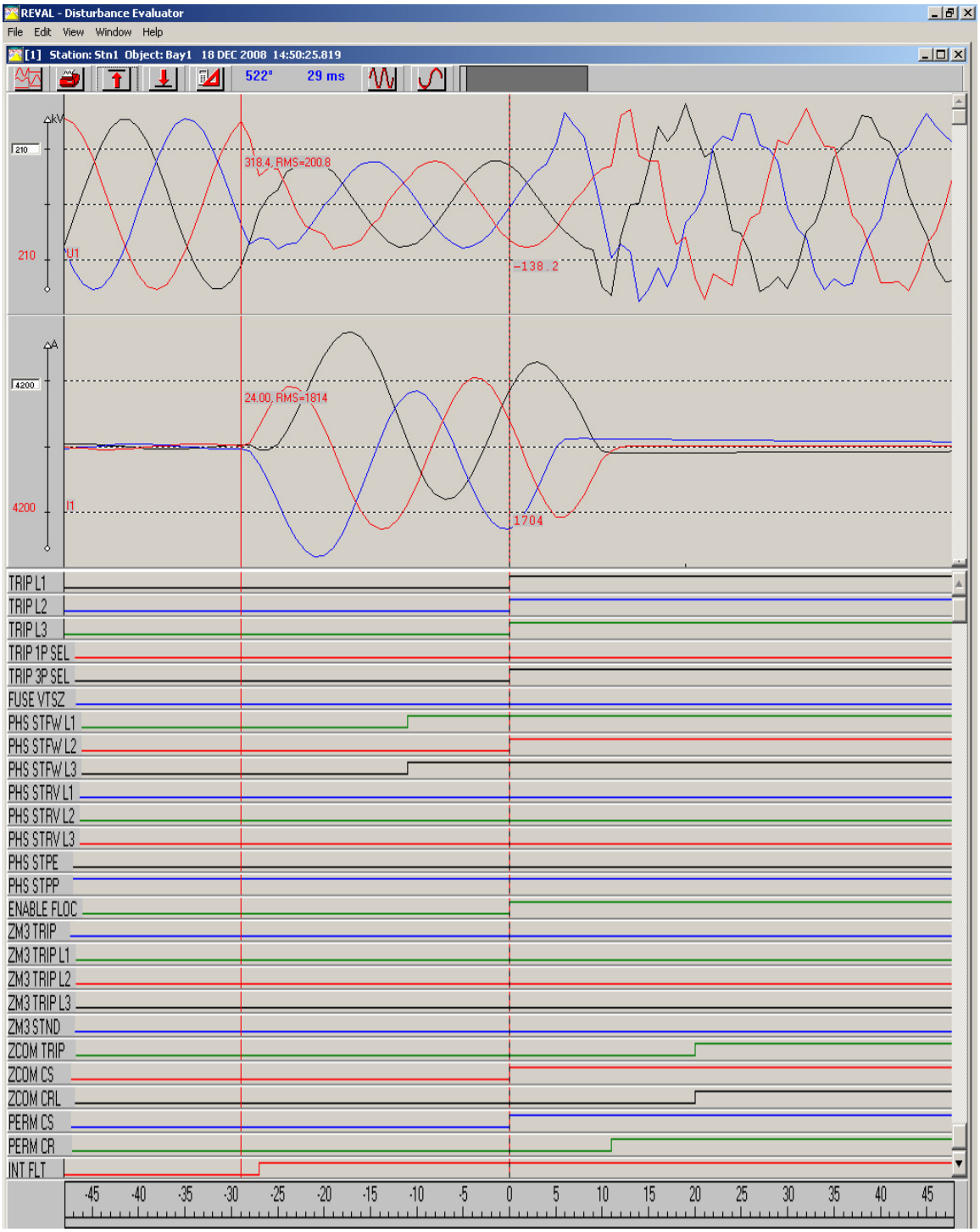

Figure B1: REL531 fault disturbance record from a single REL531 relay upload using the CAP540 software.

Table B1: Standard distance protection scheme performance testing results.

Fault location	Relay 1 performance								Relay 2 performance							
%	FLT LOC %	Trip time	Trip signal	PHS (ms)	Zone 2 STND	ZCOM CS	ZCOM CR	ZCOM TRIP	FLT LOC %	Trip time	Trip signal	PHS (ms)	Zone 2 STND	ZCOM CS	ZCOM CR	ZCOM TRIP
0	0	25	Zone 1	14	25	25	44	55	100	43	ZCOM	22	33	33	33	43
10	9.3	24	Zone 1	14	24	24	43	55	91	41	ZCOM	20	31	31	34	41
20	18.5	29	Zone 1	18	29	29	43	49	82.5	41	ZCOM	20	31	31	31	41
30	27.7	31	Zone 1	20	29	29	45	51	70.1	32	ZONE 1	21	32	32	34	42
40	49.1	23	Zone 1	23	23	23	40	53	60.5	27	ZONE 1	16	27	27	31	37
50	49.9	27	Zone 1	16	27	27	38	47	49.5	26	ZONE 1	15	26	26	36	46
60	71.4	22	Zone 1	22	22	22	39	51	39.8	26	ZONE 1	15	26	26	31	36
70	69.9	28	Zone 1	17	28	28	38	48	29.5	26	ZONE 1	15	26	26	35	46
80	83.8	44	ZCOM	24	24	24	38	44	19.6	27	ZONE 1	16	27	27	36	47
90	100	46	ZCOM	26	26	26	35	46	9.3	24	ZONE 1	24	24	24	38	44
100	100	51	ZCOM	20	31	31	42	51	3.9	30	ZONE 1	19	30	30	43	49

Table B2: The hybrid protection scheme testing results for the simple compensated line.

Relay 1 responses for AG-fault at 20.1 km (5%) from relay 1									
Event	Fault locator			Relay trip times (ms)					
#	Trip type	%	km	Trig signal	HSUR	Z1	HSORCS	Z2CS	CR
1	1 pole	4.6	18.7	HS	13	22	13	22	42
2	1 pole	5	20.2	HS	21	21	21	21	41
3	1 pole	4.7	18.7	HS	18	26	18	26	56
4	1 pole	5	20.3	HS	19	29	19	29	49
5	1 pole	4.7	18.8	HS	14	23	14	23	53
6	1 pole	4.7	18.9	HS	14	23	14	23	53
7	1 pole	4.7	18.7	HS	13	23	13	23	53
8	1 pole	5.1	20.4	HS	18	27	18	27	47
9	1 pole	4.6	18.6	HS	18	27	18	27	47
10	1 pole	5	20.3	HS	19	29	19	29	49
Relay 1 responses for ABCG-fault at 20.1 km (5%) from relay 1									
Event	Fault locator			Relay trip times (ms)					
#	Trip type	%	km	Trig signal	HSUR	Z1	HSORCS	Z2CS	CR
1	3 pole	4.8	19.3	HS	16	25	16	25	35
2	3 pole	8.9	35.6	HS	18	28	9	28	58
3	3 pole	9	36.2	HS	11	21	21	11	40
4	3 pole	4.8	19.4	HS	16	26	16	26	45
5	3 pole	4.9	19.8	HS	16	25	16	25	65
6	3 pole	8.2	33.1	HS	11	21	11	21	40
7	3 pole	9.6	38.8	HS	14	24	14	24	43
8	3 pole	5.2	20.7	HS	12	22	12	22	41
9	3 pole	7.7	31.1	HS	15	24	15	24	64
10	3 pole	8	32.3	HS	18	28	9	28	48
Relay 1 responses for AG-fault at 40.2 km (10%) from relay 1									
Event	Fault locator			Relay trip times (ms)					
#	Trip type	%	km	Trig signal	HSUR	Z1	HSORCS	Z2CS	CR
1	1 pole	9.2	36.9	HS	22	22	22	22	42
2	1 pole	9.2	37	HS	15	24	15	24	44
3	1 pole	9.3	37.5	HS	13	22	13	22	42
4	1 pole	9.3	37.4	HS	22	22	22	22	42
5	1 pole	9.2	37.1	HS	21	21	21	21	51
6	1 pole	9.2	37.1	HS	12	32	12	21	51
7	1 pole	9.2	36.8	HS	13	22	13	22	52
8	1 pole	9.3	37.4	HS	14	23	14	23	53
9	1 pole	10.1	40.7	HS	20	29	20	29	49
10	1 pole	10.1	40.5	HS	19	28	19	28	48
Relay 1 responses for ABCG-fault at 40.2 km (10%) from relay 1									
Event	Fault locator			Relay trip times (ms)					
#	Trip type	%	km	Trig signal	HSUR	Z1	HSORCS	Z2CS	CR
1	3 pole	10.3	41.4	HS	17	27	17	27	56
2	3 pole	9.5	38	HS	11	21	11	21	60
3	3 pole	14.3	57.6	HS	14	24	14	24	53
4	3 pole	4.3	17.2	HS	18	18	9	18	38
5	3 pole	10.4	41.7	HS	10	20	10	20	30
6	3 pole	9.7	39	HS	17	26	17	26	56
7	3 pole	16.1	64.6	HS	15	25	15	25	54
8	3 pole	15	60.4	HS	19	29	10	29	69
9	3 pole	14.6	58.6	HS	20	20	10	20	49
10	3 pole	13.1	52.8	HS	12	21	12	21	51

Relay 1 responses for AG-fault at 80.4 km (20%) from relay 1									
Event	Fault locator			Relay trip times (ms)					
#	Trip type	%	km	Trig signal	HSUR	Z1	HSORCS	Z2CS	CR
1	1 pole	20.4	81.9	HS	19	29	19	29	39
2	1 pole	20	80.4	HS	19	28	19	28	48
3	1 pole	18.4	74	HS	18	27	18	27	47
4	1 pole	20.5	82.3	HS	19	29	19	29	49
5	1 pole	20.2	81.2	HS	19	28	19	28	48
6	1 pole	18.3	73.4	HS	14	23	14	23	43
7	1 pole	20.2	81.3	HS	20	29	20	29	49
8	1 pole	18.5	74.3	HS	15	24	15	24	44
9	1 pole	20.1	80.7	HS	21	31	21	21	51
10	1 pole	20.2	81.1	HS	19	28	19	28	48
Relay 1 responses for ABCG-fault at 80.4 km (20%) from relay 1									
Event	Fault locator			Relay trip times (ms)					
#	Trip type	%	km	Trig signal	HSUR	Z1	HSORCS	Z2CS	CR
1	3 pole	20.6	82.9	HS	15	25	15	25	34
2	3 pole	20.6	82.7	HS	18	28	8	28	58
3	3 pole	20.4	82	HS	17	26	17	26	36
4	3 pole	20.7	83.4	HS	18	28	18	28	58
5	3 pole	20.5	82.6	HS	19	30	10	30	39
6	3 pole	26.6	107	HS	16	26	16	26	55
7	3 pole	24.8	99.6	HS	12	21	12	21	61
8	3 pole	20.5	82.2	HS	18	28	18	28	48
9	3 pole	20.6	82.9	HS	17	26	17	26	56
10	3 pole	26.7	107.2	HS	20	30	11	30	40
Relay 1 responses for AG-fault at 120.6 km (30%) from relay 1									
Event	Fault locator			Relay trip times (ms)					
#	Trip type	%	km	Trig signal	HSUR	Z1	HSORCS	Z2CS	CR
1	1 pole	30.1	121.2	HS	23	!	14	23	43
2	1 pole	27	108.4	TRIPL1	24	!	15	24	44
3	1 pole	29.6	119	HS	21	30	21	30	50
4	1 pole	27.1	108.9	HS	20	29	20	29	49
5	1 pole	29.6	119	HS	23	33	13	23	43
6	1 pole	27.1	108.9	HS	18	!	18	27	47
7	1 pole	30	120.4	HS	22	31	22	22	51
8	1 pole	27	108.4	HS	16	!	16	25	45
9	1 pole	29.9	120.3	HS	22	31	22	31	51
10	1 pole	27.0	108.4	HS	19	28	19	28	48
Relay 1 responses for ABCG-fault at 120.6 km (30%) from relay 1									
Event	Fault locator			Relay trip times (ms)					
#	Trip type	%	km	Trig signal	HSUR	Z1	HSORCS	Z2CS	CR
1	3 pole	30.8	123.8	HS	20	!	9	29	59
2	3 pole	28.9	116.4	HS	15	!	15	24	44
3	3 pole	29.4	118.1	HS	17	!	17	26	56
4	3 pole	31.1	125	HS	9	29	19	29	49
5	3 pole	29.1	116.8	HS	14	!	14	23	53
6	3 pole	33.5	134.7	HS	15	!	15	24	64
7	3 pole	29.1	117.1	HS	16	!	16	26	65
8	3 pole	29.1	116.8	HS	16	!	16	25	45
9	3 pole	30.8	123.8	HS	18	!	18	28	37
10	3 pole	28.9	116.3	HS	16	!	16	26	55

Relay 1 responses for AG-fault at 180.9 km (45%) from relay 1									
Event	Fault locator			Relay trip times (ms)					
#	Trip type	%	km	Trig signal	HSUR	Z1	HSORCS	Z2CS	CR
1	1 pole	44.7	179.7	HS	27	!	17	27	48
2	1 pole	44.2	177.8	TRIP L1	30	!	20	30	50
3	1 pole	39.5	158.8	TRIP L1	29	!	20	29	49
4	1 pole	44.9	180.4	HS	26	!	15	26	55
5	1 pole	43.7	175.5	HS	28	!	18	28	49
6	1 pole	44.4	178.6	HS	23	!	23	23	52
7	1 pole	44	177	HS	22	!	22	22	51
8	1 pole	44.6	179.4	HS	27	!	17	27	38
9	1 pole	44.7	179.7	HS	24	!	13	24	43
10	1 pole	44.5	179	TRIP L1	31	!	22	31	41
Relay 1 responses for ABCG-fault at 180.9 km (45%) from relay 1									
Event	Fault locator			Relay trip times (ms)					
#	Trip type	%	km	Trig signal	HSUR	Z1	HSORCS	Z2CS	CR
1	3 pole	46.2	185.6	HS	21	!	11	31	61
2	3 pole	46.3	186.1	Perm TR	!	!	15	25	45
3	3 pole	42.8	172	HS	17	!	17	26	36
4	3 pole	46.5	187.1	HS	20	!	9	29	59
5	3 pole	46.7	187.7	Perm TR	!	!	16	26	47
6	3 pole	48.0	192.9	TRIP L1	24	!	14	24	53
7	3 pole	47.0	188.9	Perm TR	!	!	9	19	40
8	3 pole	47.0	189	HS	19	!	19	28	48
9	3 pole	47.1	189.3	HS	21	!	11	31	51
10	3 pole	43.4	174.6	HS	16	!	16	26	45

Relay 2 responses for AG-fault at 20.1 km (5%) from relay 1									
Event	Fault locator				Relay trip times (ms)				
#	Trip type	%	km	Trig signal	HSUR	Z1	HSORCS	Z2CS	CR
1	3 pole	38.1	153	Perm TR	!	!	23	33	33
2	3 pole	35.3	142	Perm TR	!	!	22	31	42
3	3 pole	38.1	153	Perm TR	!	!	29	39	39
4	3 pole	35.1	141	Perm TR	!	!	23	33	43
5	3 pole	34.3	138	Perm TR	!	!	25	36	36
6	3 pole	34.1	137	Perm TR	!	!	28	38	38
7	3 pole	37.8	152	Perm TR	!	!	29	29	39
8	3 pole	35.6	143	Perm TR	!	!	23	33	43
9	3 pole	37.8	152	Perm TR	!	!	24	34	44
10	3 pole	34.6	139	Perm TR	!	!	29	40	40
Relay 2 responses for ABCG-fault at 20.1 km (5%) from relay 1									
Event	Fault locator				Relay trip times (ms)				
#	Trip type	%	km	Trig signal	HSUR	Z1	HSORCS	Z2CS	CR
1	3 pole	27.6	111.1	Z1	!	35	15	35	35
2	3 pole	30.2	121.4	Perm TR	!	!	!	40	30
3	3 pole	27.5	110.4	Perm TR	!	41	21	31	31
4	3 pole	30.4	122.2	Z1	!	38	18	38	38
5	3 pole	30.5	122.6	Z1	!	38	!	38	38
6	3 pole	29.7	119.5	Z1	!	34	14	34	34
7	3 pole	30.1	121.1	Z1	!	38	18	38	38
8	3 pole	28.9	116.3	Z1	!	37	17	37	37
9	3 pole	30.9	124.2	Z1	!	40	!	40	40
10	3 pole	26.9	108.1	Z1	!	36	26	36	36

Relay 2 responses for AG-fault at 40.2 km (10%) from relay 1									
Event	Fault locator			Relay trip times (ms)					
#	Trip type	%	km	Trig signal	HSUR	Z1	HSORCS	Z2CS	CR
1	3 pole	33.6	135	Perm TR	!	!	21	31	41
2	3 pole	32.8	132	Perm TR	!	!	25	35	35
3	3 pole	39.8	160	Perm TR	!	!	24	34	34
4	3 pole	30.6	123	Perm TR	!	!	24	33	44
5	3 pole	40.0	161	Perm TR	!	!	24	34	44
6	3 pole	32.3	130	Perm TR	!	!	24	35	35
7	3 pole	32.6	131	Perm TR	!	!	26	37	37
8	3 pole	40.0	161	Perm TR	!	!	26	37	37
9	3 pole	39.6	159	Perm TR	!	!	24	34	44
10	3 pole	32.6	131	Perm TR	!	!	24	34	44
Relay 2 responses for ABCG-fault at 40.2 km (10%) from relay 1									
Event	Fault locator			Relay trip times (ms)					
#	Trip type	%	km	Trig signal	HSUR	Z1	HSORCS	Z2CS	CR
1	3 pole	22.5	90.6	Z1	!	33	!	33	43
2	3 pole	27.1	108.9	Z1	!	38	!	38	38
3	3 pole	24.8	99.5	Z1	!	31	!	31	41
4	3 pole	27.1	108.8	Z1	!	36	16	36	36
5	3 pole	22.8	91.8	Perm TR	!	38	18	38	28
6	3 pole	25.5	102.4	Z1	!	36	!	36	36
7	3 pole	24.6	99.6	Z1	!	34	!	34	34
8	3 pole	27.4	109.9	Z1	!	40	!	40	30
9	3 pole	24.8	99.6	Perm TR	!	41	21	31	31
10	3 pole	24.3	97.5	Perm TR	!	43	!	33	33
Relay 2 responses for AG-fault at 80.4 km (20%) from relay 1									
Event	Fault locator			Relay trip times (ms)					
#	Trip type	%	km	Trig signal	HSUR	Z1	HSORCS	Z2CS	CR
1	3 pole	25.1	101	Perm TR	!	59	20	30	40
2	3 pole	25.1	101	Perm TR	!	58	28	39	39
3	3 pole	23.9	96.1	Perm TR	!	!	26	37	37
4	3 pole	26.1	105	Perm TR	!	58	29	39	39
5	3 pole	23.8	95.6	Perm TR	!	!	27	37	37
6	3 pole	25.9	104	Perm TR	!	51	21	31	41
7	3 pole	26.4	106	Perm TR	!	57	26	37	47
8	3 pole	26.1	105	Perm TR	!	52	22	32	42
9	3 pole	26.1	105	Perm TR	!	57	26	37	47
10	3 pole	26.4	106	Perm TR	!	53	23	32	43
Relay 2 responses for ABCG-fault at 80.4 km (20%) from relay 1									
Event	Fault locator			Relay trip times (ms)					
#	Trip type	%	km	Trig signal	HSUR	Z1	HSORCS	Z2CS	CR
1	3 pole	21.9	88.1	Z1	!	32	22	32	42
2	3 pole	21.7	87.1	Z1	!	40	!	40	30
3	3 pole	21.2	85.1	Z1	!	37	17	37	37
4	3 pole	24.1	96.9	Z1	!	39	!	39	39
5	3 pole	18.8	75.6	Perm TR	!	38	18	38	28
6	3 pole	19.9	79.9	Z1	!	34	!	34	44
7	3 pole	22.5	90.4	Z1	!	40	!	40	40
8	3 pole	19.9	79.8	Z1	!	34	24	34	44
9	3 pole	18.6	74.7	Z1	!	34	!	34	44
10	3 pole	23.7	95.4	Z1	!	37	17	27	37

Relay 2 responses for AG-fault at 120.6 km (30%) from relay 1									
Event	Fault locator			Relay trip times (ms)					
#	Trip type	%	km	Trig signal	HSUR	Z1	HSORCS	Z2CS	CR
1	3 pole	22.5	90.6	Z1	!	34	24	34	34
2	3 pole	17.3	69.6	Z1	!	34	23	34	34
3	3 pole	19.4	78	Z1	!	40	30	40	40
4	3 pole	23.6	94.7	Z1	!	38	27	38	38
5	3 pole	16.4	66	Z1	!	31	21	31	41
6	3 pole	17.1	68.6	Z1	!	34	24	34	44
7	3 pole	18.5	74.2	Z1	!	37	27	37	47
8	3 pole	17.6	70.7	Z1	!	32	22	32	42
9	3 pole	19.3	77.6	Z1	!	37	26	37	47
10	3 pole	17.4	69.9	Z1	!	32	22	32	42
Relay 2 responses for ABCG-fault at 120.6 km (30%) from relay 1									
Event	Fault locator			Relay trip times (ms)					
#	Trip type	%	km	Trig signal	HSUR	Z1	HSORCS	Z2CS	CR
1	3 pole	15.5	62.3	Z1	!	35	!	35	35
2	3 pole	19.8	79.6	Z1	!	41	21	31	41
3	3 pole	19.9	79.9	Z1	!	31	!	31	41
4	3 pole	18.4	73.9	Z1	!	33	23	33	33
5	3 pole	16.9	68.1	Z1	!	37	!	27	37
6	3 pole	16.9	68	Z1	!	36	!	36	36
7	3 pole	20.6	82.7	Z1	!	37	!	37	37
8	3 pole	20.1	80.7	Z1	!	38	!	28	38
9	3 pole	16.6	66.8	Z1	!	38	18	38	38
10	3 pole	16.1	64.7	Z1	!	35	!	35	35
Relay 2 responses for AG-fault at 180.9 km (45%) from relay 1									
Event	Fault locator			Relay trip times (ms)					
#	Trip type	%	km	Trig signal	HSUR	Z1	HSORCS	Z2CS	CR
1	3 pole	5.4	21.6	TRIP L1	34	34	24	34	44
2	3 pole	7.2	28.8	HS	26	37	26	37	46
3	3 pole	4.9	19.5	HS	24	34	24	34	44
4	3 pole	9.3	37.2	Z1	!	40	30	40	40
5	3 pole	10.3	41.6	Z1	!	31	21	31	41
6	3 pole	6.8	27.4	Z1	!	35	25	35	45
7	3 pole	10.5	42.3	Z1	!	34	24	34	44
8	3 pole	9.7	38.8	Z1	!	40	20	40	40
9	3 pole	7.2	28.8	Z1	!	34	24	34	34
10	3 pole	7.2	29.1	Z1	31	31	21	31	41
Relay 2 responses for ABCG-fault at 180.9 km (45%) from relay 1									
Event	Fault locator			Relay trip times (ms)					
#	Trip type	%	km	Trig signal	HSUR	Z1	HSORCS	Z2CS	CR
1	3 pole	7.4	29.7	Z1	!	32	!	32	32
2	3 pole	8.4	33.8	Z1	!	35	24	35	35
3	3 pole	10.2	40.9	Z1	!	36	16	26	36
4	3 pole	10.9	43.9	Z1	!	38	!	38	28
5	3 pole	8.4	33.8	Z1	!	35	25	35	35
6	3 pole	8.6	34.4	Z1	!	32	!	32	42
7	3 pole	13.6	54.5	Z1	!	37	17	27	37
8	3 pole	8.8	35.5	Z1	!	35	23	35	44
9	3 pole	13.8	55.3	Z1	!	38	!	28	38
10	3 pole	15.5	62.1	Z1	!	36	!	33	36

APPENDIX C

ESKOM CAPE TRANSMISSION NETWORK

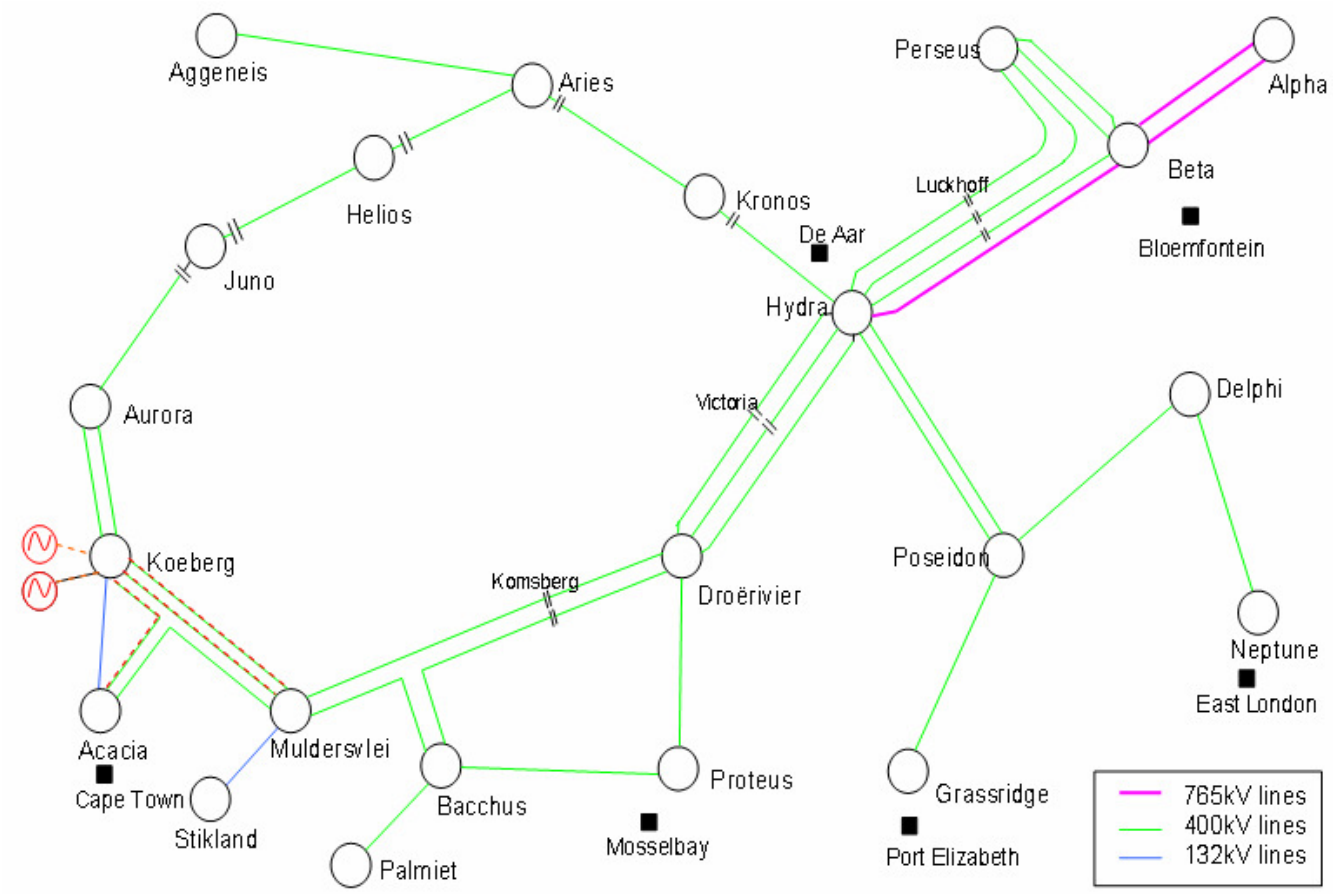

Figure C1: Eskom Cape transmission network [43].

REFERENCES

[1] Topham G., Stokes-Waller E.: "Steady-State Protection Study for the Application of Series Capacitors in the Empangeni 400kV Network", 31st Annual Western Protective Relay Conference, Spokane, Washington, Oct 2004.

[2] Topham G.H., Coney R.G., Fawkes M.G.: "Experience and Problems with the Protection of Series Compensated Lines", IEEE 4th International Conference on Development in Power Protection, Edinburgh, UK, Apr 1989, pp 177-181.

[3] ALSTOM, Network Protection and Automation Guide, First Edition, July 2002, ISBN 2-951 8589-0-0.

[4] Ricardo Dutra, Luis Fabiano, Wagner Oliveira, Murari Mohan Saha, Stig Lidstrom: "Adaptive Distance Protection for Series Compensated Transmission Lines", IEEE/PES Transmission and Distribution Conference and Exposition, Latin America, 2004, pp 581-586.

[5] Anderson P.M.: Power System Protection, IEEE Press Series on Power Engineering, John Wiley & Sons, Inc, 1999.

[6] Santos L.F., Silveira P.M.: "Evaluation of Numerical Distance Protection Algorithms for Series Compensated Transmission Lines", IEEE/PES Transmission and Distribution Conference and Exposition, Latin America, Aug 2006, pp 1-6.

[7] Kundur P.: Power System Stability and Control, EPRI Power System Engineering Series, McGraw-Hill, Inc. 1994.

[8] D. Novosel, B. Bachmann, D. Hart, Yi Hu, M.M. Saha, "Algorithm for Locating Faults on Series Compensated Lines Using Neural Network and Deterministic Methods", IEEE Transactions on Power Delivery, Vol.11 No.4 Oct 1996.

[9] D.W.P. Thomas, C. Christopoulos, "Ultra High-Speed Protection of Series Compensated Lines", IEEE Transactions on Power Delivery, Vol 7 No.1 Jan 1992.

[10] S.K. Salman, N. Rajoo, V. Leitloff, "Investigation of the Effect of the Insertion of Series Capacitors in high Voltage Transmission Lines on the Settings of Distance Protection", IEE Seventh International Conference on Developments in Power System Protection, 9-12 Apr 2001.

[11] Armando Guzmán, Joe Mooney, Gabriel Benmouyal, Normann Fischer, "Transmission Line Protection System for Increasing Power System Requirements", Schweitzer Engineering Laboratories, Inc.

[12] D. L. Goldsworthy, “A Linearized Model for MOV-Protected Series Capacitors”, IEEE Transactions on Power Delivery, Vol. 2, No. 4, November 1987.

[13] G.E. Alexander, J.G. Andrichak, S.S. Rowe, S.B. Wikinson, “Series Compensated Line Protection-A Practical Evaluation” GE Power Management, MULTILIN.

[14] Leoaneka M.C., Rigby B.S.: “Some Challenges Associated with Distance Protection of Series Compensated Transmission Lines”, Proceedings of the 16th Southern African Universities Power Engineering Conference, Cape Town, 2007.

[15] Leoaneka M.C., Rigby B.S.: “Investigation into Underreaching of Distance Relays in Heavily Series Compensated Transmission Network”, Proceedings of the 17th Southern African Universities Power Engineering Conference, Durban, 2008.

[16] Juan M. Gers, Edward J. Holmes: “Protection of Electricity Distribution Networks”, IEE Power and Energy Series 28, London, United Kingdom, 1998.

[17] J. Lewis Blackburn, Thomas J. Domin: Protective Relaying Principles and Applications, 3rd Edition, Taylor and Francis Group, LLC, 2007.

[18] Maria Lúcia C Gabino, Reginaldo C Oliveira, Davis Erwin, Manish Thakur, JC Theron, “Perfecting Performance of Distance Protective Relays and its Associated Pilot Protection Schemes in Extra High Voltage (EHV) Transmission Line Applications”, 59th Annual Conference for Protective Relay Engineers College Station, TX, April 4-6, 2006.

[19] IEEE Std C37.113-1999, “IEEE Guide for Protective Relay Applications to Transmission Lines”, Sept, 1999.

[20] ABB, REL 531 V2.3, Line Distance Protection Terminal, Reference Manuals, ABB, 2006.

[21] Armando Guzman, Jeff Roberts, Karl Zimmerman: “Applying the SEL-321 Relay to Permissive Overreaching Transfer Trip (POTT) Schemes”, SEL Application Guide, Volume I AG95-29.

[22] Stanley H. Horowitz, Arun G. Phadke, Power System Relaying, 2nd Edition. Pg 156, John Wiley & Sons, Inc, 1995.

[23] Roger A. Hedding, ABB Application Note-71L-00, Pilot Protection Alternative, Rev 0, 12/00.

[24] Floriano C.A.F, Oliveira W., Lidstrom S., Saha M.M.: “Real Time Simulation of Protection for 500 kV Series Compensated Lines”, IEEE/PES Transmission and Distribution Conference and Exposition, Latin America, 2004, pp 575-580.

[25] Grunbaum R., Jacques Pernot: “Thyristor-Controlled Series Compensation: A State of the Art Approach for Optimization of Transmission over Power Links”, library.abb.com.

[26] Anderson P.M., Farmer R.G.: Series Compensation of Power Systems, PBLSH, Inc., Encinitas, CA, 1996.

[27] Sakshaug R.C., Kresge J.S., and Miske S.A.: “A New Concept in Arrester Design”, IEEE Transactions PAS-96, no.2, March/April 1977, pp 647-656.

[28] IEEE Power Systems Relaying Committee, WK K13, Series Capacitor Bank Protection, Special publication TP-126-0, 1998.

[29] Cutler J.M., Sublich M.: “Parametric Study of Varistor Energy Requirements for 500 kV Series Capacitor”, IEEE Transactions on Power Delivery, Vol. 3, No. 4, Oct. 1988.

[30] M. M. Sara, B. Kasztenny, E. Rosolowski, J. Izykowski: “First Zone Algorithm for Protection of Series Compensated Lines”, IEEE Transactions on Power Delivery, Vol.16, No. 2, April 2001.

[31] Bogdan Kasztenny: “Distance Protection of Series Compensated Lines; Problems and Solutions”, 28th Annual Western Protective Relay Conference, Spokane, Oct. 2001.

[32] R.J. Marttila: “Performance of Distance Relay Mho Elements On MOV-Protected Series-Compensated Transmission Lines”, IEEE Transactions on Power Delivery, Vol. 7, No. 3, July 1992.

[33] S. Bin, D. Xinzhou, S. Yuanzhang: “A New Traveling Wave Differential Relay for Series Compensated EHV Transmission Line”, Seventh IEE International Conference on Developments In Power System Protection, 5-8 April 2004

[34] Thomas S Roseburg Murari M Saha, Janez Zakonjšek, “Testing and Operational Experiences with High-Speed Distance Relay in BPA 500 kV Series Compensated Network”, 32nd Annual Western Protective Relay Conference, October 25 – 27, 2005.

[35] M.M. Saha, K. Wikstrom, A. Holmstrom, “High-speed protection Scheme for EHV Transmmission Lines”, IEEE Power Engineering Society Winter Meeting, 2000.

[36] M. Chamia, S. Liberman, “Ultra high-Speed Relay for EHV/UHV Transmission Lines-Development, Design and Application”, IEEE Transactions on PAS, Vol. PAS-97, No. 6, Nov./Dec. 1978.

[37] Paul Forsyth, Trevor Maguire, Rick Kuffel, "Real Time Digital Simulator for Control and Protection Systems Testing", 35th Annual IEEE Power Electronics Specialists Conference, 2004.

[38] R. Kuffel, J. Giesbrecht, T. Maguire, R.P. Wierckx, P. McLaren, "RTDS-A Fully Digital Power System Simulator Operating in Real Time", WESCANEX 95, Communications, Power, and Computing Conference Proceedings. IEEE Volume 2, 15-16 May 1995.

[39] P.G. McLaren, R. Kuffel, R. Wwierckx, J. Giesbrecht, L. Arendt, "A Real Time Tigital Simulator for Testing Relays", IEEE Transaction on Power Delivery, Vol. 7 No.1, Jan. 1992.

[40] Smith, S.W., The Science and Engineer's Guide to Digital Signal Processing, California Technical Publishing, San Diego, CA, 1999.

[41] T. Saengsuwan, "Modelling of Distance Relays in EMTP", IPSI '99-International Conference on Power Systems Transients, June 14-20, 1999, Budapest-Hungary.

[42] Leoaneka M.C., Rigby B.S.: "Real-Time Simulator Studies into the Performance of Numerical Distance Relays in Heavily Series Compensated Transmission Networks", Southern African Power System Protection Conference, 2008.

[43] Jacob Maroga, "Western Cape Recovery Plan", 24 May 2006,

http://www.dpe.gov.za/res/Cape_Recovery_240506.ppt

[44] Bin Su, Jianping Wang, Ying Yang, Weixing Gong, Yongsheng Xu, "Setting Considerations of Distance Relays for UHV/EHV Long Transmission Lines", Power Engineering Society General Meeting, 2007. IEEE, 24-28 June 2007.

[45] A.T. Johns, S.K. Salman, Digital Protection for Power Systems, IEE Power Series 15, Peter Peregrinus Ltd, 1995.

[46] Ricardo Abboud, Walmer Ferreira soares, Fernando Goldman, "Challenges and Solution in the Protection of a Long Line in the Furnas system", www.selinc.com/techpprs.

[47] Rigby B S: "Validation of Mathematical Models Used in Real-Time Simulation", Eskom Research Report RES/RR/06/27495, February 2006.